PONTIFICIA UNIVERSIDAD CATOLICA DE CHILE
SCHOOL OF ENGINEERING

AN ACCURATE NUMERICAL-ANALYTICAL METHOD FOR COMPUTING STRESSES IN ROCK MASS AROUND MINING EXCAVATIONS

VALERIA BOCCARDO SALVO

Thesis submitted to the Office of Graduate Studies
in partial fulfillment of the requirements for the Degree of
Doctor in Engineering Sciences

Advisor:
MARIO DURAN

Santiago de Chile, Dic 2017

© MMXVII, VALERIA BOCCARDO SALVO

PONTIFICIA UNIVERSIDAD CATOLICA DE CHILE
SCHOOL OF ENGINEERING

AN ACCURATE NUMERICAL-ANALYTICAL METHOD FOR COMPUTING STRESSES IN ROCK MASS AROUND MINING EXCAVATIONS

VALERIA BOCCARDO SALVO

Members of the Committee:
MARIO DURAN
EDUARDO GODOY
GONZALO YÁÑEZ
RAFAEL BENGURIA
JEAN-CLAUDE NÉDÉLEC
JORGE VÁSQUEZ

Thesis submitted to the Office of Graduate Studies
in partial fulfillment of the requirements for the Degree of
Doctor in Engineering Sciences

Santiago de Chile, Dic 2017

© MMXVII, VALERIA BOCCARDO SALVO

A mi familia, especialmente a
Germán y Antonio, gracias por
darle sentido a mis días.

ACKNOWLEDGEMENTS

Quisiera agradecer al proyecto *MECE Educación superior PUC0710* por la ayuda recibida para realizar mis estudios.

A mi supervisor Mario por su tiempo y dedicación, y al equipo de jovenes investigadores que lidera, Ricardo Hein, Carlos Pérez, Ignacio Vargas y Juan La Rivera, pues sin ellos nada de esto habría sido posible. Especialmente mi reconocimiento a Eduardo Godoy por su constante apoyo en el desarrollo de esta tesis. Al equipo de INGMAT por sus consejos y ayuda.

A Rafael Benguria, quien desde que era una estudiante de pregrado me ha apoyado, aconsejado e inspirado. A los profesores Jean-Claude Nédélec, Gonzalo Yáñez y Jorge Vásquez les agradezco por participar en mi comisión examinadora y revisar esta tesis.

A Aldo Valcarce, Sanzia, Rafael González, Mabel Vega, Mauricio Ipinza, Daniela Cerón, Sebastián Sarmiento y Cristian Gutierrez les agradezco por su paciencia y compañia en estos años.

A mi familia, mi madre Patricia, mis hermanos Andrea, Tamara y Mauro, y mis sobrinos Franco, Stefano y Rafaella, por su amor y apoyo.

Finalmente a Germán, fuimos muy afortunados de encontrarnos, llegaste a cambiar mi vida, llenaste de luz mis ojos y de risas mis días. Gracias por ser mi compañero, y el mejor padre que podría existir para nuestro hijo Antonio.

TABLE OF CONTENTS

LIST OF FIGURES

LIST OF TABLES

ABSTRACT

The Earth's crust is subjected to a state of stress, as a result of gravitational, tectonic, and other forces. When removing material from rock masses, stresses are redistributed, which is especially important in mining, since high stress concentration areas could arise in mining excavations, resulting in undesired events such as rock-falls or slides. Therefore, there is a need for determining, in a reliable way, the state of stress generated in rock masses by mining activities, which constitutes a complex problem. The aim of this work is thus to propose an accurate mathematical methodology to compute such stresses and show its performance in a simplified case. The main strength of the proposed methodology is the effective and efficient numerical treatment of the unbounded medium that surrounds the excavation, when compared with the customary approach used by standard commercial software for the same purpose, which results in a considerable reduction of the required computational resources. The methodology is developed in two stages. In the first stage, we consider a simplified problem where the excavation is assumed to be a hemispherical pit, placed on the surface of an elastic semi-infinite domain subjected to gravity. This problem is solved by using two semi-analytical methods, where the second method is an improvement of the first one. In the second stage, we deal with an excavation of arbitrary axisymmetric geometry by means of a coupling technique, which employs the second semi-analytical method to compute an approximation of the Dirichlet-to-Neumann map (DtN) on an artificial semi-spherical boundary. The DtN map provides the exact boundary conditions that complete the mathematical problem posed in the computational domain lying between the excavation and the artificial boundary, which is then solved by the finite element method (FEM). Numerical results are provided to demonstrate the effectiveness and accuracy of the proposed methodology.

Keywords: Numerical-analytical method, mining excavation, stress, elasticity, semi-infinite domain, finite elements, Dirichlet-to-Neumann map

RESUMEN

La corteza terrestre se encuentra sometida a un estado de esfuerzos o tensiones debido a fuerzas de origen gravitacional y tectónico, entre otros. Al extraer material desde un macizo rocoso, los esfuerzos se redistribuyen, lo cual es especialmente importante en minería, debido a que pueden aparecer áreas de alta concentración de esfuerzos en excavaciones mineras, produciendo eventos no deseados como caídas de roca o deslizamientos. Por lo tanto, hay una necesidad por determinar, de manera fehaciente, el estado de esfuerzos inducido en un macizo rocoso por la actividad minera, lo cual constituye un problema complejo. El objetivo de este trabajo es entonces proponer una metodología matemática certera para calcular estos esfuerzos y mostrar su desempeño en un caso simplificado. La principal fortaleza de esta metodología es el tratamiento numérico eficiente y eficaz del medio no acotado que rodea la excavación, comparado con el enfoque habitual usado por software comercial estándar para el mismo propósito, lo que conlleva una considerable reducción del recurso computacional requerido. El desarrollo de la metodología se divide en dos etapas. En la primera etapa se considera un problema simplificado donde se asume que la excavación es un pit semiesférico situado sobre la superficie de un dominio elástico semi-infinito y sometido a gravedad. Este problema es resuelto usando dos métodos semianalíticos, donde el segundo método es una mejora del primero. En la segunda etapa, se trata el caso de una excavación de geometría axisimétrica arbitraria mediante una técnica de acoplamiento, la cual emplea el segundo método semi-analítico para calcular una aproximación del operador Dirichlet-to-Neumann (DtN) sobre una frontera artificial semi-esférica. El operador DtN provee las condiciones de borde exactas que completan el problema matemático planteado en el dominio computacional existente entre la excavación y la frontera artificial, el cual es entonces resuelto mediante el método de los elementos finitos (FEM). Se presentan resultados numéricos para demostrar la eficiencia y precisión de la metodología propuesta.

Palabras Claves: Método numérico-analítico, excavación minera, esfuerzos, elasticidad, dominio semi-infinito, elementos finitos, operador Dirichlet-to-Neumann

1. INTRODUCTION

Many productive activities involve large scale excavation works. Typical examples are the exploitation of mineral resources, hydrocarbons, or the construction of civil works. From an operational point of view, the stability of excavations represents a crucial issue. If an excavation has not been properly designed, particular zones may become unstable, resulting in undesired events such as rock-falls or slides, which could put at risk the safety of workers, equipment, infrastructure, or cause economic losses. Hence the need for predictive tools capable of determining those areas of the excavation that may be in risk of collapse, in order to take the necessary measures in advance. Previous to any excavation work, the geological structure of the rock mass is subjected to an initial state of stress of gravitational, tectonic, hydraulic or residual origin. When a large scale excavation takes place, the initial state of stress is modified, both on the new surfaces created by the excavation and in the surrounding area. The new state of stress may give rise to instabilities, particularly if certain areas of the excavation undergo high-stress concentration. A displacement field is also generated in the excavation as a consequence of the modified state of stress. Therefore, reliable and opportune information about stresses and displacements in an excavation would make possible to detect beforehand the areas in potential risk of failure.

Numerical methods are a common and powerful tool to compute the stresses and displacements around structures in a rock mass, such an excavation. Among them, one of the most widely used is the finite element method (FEM), mainly due to its advantages in treating complex geometries and material properties. Nevertheless, the FEM applied to problems in geomechanics presents a computational drawback that needs to be overcome. As the whole rock mass around an excavation is of infinitely large size, it is not possible in practice to cover the entire region with a finite element mesh. This drawback is often remedied by performing the finite element analysis only within a finite region of rock mass near the structure under study. This region is bounded by artificial boundaries, which normally consist of line segments or planes, depending on whether the study is two or three

dimensional, respectively. Some authors that have adopted this approach in underground mining are (Kulhawy, 1974), (Huttelmaier & Glockner, 1985) and (Ou, Chiou, & Wu, 1996). It has also been applied by (Griffiths & Lane, 1999) to slope stability in open pits. However, this approach is not exempt from limitations. As it was established in (Kulhawy, 1974), the artificial boundaries need to be located far away enough from the structure in order to achieve an acceptable accuracy. Hence, it is necessary to consider a sufficiently large computational domain, which will require a large number of points in order to be discretized, leading to an increasing amount in the required computational resources. This is a essential point, because the chosen boundary conditions strongly affect the numerical solution obtained. Nevertheless, it often receives little attention in related literature. What is usually done is to assume that either all displacements are zero, or tangent stresses and normal displacements are zero (cf. (Ou et al., 1996; Griffiths & Lane, 1999)). Other approximations suppose spring-like behaviours at boundaries (cf. (Huttelmaier & Glockner, 1985)). However, no mathematical justification of these boundary conditions is given.

In this thesis, we propose an accurate and efficient methodology to compute stresses and displacements around an excavation, whose main strength is the effective and efficient numerical treatment of the unbounded surrounding medium, when compared with the usual approach considered by standard commercial software to perform the same calculations. The methodology uses exact artificial boundary conditions in semi-infinite domains, which allow us to considerably minimize the size of the computational domain to be meshed and at the same time, to avoid the need of using spurious boundary conditions, resulting in an important reduction of the required computational resources. In order to demonstrate the efficiency and effectiveness of the proposed methodology, a simplified problem is considered, where the unbounded rock mass is assumed to be an elastic, isotropic and homogeneous semi-infinite medium, and the excavation shape is supposed axisymmetric. By using spherical coordinates, the partial differential equations of elastostatics are analytically solved and exact boundary conditions are determined in order to be prescribed on an artificial half-spherical boundary. Then a finite element analysis of stresses can be performed inside the computational domain lying between the structure and the artificial

boundary, where more complex characterizations of the rock mass could be assumed. As a first stage of this study, we consider a hemispherical pit in the surface of an elastic, homogeneous and isotropic half-space subject to gravitational stress. Both the infinite flat surface of the half-space and the pit are assumed to be traction-free boundaries. The complete solution of this problem is obtained in a semi-analytical way. Analogous problems have been approached for several authors in contexts different from geomechanics or mining. The first of them was (R. Eubanks, 1953), who studied analytically the stresses and displacements of an elastic half-space with a free boundary and a hemispherical cavity, induced due to a constant pressure, parallel to the flat surface of the solid. Subsequently, (Fujita, Sadayasu, Tsuchida, & Nakahara, 1978) improved some of the expressions given by Eubanks and provided a complete analytical solution. In a later work, (Fujita, Tsuchida, & Nakahara, 1982) treated the case when the external force is no longer a homogeneous pressure, but a directed force (simulating the traction or compression to which a metallic piece is subjected). The same problem was solved by (Ovsyannikov & Starikov, 1987), who proposed some variations based on singular solutions, in order to increase the efficiency of the solution method. In more recent works, most of the attention has been concentrated on stresses on hemispherical cavities when in addition there is corrosion in the metal (see (Cerit, Genel, & Eksi, 2009; Turnbull, Horner, & Connolly, 2009)). All of these articles do not deal with the volume forces due to the weight of the solid medium, which are essential in an elastic model of the infinite rock mass. Eubanks employs the so-called Boussinesq potentials to obtain an analytical solution as infinite series satisfying traction-free boundary conditions on the plane surface and decaying conditions at infinity. However, imposing boundary conditions on the surface of the pit leads to an infinite set of simultaneous linear equations for the coefficients of the series, which cannot be solved exactly. After some unwieldy algebraic manipulation, these equations are solved numerically, yielding approximate values for a finite number of coefficients. Hence, the solution given in (R. A. Eubanks, 1954) is actually not fully analytical but semi-analytical, and similar phenomena occur in (Fujita et al., 1978, 1982) and (Givoli & Vigdergauz, 1993). In addition, the numerical evaluation of the solution in (R. A. Eubanks, 1954) involves computing the sum of double series that

show a slow convergence at the surface of the pit, which is computationally expensive and further complicates obtaining explicitly the solution.

In the second stage of this study we deal with an excavation of arbitrary axisymmetric geometry placed on the surface of a half-space, assumed again elastic, isotropic and homogeneous. The boundary-value problem (BVP) that describes the stresses and displacements around the excavation is formulated on an unbounded domain. Different mathematical and numerical approaches have been devised to solve BVPs in unbounded domains. According to (Givoli, 1992, 1999b), they are classified into four main categories: boundary integral methods, infinite element methods, absorbing layer methods, and artificial boundary condition (ABC) methods. The advantages and limitations of each one of them are discussed in (Givoli, 1992). The present work is concerned with the latter category, also referred to as artificial boundary method (H. D. Han & Wu, 2013b, 2013a).

In the standard ABC method, the original unbounded domain is truncated by introducing an artificial boundary enclosing the particular area of interest, thus defining a bounded computational domain, where standard numerical methods may be used to solve the BVP. This is possible on the condition that suitable boundary conditions are set on the artificial boundary (the ABCs), which are supposed to properly represent the unbounded residual domain that was eliminated. In general, many different choices of ABCs are possible. We focus herein on ABCs based on the Dirichlet-to-Neumann (DtN) map and their use in combination with finite elements, which results in the Dirichlet-to-Neumann finite element method (DtN FEM) (Givoli, 1999b, 1999a). The main advantage of this approach is that the DtN map provides *exact* ABCs, in such a way that the resulting BVP in the computational domain is mathematically equivalent to the original unbounded BVP. Therefore, the use of the FEM to solve the former results in highly accurate and robust numerical schemes.

The DtN FEM method has been mainly developed for BVPs formulated in exterior domains, i.e. the complement of a compact set. It is customary to assume a circular or spherical artificial boundary, in order to be able to apply the method of separation of variables to solve the resulting BVP in the residual domain. Thus, an analytical solution in series form

is obtained, with coefficients that are computed exactly. From it, an explicit closed-form expression for the DtN map is deduced, given as an exact nonlocal relation between the solution and its normal derivative on the artificial boundary, which is used as a boundary condition that completes the mathematical formulation of the BVP in the computational domain, making it available for numerical solution by finite elements. This procedure has been extensively used to solve wave BVPs, namely the Helmholtz equation (Keller & Givoli, 1989), (Grote & Keller, 1995b), (Deakin & Rasmussen, 2001), the time-dependent wave equation (Grote & Keller, 1995a, 1996; Aladl, Deakin, & Rasmussen, 2002), and the elastodynamic equation, both in frequency domain (Givoli & Keller, 1990; Harari & Shohet, 1998) and time domain (Grote & Keller, 2000; Grote, 2000; Gächter & Grote, 2003). In this context, ABCs are also called *non-reflecting boundary conditions*, since they are aimed at preventing any spurious reflection of waves from the artificial boundary. The DtN FEM method has also been successfully applied to linear elliptic BVPs in exterior domains, mainly the Laplace equation and linear elastostatics (H. D. Han & Wu, 1985; Givoli & Keller, 1989; H. D. Han & Wu, 1992; H. D. Han & Zheng, 2005).

A particularly important field of application of unbounded BVPs is geophysics, where the ground is usually modelled as an unbounded elastic domain. A typical example is the problem of determining deformations and stresses around structures of interest in the ground, such as an excavation in mining or civil engineering. Even though an exterior domain may be used as a model of the ground in a first approximation, a more realistic model needs to take into account the ground surface, which is customarily assumed, for simplicity, to be a plane boundary that extends to infinity, where a traction-free (Neumann) boundary condition holds. The resulting unbounded domain is called *semi-infinite*. To apply a DtN FEM approach to such a domain, a natural approach would be to consider as artificial boundary a semi-circle or semi-sphere surrounding the structure of interest, in analogy to the exterior case. This procedure works properly for some standard 2D scalar BVPs, such as the Laplace equation (Givoli, 1992) and the Helmholtz equation (Givoli & Vigdergauz, 1993) with Dirichlet or Neumann boundary conditions holding on the infinite plane boundary, since in these cases the BVP in the residual semi-infinite domain can be

solved by separation of variables. However, the same procedure cannot be directly applied to linear elastostatics in semi-infinite domains, since in this case the method of separation of variables fails in solving the BVP in the residual domain in a fully analytical way, and thus it is not possible to get an explicit closed-form expression for the DtN map. Givoli and Vigdergauz (Givoli & Vigdergauz, 1993) proposed an alternative to deal with this drawback in the 2D case. They considered a semi-circular artificial boundary and solved the BVP in the semi-infinite residual domain using complex analysis techniques, resulting in a solution in series form, whose coefficients can only be computed in an approximated way. A different approach was used by Han, Bao and Wang (H. Han, Bao, & Wang, 1997), who employed the direct method of lines with semi-discretisation to solve the BVP in the residual domain, obtaining an approximation of the DtN map. No previous work on DtN FEM procedures for 3D elastostatics in semi-infinite domains was found in the literature.

In the last chapter, we present a DtN FEM for a semi-infinite elastic domain in 3D. A geometrical perturbation on the plane surface representing the structure of interest is considered, which is assumed to be axisymmetric about the vertical axis. Assuming further that the elastic domain is only under axisymmetric loading, the whole problem is treated as a BVP of axisymmetric elastostatics. The semi-infinite domain is truncated by introducing a semi-spherical artificial boundary surrounding the perturbation. Then a standard FEM discretisation in the resulting computational domain with exact ABCs in the artificial boundary is established at a theoretical level. As it is not possible to obtain a fully explicit closed-form expression for the DtN map, we proceed in a similar way to (Givoli & Vigdergauz, 1993), solving the BVP in the residual domain just for particular Dirichlet data on the artificial boundary, in order to approximate those boundary integral terms involving the DtN map that occur in the finite element formulation. The BVP in the residual domain for each required case is solved by a semi-analytical method, analogous to that presented in Chapter IV. By applying separation of variables, a general analytical solution is calculated, expressed as a series with unknown coefficients, which are approximated by minimising a quadratic energy functional appropriately chosen. The minimisation yields a symmetric and positive definite linear system of equations for a finite number of coefficients, which is

efficiently solved by exploiting its particular block structure, in such a way that the coefficients are computed by mere forward and backward substitutions. This procedure allows an approximate but effective coupling of the exact nonlocal ABCs provided by the DtN map with the FEM scheme. The method is validated by solving a model problem whose exact solution is available. The relative error between the numerical and the exact solution is analysed for different mesh sizes.

2. GENERAL MODEL

In this chapter, the mathematical model describing the elastic deformations and stresses in a half-space with a hemispherical pit is formulated.

2.1. Mathematical Model

Let us consider the lower half-space with a geometrical perturbation on its plane surface which is local, i.e. it is restricted to a bounded region. This type of domain is oftentimes referred to as a *locally perturbed half-space*. In addition, the perturbation is assumed to be rotationally symmetric about a vertical axis, in such a way that the whole semi-infinite domain is actually an axisymmetric solid (or solid of revolution). Therefore, its geometry is completely described by its generating cross section, which consists in a 2D domain that we denote by Ω. The boundary of Ω consists of three parts: A vertical boundary of axisymmetry coinciding with the axis of revolution, denoted by Γ_{s}, a horizontal unperturbed boundary coinciding with the infinite plane surface of the half-space, denoted by Γ_{∞}, and a perturbed bounded boundary which is assumed piecewise smooth, denoted by Γ_{h} (see Figure 2.1). The domain Ω will be described with the aid of axisymmetric cylindrical coordinates (ρ, z) or spherical coordinates (r, ϕ) as appropriate, with the origin placed at the point of intersection between the axis of revolution and the plane boundary of the unperturbed half-space. Variables ρ, z, r and ϕ are linked by the relations

$$r^2 = \rho^2 + z^2, \qquad \phi = \arctan\frac{z}{\rho}, \qquad \rho = r\sin\phi, \qquad z = r\cos\phi.$$

The unit vectors associated with variables ρ, z, r and ϕ are denoted respectively by $\hat{\boldsymbol{\rho}}$, $\hat{\boldsymbol{z}}$, $\hat{\boldsymbol{r}}$ and $\hat{\boldsymbol{\phi}}$. They are linked by the relations

$$\hat{\boldsymbol{\rho}} = \hat{\boldsymbol{r}}\sin\phi + \hat{\boldsymbol{\phi}}\cos\phi, \qquad \hat{\boldsymbol{z}} = \hat{\boldsymbol{r}}\cos\phi - \hat{\boldsymbol{\phi}}\sin\phi, \tag{2.1a}$$

$$\hat{\boldsymbol{r}} = \hat{\boldsymbol{\rho}}\sin\phi + \hat{\boldsymbol{z}}\cos\phi, \qquad \hat{\boldsymbol{\phi}} = \hat{\boldsymbol{\rho}}\cos\phi - \hat{\boldsymbol{z}}\sin\phi. \tag{2.1b}$$

Thus an arbitrary position in Ω is expressed either as (ρ, z) or (r, ϕ), depending on the chosen system of coordinates. Moreover, we denote by θ the azimuthal angle, which is not

necessary to describe geometrically the 2D domain Ω, but it is required in the axisymmetric elastostatic model.

We assume that Ω is occupied by an isotropic, homogeneous, linear elastic medium. Under the condition that the 3D axisymmetric domain is only subject to axisymmetric loading, the resulting elastic deformations will keep the axisymmetric nature of the problem. A generic displacement field defined in Ω is denoted by $\boldsymbol{u}$ and its associated stress tensor is denoted by $\boldsymbol{\sigma} = \boldsymbol{\sigma}(\boldsymbol{u})$. By virtue of the axisymmetry, $\boldsymbol{u}$ has only components u_ρ and u_z (resp. u_r and u_ϕ), whereas $\boldsymbol{\sigma}$ has normal components σ_ρ and σ_z (resp. σ_r and σ_ϕ), a shear component $\sigma_{\rho z}$ (resp. $\sigma_{r\phi}$), and an additional non-vanishing normal component σ_θ (see (Sadd, 2005) for details). It is assumed that $\boldsymbol{\sigma}$ is given in terms of $\boldsymbol{u}$ by the isotropic Hooke's law, that is,

$$\boldsymbol{\sigma}(\boldsymbol{u}) = \lambda\,(\nabla \cdot \boldsymbol{u})\,I + \mu(\nabla \boldsymbol{u} + \nabla \boldsymbol{u}^T), \tag{2.2}$$

where $\lambda,\ \mu > 0$ are the Lamé constants of the elastic solid and I is the 3×3 identity matrix. We assume the downward gravitational force to be the only body force acting on the solid medium. The elastic equilibrium is thus governed by Navier's equation:

$$-\nabla \cdot \sigma(\boldsymbol{u}) = \varrho g \hat{\boldsymbol{z}}, \tag{2.3}$$

or written in terms of the displacements

$$(\lambda + \mu)\nabla(\nabla \cdot \boldsymbol{u}) + \mu \Delta \boldsymbol{u} = -\varrho g \hat{\boldsymbol{z}}, \tag{2.4}$$

where g denotes the acceleration of gravity and $\hat{\boldsymbol{z}}$ stands for the unit vector in the direction of positive z-axis. The right-hand side of (2.3) takes into account the effect of the gravity force per unit volume of solid. It has constant magnitude ϱg and acts in the direction of $-\hat{\boldsymbol{z}}$ everywhere in $\mathbb{R}^3_-$. As the half-space is unbounded in both horizontal directions x and y, the displacement field due to the gravity force, which we shall call $\boldsymbol{u}_g$, must be in the direction of $-\hat{\boldsymbol{z}}$. On the other hand, it is assumed that the infinite plane surface of the half-space, defined by $z = 0$, is traction-free, which is mathematically expressed by

homogeneous Neumann boundary conditions:

$$\boldsymbol{\sigma}(\boldsymbol{u})\hat{\boldsymbol{z}} = \mathbf{0}. \tag{2.5}$$

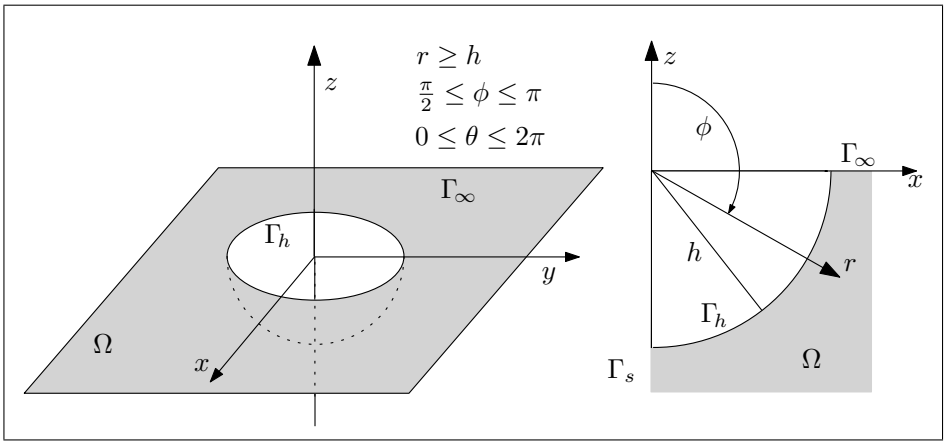

Figure 2.1. Geometrical model of the elastoestatic problem.

hemispherical boundary, by Γ_∞ its infinite horizontal boundary, and by Γ_s its vertical boundary. These sets are defined in terms of (r, ϕ) as follows:

$$\Omega = \{(r,\phi) :\ h < r < \infty,\ \pi/2 < \phi < \pi\}, \tag{2.6a}$$

$$\Gamma_h = \{(r,\phi) :\ r = h,\ \pi/2 < \phi < \pi\}, \tag{2.6b}$$

$$\Gamma_\infty = \{(r,\phi) :\ r \geq h,\ \phi = \pi/2\}, \tag{2.6c}$$

$$\Gamma_s = \{(r,\phi) :\ r \geq h,\ \phi = \pi\}. \tag{2.6d}$$

The stress (see Figure 2.2) and the displacements are related through the Hooke's law, which in this isotropic case is $\sigma_{ij} = \lambda \nabla \cdot \boldsymbol{u}\delta_{ij} + 2\mu\varepsilon_{ij}$.The Hooke's law (2.2) is written by components as

$$\sigma_\rho(\boldsymbol{u}) = (\lambda + 2\mu)\frac{\partial u_\rho}{\partial \rho} + \lambda\frac{u_\rho}{\rho} + \lambda\frac{\partial u_z}{\partial z}, \tag{2.7a}$$

$$\sigma_\theta(\boldsymbol{u}) = \lambda\frac{\partial u_\rho}{\partial \rho} + (\lambda + 2\mu)\frac{u_\rho}{\rho} + \lambda\frac{\partial u_z}{\partial z}, \tag{2.7b}$$

$$\sigma_z(\boldsymbol{u}) = \lambda\frac{\partial u_\rho}{\partial \rho} + \lambda\frac{u_\rho}{\rho} + (\lambda + 2\mu)\frac{\partial u_z}{\partial z}, \tag{2.7c}$$

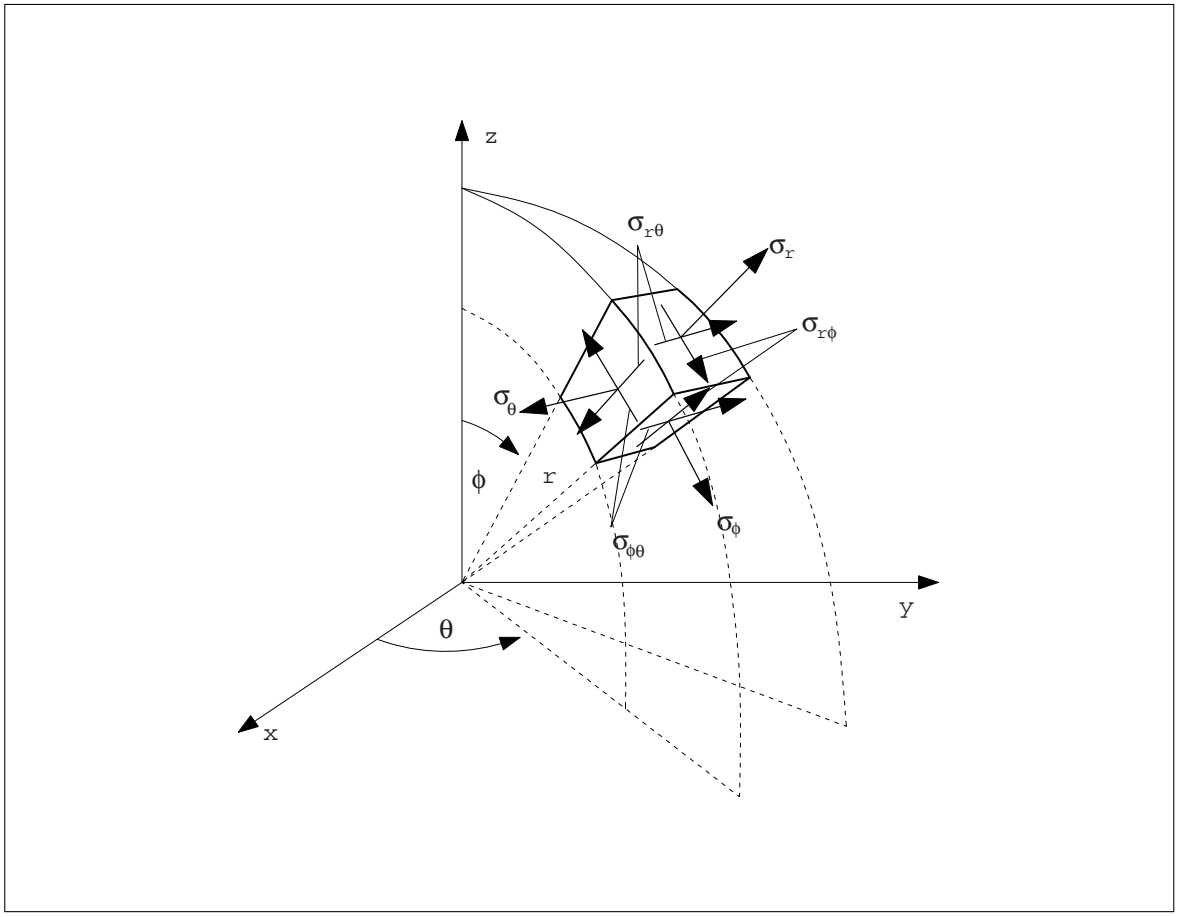

Figure 2.2. Stress components in spherical coordinates.

$$\sigma_{\rho z}(\boldsymbol{u}) = \mu\Big(\frac{\partial u_\rho}{\partial z} + \frac{\partial u_z}{\partial \rho}\Big), \tag{2.7d}$$

in cylindrical coordinates and as

$$\sigma_r(\boldsymbol{u}) = (\lambda + 2\mu)\frac{\partial u_r}{\partial r} + 2\lambda\frac{u_r}{r} + \frac{\lambda}{r}\Big(\frac{\partial u_\phi}{\partial \phi} + \cot\phi\, u_\phi\Big), \tag{2.8a}$$

$$\sigma_\phi(\boldsymbol{u}) = \lambda\frac{\partial u_r}{\partial r} + 2(\lambda + \mu)\frac{u_r}{r} + \frac{1}{r}\Big((\lambda + 2\mu)\frac{\partial u_\phi}{\partial \phi} + \lambda\cot\phi\, u_\phi\Big), \tag{2.8b}$$

$$\sigma_\theta(\boldsymbol{u}) = \lambda\frac{\partial u_r}{\partial r} + 2(\lambda + \mu)\frac{u_r}{r} + \frac{1}{r}\Big(\lambda\frac{\partial u_\phi}{\partial \phi} + (\lambda + 2\mu)\cot\phi\, u_\phi\Big), \tag{2.8c}$$

$$\sigma_{r\phi}(\boldsymbol{u}) = \mu\Big(\frac{1}{r}\frac{\partial u_r}{\partial \phi} + \frac{\partial u_\phi}{\partial r} - \frac{u_\phi}{r}\Big), \tag{2.8d}$$

in spherical coordinates (see (Sadd, 2005) for details).

The elastic equilibrium of the perturbed domain Ω subject to gravity is governed by Navier's equation, given in (2.3). On the other hand, Γ_∞ and Γ_h are both assumed to be traction-free, which means that homogeneous Neumann boundary conditions as those given in (2.5) hold on both boundaries, with $\hat{\boldsymbol{z}}$ substituted by $-\hat{\boldsymbol{r}}$ in the latter case. In addition, the vertical boundary Γ_s is assumed to be free of shear traction and constrained against normal displacement (otherwise the axisymmetry would be destroyed). Furthermore, from physical intuition it is reasonable to assume that the effect of the hemispherical pit on the displacement field in Ω is essentially local, that is, at large distances from the origin the elastic half-space deforms as if there is no geometrical perturbation. We thus assume that, as the distance from the pit tends to infinity, the displacement field $\boldsymbol{u}$ approaches asymptotically $\boldsymbol{u}_g$, i.e., the displacement field in absence of perturbation. An important related issue is the rate at which this asymptotic approach at infinity takes place, which is not a simple matter. It rather concerns questions of existence and uniqueness, which are beyond the scope of this work. We simply assume that when r tends to infinity, the difference in norm between $\boldsymbol{u}$ and $\boldsymbol{u}_g$ decays to zero as $O(1/r)$, which is sufficient for our purposes. Taking into account all these assumptions, $\boldsymbol{u}$ is obtained as a solution of the boundary-value problem: Find $\boldsymbol{u} : \Omega \to \mathbb{R}^2$ such that

$$\nabla \cdot \boldsymbol{\sigma}(\boldsymbol{u}) = -\rho g \hat{\boldsymbol{z}} \qquad \text{in } \Omega, \tag{2.9a}$$

$$\boldsymbol{\sigma}(\boldsymbol{u})\hat{\boldsymbol{z}} = \boldsymbol{0} \qquad \text{on } \Gamma_\infty, \tag{2.9b}$$

$$\boldsymbol{\sigma}(\boldsymbol{u})\hat{\boldsymbol{r}} = \boldsymbol{0} \qquad \text{on } \Gamma_h, \tag{2.9c}$$

$$\boldsymbol{\sigma}(\boldsymbol{u})\hat{\boldsymbol{\phi}} \cdot \hat{\boldsymbol{r}} = \boldsymbol{u} \cdot \hat{\boldsymbol{\phi}} = 0 \qquad \text{on } \Gamma_s, \tag{2.9d}$$

$$|\boldsymbol{u} - \boldsymbol{u}_g| = O\Big(\frac{1}{r}\Big) \qquad \text{as } r \to \infty, \tag{2.9e}$$

where $|\cdot|$ stands for the Euclidean norm. We make the change of variables $\boldsymbol{v} = \boldsymbol{u} - \frac{\varrho g z^2}{2(\lambda+2\mu)}\hat{\boldsymbol{z}}$ in order to achieve a homogeneous equation. The displacement field $\boldsymbol{u}$ is then

$$\boldsymbol{u} = \boldsymbol{u}_g + \boldsymbol{v}, \qquad \boldsymbol{u}_g(x, y, z) = -\frac{\varrho g z^2}{2(\lambda + 2\mu)}\,\hat{\boldsymbol{z}}. \tag{2.10}$$

The Navier equation in this new displacement field $\boldsymbol{v}$ is

$$(\lambda + \mu)\nabla(\nabla \cdot \boldsymbol{v}) + \mu\Delta\boldsymbol{v} = \boldsymbol{0}. \tag{2.11}$$

The problem is then: Find $\boldsymbol{v} : \Omega \to \mathbb{R}^2$ such that

$$\nabla \cdot \boldsymbol{\sigma}(\boldsymbol{v}) = \boldsymbol{0} \qquad \text{in } \Omega, \tag{2.12a}$$

$$\boldsymbol{\sigma}(\boldsymbol{v})\hat{\boldsymbol{z}} = \boldsymbol{0} \qquad \text{on } \Gamma_\infty, \tag{2.12b}$$

$$\boldsymbol{\sigma}(\boldsymbol{v})\hat{\boldsymbol{r}} = \boldsymbol{f} \qquad \text{on } \Gamma_h, \tag{2.12c}$$

$$\boldsymbol{\sigma}(\boldsymbol{v})\hat{\boldsymbol{\phi}} \cdot \hat{\boldsymbol{r}} = \boldsymbol{v} \cdot \hat{\boldsymbol{\phi}} = 0 \qquad \text{on } \Gamma_s, \tag{2.12d}$$

$$|\boldsymbol{v}| = O\Big(\frac{1}{r}\Big) \qquad \text{as } r \to \infty, \tag{2.12e}$$

where $\boldsymbol{f} : \Gamma_h \to \mathbb{R}^2$ is a vector function defined by its components in r and ϕ as

$$\boldsymbol{f}(\phi) = f_r(\phi)\,\hat{\boldsymbol{r}} + f_\phi(\phi)\,\hat{\boldsymbol{\phi}}, \qquad \frac{\pi}{2} \le \phi \le \pi, \tag{2.13}$$

with

$$f_r(\phi) = \varrho g h\,\frac{\big(\nu + (1-2\nu)\cos^2\phi\big)\cos\phi}{1-\nu}, \tag{2.14a}$$

$$f_\phi(\phi) = -\varrho g h\,\frac{(1-2\nu)\cos^2\phi\,\sin\phi}{1-\nu}, \tag{2.14b}$$

The boundary-value problem (2.12) has certain advantages over the original problem, such as a homogeneous Navier's equation (2.12a) and a solution decaying to zero at infinity (2.12e). Hence, in order to determine the displacement field $\boldsymbol{u}$, we first solve (2.12) to obtain the displacement field $\boldsymbol{v}$ and then we calculate $\boldsymbol{u}$ from (2.10), given that an explicit expression for $\boldsymbol{u}_g$ is available.

2.1.1. Papkovich-Neuber's decomposition

It should be noted that only two independent elastic constants are needed to describe the behaviour of isotropic materials. The relationships between elastic constants E, λ, μ and ν are provided in Table 2.1.

Table 2.1. Relationship between the different constants that characterise a material.

	(λ, μ)	(E, μ)	(λ, ν)	(μ, ν)	(E, ν)
E	$\mu\dfrac{3\lambda+2\mu}{\lambda+\mu}$	E	$\dfrac{\lambda(1+\nu)(1-2\nu)}{\nu}$	$2\mu(1+\nu)$	E
λ	λ	$\mu\dfrac{E-2\mu}{3\mu-E}$	λ	$\dfrac{2\mu\nu}{1-2\nu}$	$\dfrac{E\nu}{(1+\nu)(1-2\nu)}$
μ	μ	μ	$\lambda\dfrac{1-2\nu}{2\nu}$	μ	$\dfrac{E}{2(1+\nu)}$
ν	$\dfrac{\lambda}{2(\lambda+\mu)}$	$\dfrac{E}{2\mu}-1$	ν	ν	ν

We can use the Helmholtz decomposition, which states that any sufficiently continuous vector field can be represented as the sum of the gradient of a scalar potential φ and the curl of a vector potential $\boldsymbol{\phi}$, that is, $\boldsymbol{u} = \nabla\varphi + \nabla \times \boldsymbol{\phi}$. The gradient term in the decomposition has a zero curl and is referred to as the irrotational part, while the curl term has a zero divergence and is called solenoidal. Note that this representation specifies three displacement components in terms of four potential components, and furthermore the divergence of $\boldsymbol{\phi}$ is arbitrary. In order to address these problems, it is common to choose $\boldsymbol{\phi}$ with zero divergence, *i.e.*, $\nabla \cdot \boldsymbol{\phi} = 0$.

Based on the Helmholtz's decomposition, we can define φ such that $\nabla \cdot \boldsymbol{u} = \Delta\varphi$, so

$$\Delta\boldsymbol{u} + \frac{1}{(1-2\nu)}\nabla(\Delta\varphi) = -\frac{\boldsymbol{F}}{\mu}, \tag{2.15}$$

and arranging in a suitable way,

$$\Delta\left(\boldsymbol{u}+\frac{1}{(1-2\nu)}\nabla\varphi\right)=-\frac{\boldsymbol{F}}{\mu}. \tag{2.16}$$

We define the vectorial potential such that $\boldsymbol{A}=\left(2\mu\boldsymbol{u}+\frac{2\mu}{(1-2\nu)}\nabla\varphi\right)$, so for $\boldsymbol{A}=[A_r\ A_\theta\ A_z]^T$ we have the following relations

$$\Delta\boldsymbol{A}=-2\boldsymbol{F}\qquad\text{and}\qquad\nabla\cdot\boldsymbol{A}=\frac{4\mu(1-\nu)}{(1-2\nu)}\Delta\varphi. \tag{2.17}$$

The second relation follows from $\nabla\cdot\nabla\varphi=\Delta\varphi$, and by definition $\nabla\cdot\boldsymbol{u}=\Delta\varphi$.

From vectorial calculus we know that for any vectorial field $\boldsymbol{F}(\cdot)$ and a constant vector $\boldsymbol{R}$ the following relation holds,

$$\Delta(\boldsymbol{R}\cdot\boldsymbol{F})=\boldsymbol{R}\cdot\Delta\boldsymbol{F}+2(\nabla\cdot\boldsymbol{F}).$$

In particular we have,

$$\Delta(\boldsymbol{R}\cdot\boldsymbol{A})=\boldsymbol{R}\cdot\Delta\boldsymbol{A}+2(\nabla\cdot\boldsymbol{A}), \tag{2.18}$$

which is the same as,

$$\nabla\cdot\boldsymbol{A}=\frac{1}{2}\left(\Delta(\boldsymbol{R}\cdot\boldsymbol{A})+2(\boldsymbol{R}\cdot\boldsymbol{f})\right), \tag{2.19}$$

and this is equivalent to

$$\frac{4\mu(1-\nu)}{(1-2\nu)}\Delta\varphi=\frac{1}{2}\left(\Delta(\boldsymbol{R}\cdot\boldsymbol{A})+2(\boldsymbol{R}\cdot\boldsymbol{F})\right), \tag{2.20}$$

which implies

$$\Delta\left(\frac{4\mu(1-\nu)}{(1-2\nu)}\varphi-\frac{1}{2}(\boldsymbol{R}\cdot\boldsymbol{A})\right)=\boldsymbol{R}\cdot\boldsymbol{F}. \tag{2.21}$$

We introduce the scalar potential $B=\left(\frac{2\mu}{(1-2\nu)}\varphi-\frac{(\boldsymbol{R}\cdot\boldsymbol{A})}{4(1-\nu)}\right)$ in sustitution of φ, which satisfies

$$\Delta B=\frac{\boldsymbol{R}\cdot\boldsymbol{F}}{2(1-\nu)},$$

in our case we have $\boldsymbol{F}=0$, which means the potentials satisfy

$$\Delta\boldsymbol{A}=0,\quad\Delta B=0. \tag{2.22}$$

Moreover, in this axisymmetric case $A_r = A_\theta = 0$, $A_z = A_z(r, z)$ and $B = B(r, z)$, where $A_z,\ B$ are commonly called the Boussinesq potentials. If we take the definitions of $\boldsymbol{A}$ y B, it holds that

$$2\mu\boldsymbol{u} = \boldsymbol{A} - \nabla\left(B + \frac{\boldsymbol{R}\cdot\boldsymbol{A}}{4(1-\nu)}\right). \tag{2.23}$$

If we use the decomposition of Papkovich-Neuber, we can find the solution of (2.4) through the scalar potentials $B(r, \phi)$ and $A_z(r, \phi)$, which are related with $\boldsymbol{v}$ by means of the expression

$$2\mu\boldsymbol{v} = \nabla(B + zA_z) - 4(1-\nu)A_z\hat{\boldsymbol{z}}, \tag{2.24}$$

where both potentials are harmonic functions, i.e., $\Delta B = \Delta A_z = 0$, and $\boldsymbol{v}$ must satisfy the boundary conditions. The completeness of this representation was shown by (R. Eubanks & Sternberg, 1956), and thus all elasticity solutions are representable by this scheme. The solution to Navier's equation in Ω is sought with the aid of the so-called Boussinesq potentials, which are a particular case of the more general Papkovich-Neuber (or Boussinesq-Papkovich) representation (cf. (Amenzade, 1979; Sadd, 2005)). According to (R. A. Eubanks, 1954), $\boldsymbol{v}$ is defined through the following relation

$$2\mu\boldsymbol{v} = \nabla(\Phi + z\Psi) - 4(1-\nu)\Psi\,\hat{\boldsymbol{k}}, \tag{2.25}$$

where Φ and Ψ are the Boussinesq potentials, which are harmonic functions thanks to the fact that Navier's equation (2.12a) is homogeneous. Otherwise, Φ and Ψ would satisfy the Poisson equation, with nonzero right-hand sides. Expressing (2.25) by its components in r and ϕ yields

$$2\mu v_r(r,\phi) = \frac{\partial\Phi}{\partial r}(r,\phi) + r\cos\phi\,\frac{\partial\Psi}{\partial r}(r,\phi) - (3-4\nu)\cos\phi\,\Psi(r,\phi), \tag{2.26a}$$

$$2\mu v_\phi(r,\phi) = \frac{1}{r}\frac{\partial\Phi}{\partial\phi}(r,\phi) + \cos\phi\,\frac{\partial\Psi}{\partial\phi}(r,\phi) + (3-4\nu)\sin\phi\,\Psi(r,\phi). \tag{2.26b}$$

In order to calculate a solution of (2.12a), it becomes necessary to solve the Laplace equation in Ω for Φ and Ψ. Prior to this, we analyse in more detail the decaying condition at infinity for $\boldsymbol{v}$. By replacing (2.25) in (2.12e), we infer that Φ and Ψ have to satisfy certain asymptotic behaviours when r tends to infinity. Specifically, Ψ has to decay to zero as

$O(1/r)$. It is also required that the term $\nabla(z\Psi)$ appearing in (2.25) decreases to zero at the same rate. We also need that $\nabla\Phi$ decays to zero as $O(1/r)$, which is a weaker condition than the one required for Ψ. Therefore, Ψ is sought as a solution of

$$\Delta\Psi = 0 \qquad \text{in } \Omega, \tag{2.27a}$$

$$\Psi = O\Big(\frac{1}{r}\Big) \qquad \text{as } r \to \infty, \tag{2.27b}$$

and Φ is sought as a solution of

$$\Delta\Phi = 0 \qquad \text{in } \Omega, \tag{2.28a}$$

$$|\nabla\Phi| = O\Big(\frac{1}{r}\Big) \qquad \text{as } r \to \infty, \tag{2.28b}$$

where Δ stands for the Laplacian. Let us first determine Ψ. Expressing $\Psi = \Psi(r, \phi)$, the Laplace equation in axisymmetric spherical coordinates is given by

$$\Delta\Psi(r,\phi) = \frac{1}{r^2}\frac{\partial}{\partial r}\left(r^2\frac{\partial\Psi(r,\phi)}{\partial r}\right) + \frac{1}{r^2\sin\phi}\frac{\partial}{\partial\phi}\left(\sin\phi\frac{\partial\Psi(r,\phi)}{\partial\phi}\right) = 0. \tag{2.29}$$

If we apply standard separation of variables in r and ϕ to (2.29) (cf. (Arfken & Weber, 2001)), and we discard those solutions that are unbounded in Ω, we obtain that for each integer $n \geq 0$, the function Ψ_n defined as

$$\Psi_n(r,\phi) = \frac{P_n(\cos\phi)}{r^{n+1}}, \tag{2.30}$$

is a solution of (2.27a), where $P_n(\cdot)$ denotes the Legendre polynomial of order n (see Appendix 6.1). The general solution of (2.27a) is then expressed as an infinite linear combination of functions Ψ_n. By virtue of (2.30) it is immediate that

$$\Psi_n(r,\phi) = O\Big(\frac{1}{r^{n+1}}\Big) \qquad \text{as } r \to \infty,$$

which means that when r increases, the first term of the infinite linear combination (the one for $n = 0$) dominates over the rest of the terms, and as this term behaves asymptotically as $O(1/r)$, the linear combination of all terms behaves asymptotically the same way. Therefore, the obtained general solution of (2.27a) also fulfils the decaying condition (2.27b). In

addition, if we compute the terms $\nabla(z\Psi_n)$ for each $n \geq 0$, we verify that

$$|\nabla(z\Psi_n(r,\phi))| = O\Big(\frac{1}{r^{n+1}}\Big) \qquad \text{as } r \to \infty,$$

and an analogous reasoning allows us to state that when r tends to infinity, the term $\nabla(z\Psi)$ decreases asymptotically in norm as $O(1/r)$. Hence, this term does not affect the fulfilment of (2.12e). Let us now determine Φ. Proceeding analogously as for Ψ, we obtain that the functions Φ_n defined by

$$\Phi_n(r,\phi) = \frac{P_n(\cos\phi)}{r^{n+1}}, \tag{2.31}$$

satisfy (2.28a) for each integer $n \geq 0$. As done in (R. A. Eubanks, 1954), it seems reasonable to propose an infinite linear combination of functions Φ_n as the general solution of (2.28a), in analogy to the solution established for (2.27a). Nevertheless, according to the authors' opinion such a solution is not general enough, owing to the decaying condition at infinity (2.28b) imposed on Φ, which differs from that imposed on Ψ. If we calculate the gradients of functions Φ_n defined in (2.31) and we take their norms, it is easy to see that

$$|\nabla\Phi_n(r,\phi)| = O\Big(\frac{1}{r^{n+2}}\Big) \qquad \text{as } r \to \infty.$$

Consequently, if we express Φ as a linear combination of functions Φ_n defined in (2.31), and if we study the asymptotic behaviour of $|\nabla\Phi|$ as r increases, we obtain that the first term, which is again the dominating one, behaves asymptotically as $O(1/r^2)$. Thus, when r tends to infinity $|\nabla\Phi|$ decreases to zero as $O(1/r^2)$. This means that the solution Φ, just expressed as a linear combination of functions Φ_n, satisfies a more restrictive condition than (2.28b), so it is not general enough to be the sought solution of (2.28). In order to achieve the required generality in Φ, we add a new component to the set of functions Φ_n, which gives rise to an asymptotic behaviour of order $O(1/r)$ in $|\nabla\Phi|$ as r tends to infinity. This component, associated for convenience with the index $n = -1$, corresponds to the following logarithmic potential

$$\Phi_{-1}(r,\phi) = \ln(r - r\cos\phi). \tag{2.32}$$

This potential arises when solving the Boussinesq's problem, i.e., the one of a concentrated force acting normal to the free surface of an elastic half-space (cf. (Sadd, 2005)). It is also known as the Boussinesq's elementary solution of the second kind (cf. (Amenzade, 1979)). It is straightforward to verify that Φ_{-1} is a solution of (2.29). In addition, the singularity of the logarithm at zero in (2.32) does not cause problems of unboundedness, since all those points such that $\cos\phi = 1$ (i.e. $\phi = 0$) are not contained in the domain Ω. Moreover, if we compute the gradient of Φ_{-1} and we take its norm, we arrive at

$$|\nabla \Phi_{-1}(r, \phi)| = O\Big(\frac{1}{r}\Big) \qquad \text{as } r \to \infty.$$

Hence, the sought solution to (2.28) corresponds to an infinite linear combination of functions Φ_n including the case $n = -1$, since such a solution satisfies the right decaying condition at infinity (2.28b).

3. A SIMPLE SEMI-INFINITE GEOMETRY

In this chapter we want to find the displacements and the stresses in a semi-infinite region. In order to do so, we use the Papkovich-Neuber decomposition technique and by imposing different boundary conditions in the perturbation of the domain, we can obtain an expression that allows us to evaluate the displacements and the stresses in any point of our domain.

3.1. Series's solution

In order to find the solution to (2.25) we note that Laplace's equation in spherical coordinates is

$$\Delta f = \frac{1}{r^2}\frac{\partial}{\partial r}\left(r^2\frac{\partial f}{\partial r}\right) + \frac{1}{r^2\sin^2\phi}\frac{\partial^2 f}{\partial\theta^2} + \frac{1}{r^2\sin\phi}\frac{\partial}{\partial\phi}\left(\sin\phi\frac{\partial f}{\partial\phi}\right). \tag{3.1}$$

Let us consider the problem of finding solutions of the form $f(r,\phi) = g(r)h(\phi)$. By separation of variables, two differential equations result by imposing Laplace's equation. We use then $g(r) = r^n$. Furthermore, the change of variables $x = \cos\phi$ transforms this equation into the Legendre differential equation

$$(1-x^2)\frac{\partial^2 h(x)}{\partial x^2} - 2x\frac{\partial h(x)}{\partial x} + n(n+1)h(x) = 0, \tag{3.2}$$

whose bounded solutions are the Legendre polynomials. We assume a bounded perturbation, so at infinity, the expression for A_z must decay, while the gradient for B must tend to zero. Hence, we write in general the solutions in the form

$$\begin{aligned} A_z(r,\phi) &= \sum_{n=0}^{\infty} a_n r^{-(n+1)} P_n(\cos\phi), \\ B(r,\phi) &= \tilde{b}\ln(r - r\cos\phi) + \sum_{n=0}^{\infty} b_n r^{-(n+1)} P_n(\cos\phi). \end{aligned} \tag{3.3}$$

In order to solve the problem, we replace (3.3) in (2.25). For the sake of convenience, we omit henceforth the argument of the Legendre polynomials, since all of them are evaluated at $\cos\phi$ unless otherwise is indicated. We thus obtain the following expressions for the displacements

$$2\mu v_r = \frac{1}{r}\tilde{b} + \sum_{n=0}^{\infty}\left(-\frac{(n+4-4\nu)\cos\phi P_n}{r^{n+1}}a_n - \frac{(n+1)}{r^{n+2}}P_n b_n\right), \tag{3.4}$$

$$2\mu v_\phi = \frac{\sin\phi}{r(1-\cos\phi)}\tilde{b} + \sum_{n=0}^{\infty}\left(\frac{\sin\phi((3-4\nu)P_n - \cos\phi P_n')}{r^{n+1}}a_n - \frac{\sin\phi P_n'}{r^{n+2}}b_n\right). \tag{3.5}$$

We make the linear combination $A_n = (2n+1)a_n - (n+4-4\nu)b_{n-1}$ valid for $n = 0, 1, \ldots$, in order to simplify the calculation. In this axisymmetric model, it holds that $\sigma_{\phi\theta} = \sigma_{r\theta} = 0$. The remaining stresses are

$$\begin{aligned}\sigma_r &= \frac{2(2(1-\nu)+(2-\nu)\cos\phi)}{r^2}A_0 - \frac{1}{r^2}\tilde{b} \\ &+ \sum_{n=0}^{\infty}\left(\frac{(n+1)((n+1)(n+4)-2\nu)P_{n+1}}{r^{n+2}}A_n + \frac{(n+1)(n+2)}{r^{n+3}}P_n b_n\right),\end{aligned} \tag{3.6}$$

$$\begin{aligned}\sigma_\phi &= \frac{(3-2\nu+(1-2\nu)\cos\phi)\cos\phi}{(1-\cos\phi)r^2}A_0 - \frac{\cos\phi}{r^2(1-\cos\phi)}\tilde{b} \\ &+ \sum_{n=0}^{\infty}\left(-\frac{(n+1)(n^2-n+1-2\nu)P_{n+1} - (n-3+4\nu)P_n'}{r^{n+2}}A_n\right. \\ &\left.+\frac{P_{n+1}' - (n+1)(n+2)P_n}{r^{n+3}}b_n\right),\end{aligned} \tag{3.7}$$

$$\begin{aligned}\sigma_\theta &= -\frac{4(1-\nu)+(1-2\nu)(1-\cos\phi)\cos\phi}{(1-\cos\phi)r^2}A_0 + \frac{1}{r^2(1-\cos\phi)}\tilde{b} \\ &+ \sum_{n=0}^{\infty}\left(\frac{-(1+2\nu)(n+1)(2n+1)P_{n+1} - (n-3+4\nu)P_n'}{r^{n+2}}A_n - \frac{P_{n+1}}{r^{n+3}}b_n\right),\end{aligned} \tag{3.8}$$

$$\begin{aligned}\sigma_{r\phi} &= \frac{(3-2\nu+(1-2\nu)\cos\phi)}{(1-\cos\phi)r^2}\sin\phi A_0 - \frac{\sin\phi}{r^2(1-\cos\phi)}\tilde{b} \\ &+ \sum_{n=0}^{\infty}\left(\frac{(n^2+2n-1+2\nu)P_{n+1}'}{r^{n+2}}\sin\phi A_n + \frac{(n+2)\sin\phi P_n'}{r^{n+3}}b_n\right).\end{aligned} \tag{3.9}$$

3.2. First set of boundary conditions: free surface boundary condition on the surface of the plane.

We know that any picewise continuous function can be written in the base of $\{P_{2n}\}_{n=0}^{\infty}$ in the range $[-1,0]$, and also we can make a descomposition in terms of the basis $\{\sin\phi P'_{2n}\}_{n=0}^{\infty}$ in the same range (see (Brown & Churchill, 2006)), where the orthonormalization constants are

$$F(\phi)=\sum_{n=0}^{\infty}F_{2n}P_{2n}(\cos\phi), \tag{3.10}$$

$$F_{2n}=(4n+1)\int_{\pi/2}^{\pi}F(\phi)\sin\phi P_{2n}(\cos\phi)\mathrm{d}\phi, \tag{3.11}$$

$$G(\phi)=\sum_{n=0}^{\infty}G_{2n}\sin\phi P'_{2n}(\cos\phi), \tag{3.12}$$

$$G_{2n}=\frac{(4n+1)}{2n(2n+1)}\int_{\pi/2}^{\pi}G(\phi)\sin^2\phi P'_{2n}(\cos\phi)\mathrm{d}\phi. \tag{3.13}$$

In particular, Legendre's polynomials of odd degree are expressed in terms of this basis, for $-1\leq x<0$ and $k=0,1,\ldots$, as follows (see Appendix A)

$$P_{2k+1}(x)=-(2k+1)P_{2k}(0)\sum_{n=0}^{\infty}\omega_k^{(n)}P_{2n}(x), \tag{3.14}$$

$$P'_{2k+1}(x)=-(2k+1)P_{2k}(0)\sum_{n=0}^{\infty}\omega_k^{(n)}P'_{2n}(x), \tag{3.15}$$

$$\omega_k^{(n)}=\frac{(4n+1)P_{2n}(0)}{(2k+1-2n)(2k+2+2n)}. \tag{3.16}$$

In addition, by using the recurrence relations for Legendre polynomials, we find that

$$P'_{2k+1}(0)=(2k+1)P_{2k}(0), \tag{3.17}$$

$$P_{2k+2}(0)=-\frac{(2k+1)}{(2k+2)}P_{2k}(0), \tag{3.18}$$

$$P_{2k}(0)=(-1)^k\frac{(2k)!}{2^{2k}(k!)^2}. \tag{3.19}$$

In the specific case of $F(x) = \ln(1-x)$ we find that $F_0 = 2\ln 2 - 1$ and $F_n = -\frac{P_{2n}(0)}{2n(2n+1)}$.

Next, we impose the free surface boundary condition on the surface of the plane Γ_∞ $(r > h,\ \phi = \pi/2)$, whose components are $\sigma_\phi(\boldsymbol{v}) = \sigma_{r\phi}(\boldsymbol{v}) = 0$. We use for this purpose the relations $P_{2n+1}(0) = P'_{2n}(0) = 0$ for all n, and define the coefficients $\alpha_n = (n+1)^2 - 2 + 2\nu$ and $\beta_n = (n+2)(n+5) - 2\nu$. This yields the following contributions, which are arranged according to the parity of the coefficients

$$\begin{array}{lcll}
A_0 & \Rightarrow & \sigma_\phi = 0, & \sigma_{r\phi} = \frac{3-2\nu}{r^2}, \\
A_{2n+1} & \Rightarrow & \sigma_\phi = \frac{(2n+1)\alpha_{2n}}{r^{2n+3}} P_{2n}(0), & \sigma_{r\phi} = 0, \\
A_{2n+2} & \Rightarrow & \sigma_\phi = 0, & \sigma_{r\phi} = -\frac{(2n+1)(2n+3)\alpha_{2n+2}}{(2n+2)r^{2n+4}} P_{2n}(0), \\
\tilde{b} & \Rightarrow & \sigma_\phi = 0, & \sigma_{r\phi} = -\frac{1}{r^2}, \\
b_{2n} & \Rightarrow & \sigma_\phi = -\frac{(2n+1)^2}{r^{2n+3}} P_{2n}(0), & \sigma_{r\phi} = 0, \\
b_{2n+1} & \Rightarrow & \sigma_\phi = 0, & \sigma_{r\phi} = \frac{(2n+1)(2n+3)}{r^{2n+4}} P_{2n}(0).
\end{array} \tag{3.20}$$

It should be observed that the contributions to σ_ϕ are given by the odd terms of A_n and the even terms of b_n, while for $\sigma_{r\phi}$ the opposite happens. Motivated by this fact, we take linear combinations of the coefficients, in order to continue fulfilling the boundary conditions and to simplify further calculations. In particular, the displacements are

$$\begin{aligned}
2\mu v_r(r,\phi) = &\left(\frac{-1+2\nu}{r} P_0 - \frac{4(1-\nu)}{r} P_1 \right) \tilde{B} \\
&- \sum_{n=0}^{\infty} \left(\frac{(2n+1)(2n+2)(2n+5-4\nu) P_{2n+2}}{r^{2n+2}} \tilde{A}_n + \frac{(2n+1)\alpha_{2n} P_{2n}}{r^{2n+2}} \tilde{A}_n \right. \\
&\left. + \frac{(2n+2)\alpha_{2n+2} P_{2n+1}}{r^{2n+3}} \tilde{B}_n + \frac{(2n+2)(2n+3)(2n+6-4\nu) P_{2n+3}}{r^{2n+3}} \tilde{B}_n \right),
\end{aligned} \tag{3.21}$$

$$\begin{aligned}
2\mu v_\phi(r,\phi) = &\frac{\sin\phi}{r} \left(\frac{2(1-\nu)}{(1-\cos\phi)} - \frac{(3-4\nu)\cos\phi}{(1-\cos\phi)} \right) \tilde{B} \\
&- \sin\phi \sum_{n=0}^{\infty} \left(\frac{(2n+1)(2n-2+4\nu) P'_{2n+2}}{r^{2n+2}} \tilde{A}_n + \frac{\alpha_{2n} P'_{2n}}{r^{2n+2}} \tilde{A}_n \right. \\
&\left. + \frac{\alpha_{2n+2} P'_{2n+1}}{r^{2n+3}} \tilde{B}_n + \frac{(2n+2)(2n-1+4\nu) P'_{2n+3}}{r^{2n+3}} \tilde{B}_n \right).
\end{aligned} \tag{3.22}$$

The stresses are

$$\begin{aligned}
\sigma_r &= \left(\frac{1-2\nu}{r^2}P_0 + \frac{2(2-\nu)}{r^2}P_1\right)\tilde{B} \\
&+ \sum_{n=0}^{\infty}\left[\frac{(2n+1)(2n+2)}{r^{2n+3}}\left(\alpha_{2n}P_{2n}+\beta_{2n}P_{2n+2}\right)\tilde{A}_n\right. \\
&\left.+\frac{(2n+2)(2n+3)}{r^{2n+4}}\left(\alpha_{2n+2}P_{2n+1}+\beta_{2n+1}P_{2n+3}\right)\tilde{B}_n\right], \qquad (3.23)\\
\sigma_\phi &= \frac{(1-2\nu)\cos^2\phi}{(1-\cos\phi)r^2}\tilde{B} \\
&+ \sum_{n=0}^{\infty}\left[-2(2n+1)\left(\frac{(n+1)\alpha_{2n}}{r^{2n+3}}P_{2n}+\frac{(n+1)(4n^2+2n+1-2\nu)}{r^{2n+3}}P_{2n+2}\right.\right. \\
&\left.+\frac{(4n+3)(2n+2\nu-1)}{r^{2n+3}}P'_{2n+1}\right)\tilde{A}_n \\
&+\left(\frac{(5+4n)(2n+1+2\nu)}{r^{2n+4}}P'_{2n+2}\right. \\
&\left.\left.-(2n+3)(2n+2)\frac{\alpha_{2n+2}P_{2n+1}+(4n^2+6n+3-2\nu)P_{2n+3}}{r^{2n+4}}\right)\tilde{B}_n\right], \qquad (3.24)
\end{aligned}$$

$$\begin{aligned}
\sigma_\theta &= \frac{(1-2\nu)(\cos^2\phi-\cos\phi-1)}{(1-\cos\phi)r^2}\tilde{B} \\
&+ \sum_{n=0}^{\infty}\left[-(4n+3)\left(\frac{(1-2\nu)(2n+1)(2n+2)P_{2n+2}}{r^{2n+3}}+\frac{(2n-1+2\nu)P'_{2n+1}}{r^{2n+3}}\right)\tilde{A}_n\right. \\
&\left.-(4n+5)\left(\frac{(1-2\nu)(2n+2)(2n+3)P_{2n+3}}{r^{2n+4}}+\frac{(2n+1+2\nu)P'_{2n+2}}{r^{2n+4}}\right)\tilde{B}_n\right], \qquad (3.25)\\
\sigma_{r\phi} &= \frac{(1-2\nu)\sin\phi\cos\phi}{(1-\cos\phi)r^2}\tilde{B} \\
&+ \sum_{n=0}^{\infty}\left[\frac{\sin\phi}{r^{2n+3}}((2n+2)\alpha_{2n}P'_{2n}+(2n+1)\alpha_{2n+1}P'_{2n+2})\tilde{A}_n\right. \qquad (3.26)\\
&\left.+\frac{\sin\phi}{r^{2n+4}}\alpha_{2n+2}((2n+2)P'_{2n+3}+(2n+3)P'_{2n+1})\tilde{B}_n\right].
\end{aligned}$$

3.3. Second set of boundary conditions: boundary conditions on the surface of the semiesphere

Until now we have the solution for the following model

$$(P)\begin{cases} \text{Find } \boldsymbol{v}(r,\phi) = \begin{bmatrix} v_r(r,\phi) \\ v_\phi(r,\phi) \end{bmatrix} \text{ such that:} & & \\ (\lambda+\mu)\nabla(\nabla\cdot\boldsymbol{v}) + \mu\Delta\boldsymbol{v} = 0 & \text{in } \Omega, & (3.27) \\ \sigma_\phi(\boldsymbol{v}) = \sigma_{r\phi}(\boldsymbol{v}) = 0 & \text{on } \Gamma_\infty, & (3.28) \\ \boldsymbol{v} \to \boldsymbol{0} & r \to \infty. & (3.29) \end{cases}$$

We still have to impose the second set of boundary conditions on the boundary Γ_h (the surface of the semiesphere). To achieve this we use various options (with respect to the boundary conditions) in the following sections.

3.3.1. Traction-free boundary

In this case we set $\sigma_r(\boldsymbol{u}) = \sigma_{r\phi}(\boldsymbol{u}) = 0$. We make a change of variables (which we already use in (2.10)), and combining with (3.14) we get

$$\begin{aligned} \sigma_r(\boldsymbol{v}) &= \varrho g h\cos\phi\left(\frac{\nu+(1-2\nu)\cos^2\phi}{1-\nu}\right) \\ &= \frac{\varrho g h}{1-\nu}\left(\frac{1}{5}(3-\nu)P_1 + \frac{2}{5}(1-2\nu)P_3\right) \\ &= -\frac{\varrho g h}{5(1-\nu)}\sum_{n=0}^{\infty}\left((3-\nu)\omega_0^{(n)} - 3(1-2\nu)\omega_1^{(n)}\right)P_{2n}, \qquad (3.30) \\ \sigma_{r\phi}(\boldsymbol{v}) &= -\varrho g h\cos^2\phi\sin\phi\left(\frac{1-2\nu}{1-\nu}\right) \\ &= -\varrho g h\sin\phi\left(\frac{1-2\nu}{1-\nu}\right)\frac{1}{15}\left(3P_1' + 2P_3'\right) \\ &= -\frac{1}{5}\varrho g h\left(\frac{1-2\nu}{1-\nu}\right)\sum_{n=0}^{\infty}\left(\omega_1^{(n)} - \omega_0^{(n)}\right)\sin\phi P_{2n}'. \qquad (3.31) \end{aligned}$$

We replace (3.23) in (3.30). Rearranging the terms appropiately and introducing a Kronecker delta gives

$$\sum_{n=0}^{\infty}\Bigg(\Bigg[\frac{\varrho gh}{5(1-\nu)}\left((3-\nu)\omega_0^{(n)}-3(1-2\nu)\omega_1^{(n)}\right)+\alpha_{2n}\frac{(2n+1)(2n+2)}{h^{2n+3}}\tilde{A}_n$$
$$+\left(\frac{1-2\nu}{h^2}\delta_0^{(n)}-\frac{2(2-\nu)}{h^2}\omega_0^{(n)}\right)\tilde{B}$$
$$-\sum_{k=0}^{\infty}\frac{(2k+1)(2k+3)P_{2k}(0)}{h^{2k+4}}\left((2k+2)\alpha_{2k+2}\omega_k^{(n)}-(2k+3)\beta_{2k+1}\omega_{k+1}^{(n)}\right)\tilde{B}_k\Bigg]P_{2n}$$
$$+\beta_{2n}\frac{(2n+1)(2n+2)}{h^{2n+3}}\tilde{A}_nP_{2n+2}\Bigg)=0. \tag{3.32}$$

Defining the coefficients $\tilde{C}=\tilde{B}$ and $C_k=(2k+1)(2k+3)P_{2k}(0)\tilde{B}_k$, the first boundary condition at Γ_h becomes

$$\alpha_{2n}\frac{(2n+1)(2n+2)}{h^{2n+3}}\tilde{A}_n+\beta_{2n-2}\frac{2n(2n-1)}{h^{2n+1}}\tilde{A}_{n-1}+\left(\frac{1-2\nu}{h^2}\delta_0^{(n)}-\frac{2(2-\nu)}{h^2}\omega_0^{(n)}\right)\tilde{C}$$
$$+\sum_{k=0}^{\infty}\frac{C_k}{h^{2k+4}}\left(-(2k+2)\alpha_{2k+2}\omega_k^{(n)}+(2k+3)\beta_{2k+1}\omega_{k+1}^{(n)}\right)$$
$$+\frac{\varrho gh}{5(1-\nu)}\left((3-\nu)\omega_0^{(n)}-3(1-2\nu)\omega_1^{(n)}\right)=0. \tag{3.33}$$

In the same way as we proceeded before, we substitute (3.26) in (3.31)

$$\sum_{n=0}^{\infty}\Bigg(\Bigg[\varrho gh\frac{1-2\nu}{5(1-\nu)}\left(\omega_1^{(n)}-\omega_0^{(n)}\right)+\frac{(1-2\nu)}{h^2}\left(\omega_0^{(n)}+\frac{(4n+1)}{2n(2n+1)}P_{2n}(0)\right)\tilde{B}$$
$$+\frac{\alpha_{2n}(2n+2)}{h^{2n+3}}\tilde{A}_n+\frac{(2n+1)\alpha_{2n+1}}{h^{2n+3}}P'_{2n+2}\tilde{A}_n$$
$$+\sum_{k=0}^{\infty}\frac{(2k+1)(2k+3)\alpha_{2k+2}P_{2k}(0)}{h^{2k+4}}\left(\omega_{k+1}^{(n)}-\omega_k^{(n)}\right)\tilde{B}_k\Bigg]P'_{2n}\Bigg)=0. \tag{3.34}$$

The second boundary condition is

$$\alpha_{2n}\frac{2n+2}{h^{2n+3}}\tilde{A}_n + \alpha_{2n-1}\frac{2n-1}{h^{2n+1}}\tilde{A}_{n-1} + \frac{1-2\nu}{h^2}\left(\omega_0^{(n)} + \frac{(4n+1)}{2n(2n+1)}P_{2n}(0)\right)\tilde{C}$$
$$+\sum_{k=0}^{\infty}\frac{\alpha_{2k+2}}{h^{2k+4}}\left(\omega_{k+1}^{(n)} - \omega_k^{(n)}\right)C_k + \varrho g h\frac{1-2\nu}{5(1-\nu)}\left(\omega_1^{(n)} - \omega_0^{(n)}\right) = 0. \tag{3.35}$$

Resolution by a system of equations: Defining the coefficients $A'_n = \frac{\tilde{A}_n}{\varrho g h^{2n+4}}$ and $C'_n = \frac{C_n}{\varrho g h^{2n+5}}$, we can express the problem as the following system of equations

$$\begin{cases} \alpha_{2n}(2n+1)(2n+2)A'_n + \beta_{2n-2}2n(2n-1)A'_{n-1} = D_n^1, \\ \alpha_{2n}(2n+2)A'_n + \alpha_{2n-1}(2n-1)A'_{n-1} = D_n^2, \end{cases} \tag{3.36}$$

where

$$D_n^1 = \tilde{C}\left(2(2-\nu)\omega_0^{(n)} - (1-2\nu)\delta_0^{(n)}\right) + \sum_{k=0}^{\infty}C'_k\left((2k+2)\alpha_{2k+2}\omega_k^{(n)}\right.$$
$$\left.-(2k+3)\beta_{2k+1}\omega_{k+1}^{(n)}\right) - \frac{(3-\nu)\omega_0^{(n)} - 3(1-2\nu)\omega_1^{(n)}}{5(1-\nu)}, \tag{3.37}$$
$$D_n^2 = \tilde{C}(1-2\nu)\left(-\frac{(4n+1)}{2n(2n+1)}P_{2n}(0) - \omega_0^{(n)}\right) + \sum_{k=0}^{\infty}C'_k\alpha_{2k+2}\left(\omega_k^{(n)} - \omega_{k+1}^{(n)}\right)$$
$$-\frac{(1-2\nu)}{5(1-\nu)}\left(\omega_1^{(n)} - \omega_0^{(n)}\right). \tag{3.38}$$

This is equivalent to the matrix system

$$\begin{pmatrix} 2n(2n-1)\beta_{2n-2} & (2n+1)(2n+2)\alpha_{2n} \\ (2n-1)\alpha_{2n-1} & (2n+2)\alpha_{2n} \end{pmatrix}\begin{pmatrix} A'_{n-1} \\ A'_n \end{pmatrix} = \begin{pmatrix} D_n^1 \\ D_n^2 \end{pmatrix}, \tag{3.39}$$

whose determinant is $\Delta_n = (2n-1)(2n+2)\alpha_{2n}(2n\beta_{2n-2} - (2n+1)\alpha_{2n-1})$. The solutions ($A'_n$ and A'_{n-1}) for this system of equations are

$$\begin{aligned}
A'_{n-1} = \frac{(2n+2)\alpha_{2n}}{\Delta_n}\Bigg(& -\frac{(2n+4-(4n+3)\nu)\omega_0^{(n)}}{5(1-\nu)} + \frac{(1-2\nu)(2n+4)\omega_1^{(n)}}{5(1-\nu)} \\
& + \left[(2n+5-4\nu(n+1))\omega_0^{(n)} + (1-2\nu)\frac{(4n+1)}{2n}P_{2n}(0)\right]\tilde{C} \\
& + \sum_{k=0}^{\infty}\left[\alpha_{2k+2}(2k-2n+1)\omega_k^{(n)} + \big(\alpha_{2k+2}(2n+1) - \beta_{2k+1}(2k+3)\big)\omega_{k+1}^{(n)}\right]C'_k\Bigg), \qquad (3.40) \\
A'_n = \frac{(2n-1)}{\Delta_n}\Bigg(& \frac{\big((1-2\nu)2n\beta_{2n-2} + (3-\nu)\alpha_{2n-1}\big)\omega_0^{(n)}}{5(1-\nu)} - \frac{(1-2\nu)(2n\beta_{2n-2}+3\alpha_{2n-1})\omega_1^{(n)}}{5(1-\nu)} \\
& + \left[\alpha_{2n-1}\left((1-2\nu)\delta_0^{(n)} - 2(2-\nu)\omega_0^{(n)}\right) - 2n\beta_{2n-2}(1-2\nu)\left(\omega_0^{(n)} + \frac{(4n+1)}{2n(2n+1)}P_{2n}(0)\right)\right]\tilde{C}' \\
& + \sum_{k=0}^{\infty}\Big[\alpha_{2k+2}\big(2n\beta_{2n-2} - (2k+2)\alpha_{2n-1}\big)\omega_k^{(n)} \\
& + \big((2k+3)\alpha_{2n-1}\beta_{2k+1} - 2n\beta_{2n-2}\alpha_{2k+2}\big)\omega_{k+1}^{(n)}\Big]C'_k\Bigg). \qquad (3.41)
\end{aligned}$$

By evaluating (3.40) at $(n+1)$ and combining with (3.41), we obtain

$$\begin{aligned}
&\Big[\Delta_n(2n+4)\alpha_{2n+2}\left((2n+7-4\nu(n+2))\omega_0^{(n+1)}+(1-2\nu)\frac{(4n+5)}{(2n+2)}P_{2n+2}(0)\right)\\
&-\Delta_{n+1}(2n-1)\left(\alpha_{2n-1}\left((1-2\nu)\delta_0^{(n)}-2(2-\nu)\omega_0^{(n)}\right)\right.\\
&\left.-2n\beta_{2n-2}(1-2\nu)\left(\omega_0^{(n)}+\frac{(4n+1)}{2n(2n+1)}P_{2n}(0)\right)\right)\Big]\tilde{C}'\\
&+\sum_{k=0}^{\infty}\Bigg[\Delta_n(2n+4)\alpha_{2n+2}\Big[\alpha_{2k+2}(2k-2n-1)\omega_k^{(n+1)}\\
&+\big((2n+3)\alpha_{2k+2}-(2k+3)\beta_{2k+1}\big)\omega_{k+1}^{(n+1)}\Big]\\
&-\Delta_{n+1}(2n-1)\Big[\alpha_{2k+2}\big(2n\beta_{2n-2}-(2k+2)\alpha_{2n-1}\big)\omega_k^{(n)}\\
&+\big((2k+3)\alpha_{2n-1}\beta_{2k+1}-2n\alpha_{2k+2}\beta_{2n-2}\big)\omega_{k+1}^{(n)}\Big]\Bigg]C_k'\\
&=\frac{-1}{5(1-\nu)}\Bigg[(2n+4)\alpha_{2n+2}\Delta_n\left((1-2\nu)(2n+6)\omega_1^{(n+1)}-(2n+6-(4n+7)\nu)\omega_0^{(n+1)}\right)\\
&-(2n-1)\Delta_{n+1}\left((1-2\nu)(2n\beta_{2n-2}+3\alpha_{2n-1})\omega_1^{(n)}\right.\\
&\left.-((1-2\nu)2n\beta_{2n-2}+(3-\nu)\alpha_{2n-1})\omega_0^{(n)}\right)\Bigg]. \qquad (3.42)
\end{aligned}$$

By truncating the infinite series in (3.42) at a finite order N, we get a linear system of equations for coefficients $\tilde{C}', C_0', C_1', \ldots, C_N'$. Once we have solved this system, we can obtain the solution to the displacements and stresses with the expressions (3.21) to (3.26).

3.3.2. Loaded boundary

In this case we take $\sigma_r(\boldsymbol{v}) = g_1(\cos\phi)$ and $\sigma_{r\phi}(\boldsymbol{v}) = g_2(\cos\phi)$. We decompose these functions in terms of the basis of Legendre polynomials, and call the associated coefficients l_{2n} and m_{2n}, in the case that the basis is $\{P_{2n}\}_{n=0}^{\infty}$ or $\{\sin\phi P_{2n}'\}_{n=0}^{\infty}$.

In the case of the first boundary condition (which involves g_1), we have that

$$\left(\frac{1-2\nu}{h^2}P_0+\frac{2(2-\nu)}{h^2}P_1\right)\tilde{B}+\sum_{n=0}^{\infty}\left\{\frac{(2n+1)(2n+2)}{h^{2n+3}}[\alpha_{2n}P_{2n}+\beta_{2n}P_{2n+2}]\tilde{A}_n\right.$$
$$\left.+\sum_{k=0}^{\infty}\frac{(2k+1)(2k+3)P_{2k}(0)}{h^{2k+4}}\left[-\alpha_{2k+2}(2k+2)\omega_k^{(n)}+\beta_{2k+1}(2k+3)\omega_{k+1}^{(n)}\right]P_{2n}\tilde{B}_k\right\}$$
$$=\sum_{n=0}^{\infty}l_{2n}P_{2n}. \tag{3.43}$$

Rearranging the terms appropiately, introducing a Kronecker delta, and defining the coefficients $\tilde{C}=\tilde{B}$ and $C_k=(2k+1)(2k+3)P_{2k}(0)\tilde{B}_k$, gives us

$$\frac{2n(2n-1)}{h^{2n+1}}\beta_{2n-2}\tilde{A}_{n-1}+\frac{(2n+1)(2n+2)}{h^{2n+3}}\alpha_{2n}\tilde{A}_n+\frac{1-2\nu}{h^2}\delta_0^{(n)}\tilde{C}-\frac{2(2-\nu)\omega_0(n)}{h^2}\tilde{C}$$
$$+\sum_{k=0}^{\infty}\frac{1}{h^{2k+4}}\left[-\alpha_{2k+2}(2k+2)\omega_k^{(n)}+\beta_{2k+1}(2k+3)\omega_{k+1}^{(n)}\right]C_k-l_{2n}=0 \tag{3.44}$$

If we proceed in the same way as before, then the second boundary condition is

$$\frac{(2n-1)\alpha_{2n-1}}{h^{2n+1}}\tilde{A}_{n-1}+\frac{(2n+2)\alpha_{2n}}{h^{2n+3}}\tilde{A}_n+\frac{(1-2\nu)}{h^2}\left(\omega_0^{(n)}+\frac{(4n+1)}{2n(2n+1)}P_{2n}(0)\right)\tilde{C}$$
$$+\sum_{k=0}^{\infty}\frac{\alpha_{2k+2}}{h^{2k+4}}\left(\omega_{k+1}^{(n)}-\omega_k^{(n)}\right)C_k-m_{2n}=0. \tag{3.45}$$

Resolution by a system of equations We make the change of variables $A'_n=\frac{\tilde{A}_n}{h^{2n+3}}$, $C'_n=\frac{C_n}{h^{2n+4}}$ and $\tilde{C}'=\frac{\tilde{C}}{h^2}$. In order to find the stresses, we must solve the system of equations generated by (3.44) and (3.45)

$$\begin{cases}\alpha_{2n}(2n+1)(2n+2)A'_n & + & \beta_{2n-2}2n(2n-1)A'_{n-1} & = D_n^1,\\ \alpha_{2n}(2n+2)A'_n & + & \alpha_{2n-1}(2n-1)A'_{n-1} & = D_n^2,\end{cases} \tag{3.46}$$

where

$$D_n^1 = l_{2n} - (1-2\nu)\delta_0^{(n)}\tilde{C}' + 2(2-\nu)\omega_0^{(n)}\tilde{C}' + \sum_{k=0}^{\infty}\left[\alpha_{2k+2}(2k+2)\omega_k^{(n)} - \beta_{2k+1}(2k+3)\omega_{k+1}^{(n)}\right]C_k', \tag{3.47}$$

$$D_n^2 = m_{2n} - (1-2\nu)\left(\omega_0^{(n)} + \frac{(4n+1)}{2n(2n+1)}P_{2n}\right)\tilde{C}' - \sum_{k=0}^{\infty}\alpha_{2k+2}\left(\omega_{k+1}^{(n)} - \omega_k^{(n)}\right)C_k'. \tag{3.48}$$

Using matrix notation, this becomes

$$\begin{pmatrix} 2n(2n-1)\beta_{2n-2} & (2n+1)(2n+2)\alpha_{2n} \\ (2n-1)\alpha_{2n-1} & (2n+2)\alpha_{2n} \end{pmatrix}\begin{pmatrix} A_{n-1}' \\ A_n' \end{pmatrix} = \begin{pmatrix} D_n^1 \\ D_n^2 \end{pmatrix} \tag{3.49}$$

where the determinant is $\Delta_n = (2n-1)(2n+2)\alpha_{2n}(2n\beta_{2n-2} - (2n+1)\alpha_{2n-1})$. Using this we can find the solutions A_n' and A_{n-1}', which are given by

$$\begin{aligned} A_{n-1} &= \frac{(2n+2)\alpha_{2n}}{\Delta_n}\left(D_n^1 - (2n+1)D_n^2\right), \\ A_n &= \frac{(2n-1)}{\Delta_n}\left(-\alpha_{2n-1}D_n^1 + 2n\beta_{2n-2}D_n^2\right). \end{aligned} \tag{3.50}$$

This is equivalent to

$$
\begin{aligned}
A'_{n-1} = \frac{(2n+2)\alpha_{2n}}{\Delta_n}\Bigg[& l_{2n} - (2n+1)m_{2n} \\
& + \left[(2n+5-4\nu(n+1))\omega_0^{(n)} + (1-2\nu)\frac{(4n+1)}{2n}P_{2n}(0)\right]\tilde{C}' \\
& + \sum_{k=0}^{\infty}\Big[\alpha_{2k+2}(2k-2n+1)\omega_k^{(n)} + \big(\alpha_{2k+2}(2n+1) - \beta_{2k+1}(2k+3)\big)\omega_{k+1}^{(n)}\Big]C'_k\Bigg],
\end{aligned}
\tag{3.51}
$$

$$
\begin{aligned}
A'_n = \frac{(2n-1)}{\Delta_n}\Bigg[& -l_{2n}\alpha_{2n-1} + 2nm_{2n}\beta_{2n-2} \\
& + \Big[\alpha_{2n-1}\left((1-2\nu)\delta_0^{(n)} - 2(2-\nu)\omega_0^{(n)}\right) \\
& -2n\beta_{2n-2}(1-2\nu)\left(\omega_0^{(n)} + \frac{(4n+1)}{2n(2n+1)}P_{2n}(0)\right)\Big]\tilde{C}' \\
& + \sum_{k=0}^{\infty}\Big[\alpha_{2k+2}\big(2n\beta_{2n-2} - (2k+2)\alpha_{2n-1}\big)\omega_k^{(n)} \\
& + \big((2k+3)\alpha_{2n-1}\beta_{2k+1} - 2n\alpha_{2k+2}\beta_{2n-2}\big)\omega_{k+1}^{(n)}\Big]C'_k\Bigg].
\end{aligned}
\tag{3.52}
$$

Evaluating (3.51) at $(n+1)$, we find that

$$
\begin{aligned}
& \Bigg[\frac{\Delta_n}{2n-1}\alpha_{2n+2}\left((2n+7-4\nu(n+2))\omega_0^{(n+1)} + (1-2\nu)\frac{(4n+5)}{(2n+2)}P_{2n+2}(0)\right) \\
& - \frac{\Delta_{n+1}}{2n+4}\left(\alpha_{2n-1}\Big((1-2\nu)\delta_0^{(n)} - 2(2-\nu)\omega_0^{(n)}\Big) - 2n\beta_{2n-2}(1-2\nu)\left(\omega_0^{(n)} + \frac{(4n+1)}{2n(2n+1)}P_{2n}\right)\right)\Bigg]\tilde{C}' \\
& + \sum_{k=0}^{\infty}\Bigg[\frac{\Delta_n}{2n-1}\alpha_{2n+2}\Big[\alpha_{2k+2}(2k-2n-1)\omega_k^{(n+1)} + \big((2n+3)\alpha_{2k+2} - (2k+3)\beta_{2k+1}\big)\omega_{k+1}^{(n+1)}\Big] \\
& - \frac{\Delta_{n+1}}{2n+4}\Big[\alpha_{2k+2}\big(2n\beta_{2n-2} - (2k+2)\alpha_{2n-1}\big)\omega_k^{(n)} + \big((2k+3)\alpha_{2n-1}\beta_{2k+1} - 2n\alpha_{2k+2}\beta_{2n-2}\big)\omega_{k+1}^{(n)}\Big]\Bigg]C'_k \\
& = -\frac{\Delta_n}{2n-1}\alpha_{2n+2}\left(l_{2n+2} - (2n+3)m_{2n+2}\right) + \frac{\Delta_{n+1}}{2n+4}\left(l_{2n}\alpha_{2n-1} - 2nm_{2n}\beta_{2n-2}\right).
\end{aligned}
\tag{3.53}
$$

By truncating the infinite series in (3.53) at a finite order N, we get a linear system of equations for coefficients $\tilde{C}', C'_0, C'_1, \ldots, C'_N$. Once we have solved this system, we can obtain the solution to the displacements and stresses with the expressions (3.21) to (3.26).

3.3.3. Zero displacement

If we take $\boldsymbol{u} = 0$, then the change of variables given in (2.10), becomes

$$\begin{aligned} 2\mu v_r(r,\phi) &= -\left(\frac{1-2\nu}{2-2\nu}\right)\varrho g h^2 \cos^3\phi, \\ 2\mu v_\phi(r,\phi) &= \left(\frac{1-2\nu}{2-2\nu}\right)\varrho g h^2 \sin\phi\cos^2\phi. \end{aligned} \tag{3.54}$$

Due to linearity, it is natural to replace the boundary conditions on Γ_h by the simpler ones $2\mu v_r = -\cos^3\phi$ and $2\mu v_\phi = \sin\phi\cos^2\phi$, and once the problem is solved, the resulting solution must be multiplied by the constant $\left(\frac{1-2\nu}{2-2\nu}\right)\varrho g h^2$. If we write these conditions in terms of the Legendre basis, we obtain that

$$\begin{aligned} 2\mu v_r(r,\phi) &= -\frac{1}{5}(3P_1 + 2P_3) \\ &= \frac{3}{5}\sum_{n=0}^{\infty}\left(\omega_0^{(n)} - \omega_1^{(n)}\right)P_{2n}, \end{aligned} \tag{3.55}$$

$$\begin{aligned} 2\mu v_\phi(r,\phi) &= \sin\phi\frac{\mathrm{d}}{\mathrm{d}\phi}\frac{\cos^3\phi}{3} = \sin\phi\frac{\mathrm{d}}{\mathrm{d}\phi}\left(\frac{1}{5}(3P_1+2P_3)\right) \\ &= -\frac{\sin\phi}{5}\sum_{n=0}^{\infty}\left(\omega_0^{(n)} - \omega_1^{(n)}\right)P'_{2n}. \end{aligned} \tag{3.56}$$

Substituting (3.21) in (3.55),exchanging the summations, collecting the terms according to the order of Legendre polynomials and introducing a Kronecker delta, we arrive at

$$\begin{aligned} &\sum_{n=0}^{\infty}\Bigg(\Bigg[\frac{3}{5}\left(\omega_0^{(n)} - \omega_1^{(n)}\right) + \alpha_{2n}\frac{(2n+1)}{h^{2n+2}}\tilde{A}_n + \left(\frac{1-2\nu}{h}\delta_0^{(n)} - \frac{4(1-\nu)}{h}\omega_0^{(n)}\right)\tilde{B} \\ &- \sum_{k=0}^{\infty}\frac{(2k+1)P_{2k}(0)}{h^{2k+3}}\left((2k+2)\alpha_{2k+2}\omega_k^{(n)} - (2k+3)^2(2k+6-4\nu)\omega_{k+1}^{(n)}\right)\tilde{B}_k\Bigg]P_{2n} \\ &+ \frac{(2n+1)(2n+2)(2n+5-4\nu)}{h^{2n+2}}\tilde{A}_n P_{2n+2}\Bigg) = 0. \end{aligned} \tag{3.57}$$

By using the orthogonality of the basis $\{P_{2n}\}_{n=0}^{\infty}$ in the range $[-1,0]$, this condition becomes

$$\alpha_{2n}\frac{(2n+1)}{h^{2n+2}}\tilde{A}_n+\frac{2n(2n-1)(2n+3-4\nu)}{h^{2n}}\tilde{A}_{n-1}$$
$$-\sum_{k=0}^{\infty}\frac{(2k+1)P_{2k}(0)}{h^{2k+3}}\left((2k+2)\alpha_{2k+2}\omega_k^{(n)}-(2k+3)^2(2k+6-4\nu)\omega_{k+1}^{(n)}\right)\tilde{B}_k$$
$$+\left(\frac{1-2\nu}{h}\delta_0^{(n)}-\frac{4(1-\nu)}{h}\omega_0^{(n)}\right)\tilde{B}+\frac{3}{5}\left(\omega_0^{(n)}-\omega_1^{(n)}\right)=0. \quad (3.58)$$

In the same way as we did before, we substitute (3.56) in (3.22), yielding

$$\sum_{n=1}^{\infty}\left(\left[\frac{\alpha_{2n}}{h^{2n+2}}\tilde{A}_n+\left(\frac{(3-4\nu)}{h}\omega_0^{(n)}-\frac{(1-2\nu)(4n+1)P_{2n}(0)}{2n(2n+1)h}\right)\tilde{B}\right.\right.$$
$$+\sum_{k=0}^{\infty}\frac{(2k+1)P_{2k}(0)}{h^{2k+3}}\left((2k+3)(2k-1+4\nu)\omega_{k+1}^{(n)}-\alpha_{2k+2}\omega_k^{(n)}\right)\tilde{B}_k$$
$$\left.\left.-\frac{1}{5}\left(\omega_0^{(n)}-\omega_1^{(n)}\right)\right]\sin\phi P'_{2n}+\frac{(2n+1)(2n-2+4\nu)}{h^{2n+2}}\tilde{A}_n\sin\phi P'_{2n+2}\right)=0. \quad (3.59)$$

By using the orthogonality of the basis $\{\sin\phi P'_{2n}\}_{n=1}^{\infty}$ in the range $[-1,0]$, the second boundary condition becomes

$$\frac{\alpha_{2n}}{h^{2n+2}}\tilde{A}_n+\left(\frac{(3-4\nu)}{h}\omega_0^{(n)}-\frac{(1-2\nu)(4n+1)P_{2n}(0)}{2n(2n+1)h}\right)\tilde{B}$$
$$+\sum_{k=0}^{\infty}\frac{(2k+1)P_{2k}(0)}{h^{2k+3}}\left((2k+3)(2k-1+4\nu)\omega_{k+1}^{(n)}-\alpha_{2k+2}\omega_k^{(n)}\right)\tilde{B}_k$$
$$-\frac{1}{5}\left(\omega_0^{(n)}-\omega_1^{(n)}\right)+\frac{(2n-1)(2n-4+4\nu)}{h^{2n}}\tilde{A}_{n-1}=0. \quad (3.60)$$

Resolution by a system of equations: If we make the change of variables $A'_n=\frac{\tilde{A}_n}{h^{2n+2}}$, $C'_n=\frac{(2n+1)P_{2n}(0)\tilde{B}_n}{h^{2n+3}}$ and $\tilde{C}'=\frac{\tilde{B}}{h}$, then the system we must solve is

$$\begin{cases}\alpha_{2n}(2n+1)\tilde{A}'_n & + & 2n(2n-1)(2n+3-4\nu)\tilde{A}'_{n-1} & = D_n^1,\\ \alpha_{2n}\tilde{A}'_n & + & (2n-1)(2n-4+4\nu)\tilde{A}'_{n-1} & = D_n^2,\end{cases} \quad (3.61)$$

where

$$D_n^1 = \left(4(1-\nu)\omega_0^{(n)} - (1-2\nu)\delta_0^{(n)}\right)\tilde{C}' + \sum_{k=0}^{\infty}\Big((2k+2)\alpha_{2k+2}\omega_k^{(n)} - (2k+3)^2(2k+6-4\nu)\omega_{k+1}^{(n)}\Big)C_k' - \frac{3}{5}\left(\omega_0^{(n)} - \omega_1^{(n)}\right), \tag{3.62}$$

$$D_n^2 = -\left((3-4\nu)\omega_0^{(n)} - (1-2\nu)\frac{(4n+1)}{2n(2n+1)}P_{2n}(0)\right)\tilde{C}' + \sum_{k=0}^{\infty}\Big(\alpha_{2k+2}\omega_k^{(n)} - (2k+3)(2k-1+4\nu)\omega_{k+1}^{(n)}\Big)C_k' + \frac{1}{5}\left(\omega_0^{(n)} - \omega_1^{(n)}\right). \tag{3.63}$$

Using matrix notation, this becomes

$$\begin{pmatrix} 2n(2n-1)(2n+3-4\nu) & (2n+1)\alpha_{2n} \\ (2n-1)(2n-4+4\nu) & \alpha_{2n} \end{pmatrix}\begin{pmatrix} A_{n-1}' \\ A_n' \end{pmatrix} = \begin{pmatrix} D_n^1 \\ D_n^2 \end{pmatrix}, \tag{3.64}$$

where the determinant is $\Delta_n = 4\alpha_{2n}(2n-1)((3-4\nu)n+1-\nu)$. The solutions A_n' and A_{n-1}' are

$$A_{n-1}' = \frac{\alpha_{2n}}{\Delta_n}\Bigg(\frac{2(n+2)}{5}\left(\omega_1^{(n)} - \omega_0^{(n)}\right) + \Big[(2(3-4\nu)n+7-8\nu)\omega_0^{(n)} + (1-2\nu)\frac{(4n+1)}{2n}P_{2n}(0)\Big]\tilde{C}' + \sum_{k=0}^{\infty}\Big[(2k-2n+1)\alpha_{2k+2}\omega_k^{(n)} + (2k+3)\big((2n+1)(2k-1+4\nu) - (2k+3)(2k+6-4\nu)\big)\omega_{k+1}^{(n)}\Big]C_k'\Bigg), \tag{3.65}$$

$$A'_n = -\frac{(2n-1)}{\Delta_n}\Bigg(\frac{4}{5}(n(n+3-2\nu)-3(1-\nu))\left(\omega_1^{(n)}-\omega_0^{(n)}\right)$$
$$-\Bigg[(1-2\nu)\left((2n-4+4\nu)\delta_0^{(n)}+(2n+3-4\nu)\frac{(4n+1)}{(2n+1)}P_{2n}(0)\right)$$
$$-2(2n-1)\big((3-4\nu)n+8(1-\nu)^2\big)\omega_0^{(n)}\Bigg]\tilde{C}'$$
$$+\sum_{k=0}^{\infty}\Big[-\big(2n(2n-2k+1-4\nu)+8(k+1)(1-\nu)\big)\alpha_{2k+2}\omega_k^{(n)}$$
$$+2(2n-2k-3)(2k+3)\big(n(2k-1+4\nu)-4(k+3-2\nu)(1-\nu)\big)\omega_{k+1}^{(n)}\Big]C'_k\Bigg). \quad (3.66)$$

We evaluate (3.65) at $(n+1)$ and obtain

$$\alpha_{2n+2}\Delta_n\Bigg(\frac{2(n+3)}{5}\left(\omega_1^{(n+1)}-\omega_0^{(n+1)}\right)+\Big[(2(3-4\nu)(n+1)+7-8\nu)\omega_0^{(n+1)}$$
$$+(1-2\nu)\frac{(4n+5)}{(2n+2)}P_{2n+2}(0)\Big]\tilde{C}'+\sum_{k=0}^{\infty}\Big[(2k-2n-1)\alpha_{2k+2}\omega_k^{(n+1)}$$
$$+(2k+3)\big((2n+3)(2k-1+4\nu)-(2k+3)(2k+6-4\nu)\big)\omega_{k+1}^{(n+1)}\Big]C'_k\Bigg)$$
$$+(2n-1)\Delta_{n+1}\Bigg(\frac{4}{5}(n(n+3-2\nu)-3(1-\nu))\left(\omega_1^{(n)}-\omega_0^{(n)}\right)$$
$$-\Bigg[(1-2\nu)\left((2n-4+4\nu)\delta_0^{(n)}+(2n+3-4\nu)\frac{(4n+1)}{(2n+1)}P_{2n}(0)\right)$$
$$-2(2n-1)\big((3-4\nu)n+8(1-\nu)^2\big)\omega_0^{(n)}\Bigg]\tilde{C}'$$
$$+\sum_{k=0}^{\infty}\Big[2(2n-2k-3)(2k+3)\big(n(2k-1+4\nu)-4(k+3-2\nu)(1-\nu)\big)\omega_{k+1}^{(n)}$$
$$-\big(2n(2n-2k+1-4\nu)+8(k+1)(1-\nu)\big)\alpha_{2k+2}\omega_k^{(n)}\Big]C'_k\Bigg)=0. \quad (3.67)$$

By truncating the infinite series in (3.67) at a finite order N, we get a linear system of equations for coefficients $\tilde{C}', C'_0, C'_1, \ldots, C'_N$. Once we have solved this system, we can obtain the solution to the displacements and stresses with the expressions (3.21) to (3.26).

3.3.4. Prescribed displacements

In this case we use as boundary conditions $2\mu \boldsymbol{v}_r = g_1(\cos\phi)$ and $2\mu \boldsymbol{v}_\phi = g_2(\cos\phi)$. We decompose these functions in terms of the basis of Legendre polynomials as we did before in Section 3.3.2. Then, the first boundary condition is given by

$$\sum_{n=0}^{\infty}\Bigg(\Bigg[l_{2n}+\alpha_{2n}\frac{(2n+1)}{h^{2n+2}}\tilde{A}_n+\left(\frac{1-2\nu}{h}\delta_0^{(n)}-\frac{4(1-\nu)}{h}\omega_0^{(n)}\right)\tilde{B}$$
$$-\sum_{k=0}^{\infty}\frac{(2k+1)P_{2k}(0)}{h^{2k+3}}\left((2k+2)\alpha_{2k+2}\omega_k^{(n)}-(2k+3)^2(2k+6-4\nu)\omega_{k+1}^{(n)}\right)\tilde{B}_k\Bigg]P_{2n}$$
$$+\frac{(2n+1)(2n+2)(2n+5-4\nu)}{h^{2n+2}}\tilde{A}_nP_{2n+2}\Bigg)=0. \tag{3.68}$$

The use of the orthogonality of the basis $\{P_{2n}\}_{n=0}^{\infty}$ in the range $[-1,0]$, turns this condition in

$$l_{2n}+\left(\frac{1-2\nu}{h}\delta_0^{(n)}-\frac{4(1-\nu)}{h}\omega_0^{(n)}\right)\tilde{B}+\frac{2n(2n-1)(2n+3-4\nu)}{h^{2n}}\tilde{A}_{n-1}+\frac{(2n+1)\alpha_{2n}}{h^{2n+2}}\tilde{A}_n$$
$$+\sum_{k=0}^{\infty}\left((2k+3)^2(2k+6-4\nu)\omega_{k+1}^{(n)}-(2k+2)\alpha_{2k+2}\omega_k^{(n)}\right)\frac{(2k+1)}{h^{2k+3}}P_{2k}(0)\tilde{B}_k=0. \tag{3.69}$$

Now we use the condition for v_ϕ, which gives us

$$\sum_{n=1}^{\infty}\Bigg(\Bigg[m_{2n}+\frac{\alpha_{2n}}{h^{2n+2}}\tilde{A}_n+\left(\frac{(3-4\nu)}{h}\omega_0^{(n)}-\frac{(1-2\nu)(4n+1)P_{2n}(0)}{2n(2n+1)h}\right)\tilde{B}$$
$$+\sum_{k=0}^{\infty}\left(\frac{(2k+1)P_{2k}(0)}{h^{2k+3}}\left((2k+3)(2k-1+4\nu)\omega_{k+1}^{(n)}-\alpha_{2k+2}\omega_k^{(n)}\right)\tilde{B}_k\right)\Bigg]\sin\phi P_{2n}'$$
$$+\frac{(2n+1)(2n-2+4\nu)}{h^{2n+2}}\tilde{A}_n\sin\phi P_{2n+2}'\Bigg)=0. \tag{3.70}$$

Using the orthogonality of the basis $\{\sin\phi P'_{2n}(\cos\phi)\}_{n=0}^{\infty}$ in $[-1,0]$, gives us

$$\frac{\alpha_{2n}}{h^{2n+2}}\tilde{A}_n+\frac{(2n-1)(2n-4+4\nu)}{h^{2n}}\tilde{A}_{n-1}+\left(\frac{(3-4\nu)}{h}\omega_0^{(n)}-\frac{(1-2\nu)(4n+1)P_{2n}(0)}{2n(2n+1)h}\right)\tilde{B}$$
$$+\sum_{k=0}^{\infty}\left(\frac{(2k+1)P_{2k}(0)}{h^{2k+3}}\left((2k+3)(2k-1+4\nu)\omega_{k+1}^{(n)}-\alpha_{2k+2}\omega_k^{(n)}\right)\tilde{B}_k+m_{2n}\right)=0. \tag{3.71}$$

Resolution by a system of equations: We make the change of variables $A'_n=\frac{\tilde{A}_n}{h^{2n+2}}$, $C'_n=\frac{(2n+1)P_{2n}(0)\tilde{B}_n}{h^{2n+3}}$ and $\tilde{C}'=\frac{\tilde{B}}{h}$, which gives us

$$\begin{cases} \alpha_{2n}(2n+1)\tilde{A}'_n & + & 2n(2n-1)(2n+3-4\nu)\tilde{A}'_{n-1} & = D_n^1, \\ \alpha_{2n}\tilde{A}'_n & + & (2n-1)(2n-4+4\nu)\tilde{A}'_{n-1} & = D_n^2, \end{cases} \tag{3.72}$$

where

$$D_n^1=\left(4(1-\nu)\omega_0^{(n)}-(1-2\nu)\delta_0^{(n)}\right)\tilde{C}'-l_{2n}$$
$$-\sum_{k=0}^{\infty}\left((2k+3)^2(2k+6-4\nu)\omega_{k+1}^{(n)}-(2k+2)\alpha_{2k+2}\omega_k^{(n)}\right)\tilde{C}'_k, \tag{3.73}$$
$$D_n^2=-\left((3-4\nu)\omega_0^{(n)}-(1-2\nu)\frac{(4n+1)}{2n(2n+1)}P_{2n}(0)\right)\tilde{C}'-m_{2n}$$
$$+\sum_{k=0}^{\infty}\left(\alpha_{2k+2}\omega_k^{(n)}-(2k+3)(2k-1+4\nu)\omega_{k+1}^{(n)}\right)\tilde{C}'_k. \tag{3.74}$$

By writing this in matrix form, we have

$$\begin{pmatrix} 2n(2n-1)(2n+3-4\nu) & (2n+1)\alpha_{2n} \\ (2n-1)(2n-4+4\nu) & \alpha_{2n} \end{pmatrix}\begin{pmatrix} A'_{n-1} \\ A'_n \end{pmatrix}=\begin{pmatrix} D_n^1 \\ D_n^2 \end{pmatrix}, \tag{3.75}$$

where the determinant is $\Delta_n = 4\alpha_{2n}(2n-1)((3-4\nu)n+1-\nu)$. Using this we find the solutions A'_n and A'_{n-1}, which are given by

$$\begin{aligned}
A'_{n-1} = \frac{\alpha_{2n}}{\Delta_n}\Bigg(& (2n+1)m_{2n} - l_{2n} \\
& + \left[(2(3-4\nu)n+7-8\nu)\omega_0^{(n)} - (1-2\nu)\frac{(4n+1)}{2n}P_{2n}(0)\right]\tilde{C}' \\
& + \sum_{k=0}^{\infty}\Big[(2k-2n+1)\alpha_{2k+2}\omega_k^{(n)} \\
& + (2k+3)\big((2n+1)(2k-1+4\nu) - (2k+3)(2k+6-4\nu)\big)\omega_{k+1}^{(n)}\Big]C'_k\Bigg), \qquad (3.76)
\end{aligned}$$

$$\begin{aligned}
A'_n = -\frac{(2n-1)}{\Delta_n}\Bigg(& 2n(2n+3-4\nu)m_{2n} - 2(n+2\nu-2)l_{2n} \\
& - \Bigg[(1-2\nu)\left((2n-4+4\nu)\delta_0^{(n)} + (2n+3-4\nu)\frac{(4n+1)}{(2n+1)}P_{2n}(0)\right) \\
& -2(2n-1)\big((3-4\nu)n + 8(1-\nu)^2\big)\omega_0^{(n)}\Bigg]\tilde{C}' \\
& + \sum_{k=0}^{\infty}\Big[-\big(2n(2n-2k+1-4\nu) + 8(k+1)(1-\nu)\big)\alpha_{2k+2}\omega_k^{(n)} \\
& +2(2n-2k-3)(2k+3)\big(n(2k-1+4\nu) - 4(k+3-2\nu)(1-\nu)\big)\omega_{k+1}^{(n)}\Big]C'_k\Bigg). \qquad (3.77)
\end{aligned}$$

Finally, we evaluate (3.76) at $(n+1)$ and obtain

$$\begin{aligned}
&\alpha_{2n+2}\Delta_n\Bigg((2n+3)m_{2n+2}-l_{2n+2}+\Big[(2(3-4\nu)(n+1)+7-8\nu)\omega_0^{(n+1)}\\
&-(1-2\nu)\frac{(4n+5)}{(2n+2)}P_{2n+2}(0)\Big]\tilde{C}'+\sum_{k=0}^{\infty}\Big[(2k-2n-1)\alpha_{2k+2}\omega_k^{(n+1)}\\
&+(2k+3)\big((2n+3)(2k-1+4\nu)-(2k+3)(2k+6-4\nu)\big)\omega_{k+1}^{(n+1)}\Big]C_k'\Bigg)\\
&+(2n-1)\Delta_{n+1}\Bigg(-2(n+2\nu-2)l_{2n}+2n(2n+3-4\nu)m_{2n}\\
&-\Bigg[(1-2\nu)\left((2n-4+4\nu)\delta_0^{(n)}+(2n+3-4\nu)\frac{(4n+1)}{(2n+1)}P_{2n}(0)\right)\\
&-2(2n-1)\big((3-4\nu)n+8(1-\nu)^2\big)\omega_0^{(n)}\Big]\tilde{C}'\\
&+\sum_{k=0}^{\infty}\Big[2(2n-2k-3)(2k+3)\big(n(2k-1+4\nu)-4(k+3-2\nu)(1-\nu)\big)\omega_{k+1}^{(n)}\\
&-\big(2n(2n-2k+1-4\nu)+8(k+1)(1-\nu)\big)\alpha_{2k+2}\omega_k^{(n)}\Big]C_k'\Bigg)=0. \qquad (3.78)
\end{aligned}$$

By truncating the infinite series in (3.78) at a finite order N, we get a linear system of equations for coefficients $\tilde{C}', C_0', C_1', \ldots, C_N'$. Once we have solved this system, we can obtain the solution to the displacements and stresses with the expressions (3.21) to (3.26).

3.4. Accelerating the convergence of series

In each of the above cases (for the stresses see (3.42), (3.53) and for the displacements see (3.67), (3.78)), after we have truncated the series at a finite order N, we get a system of $N+2$ equations and $N+2$ unknows for the coefficients C_k', which can be solved by some standard procedure to that purpose. To determine the stress values (and the displacement values), it is necessary to find the values of coefficients A_n', but these series have a slow convergence. To overcome this difficulty, we use the technique of transformation of Kummer for series (see (Abramowitz & Stegun, 1965)), *i.e.*, we obtain and calculate

numerically the dominant asymptotic term for (3.40) (respectively for (3.51), (3.65) and (3.76)). The values of these key terms are used to estimate the value of the series for A'_n, by subtracting the asymptotic term in order to accelerate convergence, and once we have the value of the series, we must add the value of the asymptotic term. To do this, we write the term A_{n-1} in the following way

$$A_{n-1} = F_n + \sum_{k=-1}^{\infty} G_n^{(k)} C_k, \tag{3.79}$$

where F_n and $G_n^{(k)}$ will depend on the case under consideration. We define s to be the contribution to the general solution given by the terms that multiply the coefficients A_n, that is,

$$s = \sum_{n=1}^{\infty} A_{n-1} s_{n-1}. \tag{3.80}$$

Using the decomposition of A_{n-1}, we can isolate the three contributions

$$\begin{aligned} s &= \sum_{n=1}^{\infty} \left[F_n + \sum_{k=-1}^{\infty} G_n^{(k)} C_k \right] s_{n-1} \\ &= \sum_{n=1}^{\infty} F_n s_{n-1} + \sum_{k=-1}^{\infty} \sum_{n=1}^{\infty} \left[G_n^{(k)} s_{n-1} \right] C_k \\ &= \sum_{n=1}^{\infty} F_n s_{n-1} + \sum_{n=1}^{\infty} \left[G_n^{(-1)} s_{n-1} \right] \tilde{C}' + \sum_{k=0}^{\infty} \sum_{n=1}^{\infty} \left[G_n^{(k)} s_{n-1} \right] C_k \\ &= F + Q_{-1} + \sum_{k=0}^{\infty} Q_k, \end{aligned} \tag{3.81}$$

where the terms s_{n-1} depend on the stresses (or displacements) that we are considering. We review the terms of the stresses given in (3.21)-(3.26) and evaluated in $n = n - 1$. For the sake of convenience we use the dimensionless parameter h/r instead $1/r$ in these equations. Thus we have

$$s_{n-1}(v_r) = (2n-1) \left(\frac{h}{r} \right)^{2n} \big(- ((2n-1)^2 - 2 + 2\nu) P_{2n-2} - 2n(2n+3-4\nu) P_{2n} \big), \tag{3.82}$$

$$s_{n-1}(v_\phi) = -\sin\phi \left(\frac{h}{r}\right)^{2n} \left(((2n-1)^2 - 2 + 2\nu)P'_{2n-2} + (2n-1)(2n-4+4\nu)P'_{2n}\right), \tag{3.83}$$

$$s_{n-1}(\sigma_r) = 2n(2n-1)\left(\frac{h}{r}\right)^{2n+1} \left(((2n-1)^2 - 2 + 2\nu)P_{2n-2} + (2n(2n+3) - 2\nu)P_{2n}\right), \tag{3.84}$$

$$\begin{aligned} s_{n-1}(\sigma_\phi) = \left(\frac{h}{r}\right)^{2n+1} \Big((4n-1)(2n+2\nu-3)P'_{2n-1} \\ - 2n(2n-1)(((2n-1)^2 - 2 + 2\nu)P_{2n-2} + (4n^2 - 6n + 3 - 2\nu)P_{2n})\Big), \end{aligned} \tag{3.85}$$

$$s_{n-1}(\sigma_\theta) = -(4n-1)\left(\frac{h}{r}\right)^{2n+1} \left(2n(2n-1)(1-2\nu)P_{2n} + (2n-3+2\nu)P'_{2n-1}\right), \tag{3.86}$$

$$s_{n-1}(\sigma_{r\phi}) = \sin\phi \left(\frac{h}{r}\right)^{2n+1} \left(2n((2n-1)^2 - 2 + 2\nu)P'_{2n-2} + (2n-1)(2n(2n+3) - 2\nu)P'_{2n}\right). \tag{3.87}$$

3.4.1. Asymptotic behaviour of Legendre's polynomials

For large n, the following asymptotic behaviour holds (see (Abramowitz & Stegun, 1965))

$$P_n(\cos\phi) = \frac{\Gamma(n+1)}{\Gamma\left(n+\frac{3}{2}\right)} \left(\frac{1}{2}\pi\sin\phi\right)^{-\frac{1}{2}} \cos\left[\left(n+\frac{1}{2}\right)\phi - \frac{\pi}{4}\right]. \tag{3.88}$$

We use one of the classical properties for the gamma function, namely

$$\Gamma\left(n+\frac{3}{2}\right) = \Gamma\left(\left(n+\frac{1}{2}\right)+1\right) = \left(n+\frac{1}{2}\right)\Gamma\left(n+\frac{1}{2}\right) = \left(n+\frac{1}{2}\right)\frac{\sqrt{\pi}}{2^{2n-1}}\frac{(2n)!}{n!}. \tag{3.89}$$

With this, (3.88) becomes

$$P_n(\cos\phi) = \frac{2^{2n-1}(n!)^2}{\left(n+\frac{1}{2}\right)\sqrt{\pi}(2n)!} \left(\frac{1}{2}\pi\sin\phi\right)^{-\frac{1}{2}} \cos\left[\left(n+\frac{1}{2}\right)\phi - \frac{\pi}{4}\right]. \tag{3.90}$$

We use the Stirling formula, in order to approximate the factorials of high order, this gives us

$$\frac{(n!)^2}{(2n)!} = \frac{\left(\sqrt{2\pi n}\left(\frac{n}{e}\right)^n\right)^2\left(1+\frac{1}{12n}\right)^2}{\sqrt{4\pi n}\left(\frac{2n}{e}\right)^{2n}\left(1+\frac{1}{24n}\right)} = \sqrt{\pi n}2^{-2n}\left(1+\frac{1}{8n}+\frac{1}{576n^2}-\ldots\right). \tag{3.91}$$

If we only keep the dominant term, then we have for a larger n the following expression

$$P_n(\cos\phi) \approx \sqrt{\frac{2}{n\pi\sin\phi}}\cos\left[\left(n+\frac{1}{2}\right)\phi-\frac{\pi}{4}\right]. \tag{3.92}$$

If we calculate $\mathrm{d}P_n(x)/\mathrm{d}x$ in (3.92), then we obtain for the derivatives of the Legendre polynomials the following expression

$$\begin{aligned} P_n'(\cos\phi) = &\frac{\cos\phi}{\sin^2\phi\sqrt{2n\pi\sin\phi}}\cos\left[\left(n+\frac{1}{2}\right)\phi-\frac{\pi}{4}\right] \\ &+\sqrt{\frac{2}{n\pi\sin\phi}}\left(n+\frac{1}{2}\right)\frac{1}{\sin\phi}\sin\left[\left(n+\frac{1}{2}\right)\phi-\frac{\pi}{4}\right]. \end{aligned} \tag{3.93}$$

Then, for large n we arrive at

$$P_n'(\cos\phi) \approx \sqrt{\frac{2n}{\pi\sin\phi}}\frac{1}{\sin\phi}\cos\left[\left(n+\frac{1}{2}\right)\phi-\frac{3\pi}{4}\right]. \tag{3.94}$$

Using again Stirling's formula, it is easy to see that for larger n we have

$$P_{2n}(0) = (-1)^n\frac{1}{\sqrt{\pi n}}. \tag{3.95}$$

In the case we need to consider the approximation to second order for the Legendre polynomials, we use

$$\begin{aligned} P_n(\cos\phi) \approx &\sqrt{\frac{2}{n\pi\sin\phi}}\left[\left(1-\frac{3}{8n}\right)\cos\left[\left(n+\frac{1}{2}\right)\phi-\frac{\pi}{4}\right]\right. \\ &\left.+\frac{1}{8n}\frac{1}{\sin\phi}\cos\left[\left(n+\frac{3}{2}\right)\phi-\frac{3\pi}{4}\right]\right], \end{aligned} \tag{3.96}$$

$$P_n'(\cos\phi) \approx \sqrt{\frac{2}{n\pi\sin^3\phi}}\Bigg[-n\cos\left[\left(n+\frac{1}{2}\right)\phi+\frac{\pi}{4}\right] - \frac{1}{8}\cos\left[\left(n+\frac{1}{2}\right)\phi+\frac{\pi}{4}\right]$$
$$+\frac{1}{8\sin\phi}\cos\left[\left(n+\frac{3}{2}\right)\phi-\frac{\pi}{4}\right] + \frac{1}{2}\frac{\cos\phi}{\sin\phi}\cos\left[\left(n+\frac{1}{2}\right)\phi-\frac{\pi}{4}\right]$$
$$+\frac{1}{n}\left(\frac{3}{16}\cos\left[\left(n+\frac{1}{2}\right)\phi+\frac{\pi}{4}\right] - \frac{1}{8}\frac{\cos\phi}{\sin^2\phi}\cos\left[\left(n+\frac{3}{2}\right)\phi+\frac{\pi}{4}\right]\right.$$
$$\left. -\frac{3}{16}\frac{1}{\sin\phi}\cos\left[\left(n+\frac{3}{2}\right)\phi-\frac{\pi}{4}\right]\right)$$
$$-\frac{1}{16}\frac{\cos\phi}{n\sin\phi}\left(3\cos\left[\left(n+\frac{1}{2}\right)\phi-\frac{\pi}{4}\right]+\frac{1}{\sin\phi}\cos\left[\left(n+\frac{3}{2}\right)\phi+\frac{\pi}{4}\right]\right)\Bigg]. \quad (3.97)$$

This second order approximation in the case $\phi = \pi/2$ gives us

$$P_{2n}(0) \approx \frac{(-1)^n}{\sqrt{n\pi}}\left(1-\frac{1}{8n}\right). \quad (3.98)$$

These approximations are valid for $\phi \neq \pi$. In the case $\phi = \pi$, we have that

$$P_n(\cos\pi) = (-1)^n, \qquad \text{y} \qquad P_n'(\cos\pi) = -\frac{(-1)^n}{2}n(n+1). \quad (3.99)$$

Using (3.92) and (3.94), we obtain the following asymptotic behaviour of the terms s_{n-1} in each case of interest

$$s_{n-1}(v_r) = -\frac{(2n)^3}{\sqrt{n\pi\sin\phi}}\left(\frac{h}{r}\right)^{2n}\left[\cos\left(\left(2n-\frac{3}{2}\right)\phi-\frac{\pi}{4}\right)+\cos\left(\left(2n+\frac{1}{2}\right)\phi-\frac{\pi}{4}\right)\right]$$
$$= \frac{(2n)^3}{\sqrt{n\pi\sin\phi}}\left(\frac{h}{r}\right)^{2n}\mathfrak{Re}\left(\frac{i-1}{\sqrt{2}}\left(e^{-\frac{3}{2}i\phi}+e^{\frac{i}{2}\phi}\right)e^{2in\phi}\right), \quad (3.100)$$
$$s_{n-1}(v_\phi) = \frac{(2n)^3}{\sqrt{n\pi\sin\phi}}\left(\frac{h}{r}\right)^{2n}\left[\cos\left(\left(2n-\frac{3}{2}\right)\phi+\frac{\pi}{4}\right)+\cos\left(\left(2n+\frac{1}{2}\right)\phi+\frac{\pi}{4}\right)\right]$$
$$= \frac{(2n)^3}{\sqrt{n\pi\sin\phi}}\left(\frac{h}{r}\right)^{2n}\mathfrak{Re}\left(\frac{1+i}{\sqrt{2}}\left(e^{-\frac{3}{2}i\phi}+e^{\frac{i}{2}\phi}\right)e^{2in\phi}\right), \quad (3.101)$$
$$s_{n-1}(\sigma_r) = \frac{(2n)^4}{\sqrt{n\pi\sin\phi}}\left(\frac{h}{r}\right)^{2n+1}\left[\cos\left(\left(2n-\frac{3}{2}\right)\phi-\frac{\pi}{4}\right)+\cos\left(\left(2n+\frac{1}{2}\right)\phi-\frac{\pi}{4}\right)\right]$$
$$= \frac{(2n)^4}{\sqrt{n\pi\sin\phi}}\left(\frac{h}{r}\right)^{2n+1}\mathfrak{Re}\left(\frac{1-i}{\sqrt{2}}\left(e^{-\frac{3}{2}i\phi}+e^{\frac{i}{2}\phi}\right)e^{2in\phi}\right), \quad (3.102)$$

$$s_{n-1}(\sigma_\phi) = \frac{-(2n)^4}{\sqrt{n\pi\sin\phi}}\left(\frac{h}{r}\right)^{2n+1}\left[\cos\left(\left(2n-\frac{3}{2}\right)\phi-\frac{\pi}{4}\right)+\cos\left(\left(2n+\frac{1}{2}\right)\phi-\frac{\pi}{4}\right)\right]$$
$$= \frac{(2n)^4}{\sqrt{n\pi\sin\phi}}\left(\frac{h}{r}\right)^{2n+1}\mathfrak{Re}\left(\frac{i-1}{\sqrt{2}}\left(e^{-\frac{3}{2}i\phi}+e^{\frac{i}{2}\phi}\right)e^{2in\phi}\right), \tag{3.103}$$

$$s_{n-1}(\sigma_\theta) = \frac{-2(2n)^3}{\sqrt{n\pi\sin\phi}}\left(\frac{h}{r}\right)^{2n+1}\left[(1-2\nu)\cos\left(\left(2n+\frac{1}{2}\right)\phi-\frac{\pi}{4}\right)\right.$$
$$\left.+\frac{1}{\sin\phi}\cos\left(\left(2n+\frac{1}{2}\right)\phi-\frac{3\pi}{4}\right)\right], \tag{3.104}$$

$$s_{n-1}(\sigma_{r\phi}) = \frac{(2n)^4}{\sqrt{n\pi\sin\phi}}\left(\frac{h}{r}\right)^{2n+1}\left[\cos\left(\left(2n-\frac{3}{2}\right)\phi-\frac{3\pi}{4}\right)+\cos\left(\left(2n+\frac{1}{2}\right)\phi-\frac{3\pi}{4}\right)\right]$$
$$= \frac{(2n)^4}{\sqrt{n\pi\sin\phi}}\left(\frac{h}{r}\right)^{2n+1}\mathfrak{Re}\left(-\frac{1+i}{\sqrt{2}}\left(e^{-\frac{3}{2}i\phi}+e^{\frac{i}{2}\phi}\right)e^{2in\phi}\right). \tag{3.105}$$

In the case of $\phi = \pi$, this becomes

$$s_{n-1}(v_r) = -16n^3\left(\frac{h}{r}\right)^{2n}, \tag{3.106}$$

$$s_{n-1}(v_\phi) = 0, \tag{3.107}$$

$$s_{n-1}(\sigma_r) = 32n^4\left(\frac{h}{r}\right)^{2n+1}, \tag{3.108}$$

$$s_{n-1}(\sigma_\phi) = -(2n)^4\left(\frac{h}{r}\right)^{2n+1}, \tag{3.109}$$

$$s_{n-1}(\sigma_\theta) = -(2n)^4\left(\frac{h}{r}\right)^{2n+1}, \tag{3.110}$$

$$s_{n-1}(\sigma_{r\phi}) = 0. \tag{3.111}$$

We just need to find the value of F_n and $G_n^{(k)}$ to calculate the value of the coefficients.

3.4.2. Traction-free boundary and loaded boundary

We write the term A_{n-1} from the equation (3.40) and (3.51) in the following way:

$$A_{n-1} = F_n + \sum_{k=-1}^{\infty} G_n^{(k)} C_k, \tag{3.112}$$

where we have two possible expressions for F_n depending on whether it is free or loaded boundary

$$F_n = \frac{(2n+2)\alpha_{2n}}{\Delta_n}\left[\frac{(2n+4-(4n+3)\nu)\omega_0^{(n)}}{5(1-\nu)} - \frac{(1-2\nu)(2n+4)\omega_1^{(n)}}{5(1-\nu)}\right], \quad (3.113)$$

$$\text{or } F_n = \frac{(2n+2)\alpha_{2n}}{\Delta_n}\left[l_{2n} - (2n+1)m_{2n}\right], \quad (3.114)$$

$$G_n^{(-1)} = \frac{(2n+2)\alpha_{2n}}{\Delta_n}\left[(2n+5-4\nu(n+1))\omega_0^{(n)} + (1-2\nu)\frac{(4n+1)}{2n}P_{2n}(0)\right], \quad (3.115)$$

$$G_n^{(k)} = \frac{(2n+2)\alpha_{2n}}{\Delta_n}\Big[(2k-2n+1)\alpha_{2k+2}\omega_k^{(n)} + \big((2n+1)\alpha_{2k+2} - (2k+3)\beta_{2k+1}\big)\omega_{k+1}^{(n)}\Big]. \quad (3.116)$$

Then we have to calculate three different sums in the case of traction-free boundary, the first one involves the free term (F_n) and the other two (which we also use in the case of loaded boundary) are

$$Q_{-1} = \sum_{n=1}^{\infty}\left[G_n^{(-1)}s_{n-1}\right]\tilde{C} \qquad \text{and} \qquad Q_k = \sum_{n=1}^{\infty} G_n^{(k)}s_{n-1}C_k \quad k = 0, 1, \ldots \quad (3.117)$$

We need to find the asymptotic behaviour of the series, so we must find the dominant term in each case, i.e.,

$$F_n \approx \frac{-\nu}{(1-\nu)}\frac{1}{16n^4}\frac{(-1)^n}{\sqrt{\pi n}}, \quad (3.118)$$

$$G_n^{(-1)} \approx -\frac{1}{8}\frac{(2-\nu)}{n^4}\frac{(-1)^n}{\sqrt{\pi n}}, \quad (3.119)$$

$$G_n^{(k)} \approx \frac{1}{8}\frac{(4k+5)(2k+4-\nu)}{n^4}\frac{(-1)^n}{\sqrt{\pi n}}. \quad (3.120)$$

We use the following sums

$$\sum_{n=1}^{\infty}(-1)^n n\left(\frac{h}{r}\right)^{2n+1}e^{2in\phi}=-\left(\frac{h}{r}\right)^{3}e^{2i\phi}\frac{1}{\left(1+\left(\frac{h}{r}\right)^{2}e^{2i\phi}\right)^{2}}, \tag{3.121}$$

$$\sum_{n=1}^{\infty}(-1)^n \left(\frac{h}{r}\right)^{2n+1}e^{2in\phi}=-\left(\frac{h}{r}\right)^{3}e^{2i\phi}\frac{1}{1+\left(\frac{h}{r}\right)^{2}e^{2i\phi}}, \tag{3.122}$$

$$\sum_{n=1}^{\infty}\frac{(-1)^n}{n}\left(\frac{h}{r}\right)^{2n+1}e^{2in\phi}=-\left(\frac{h}{r}\right)\ln\left(1+\left(\frac{h}{r}\right)^{2}e^{2i\phi}\right). \tag{3.123}$$

Then, the terms that we need include in the sums $\phi<\pi$ are

$$F(\sigma_r)=\mathfrak{Re}\left(\frac{\nu}{(1-\nu)}\frac{1}{\pi\sqrt{\sin\phi}}\frac{(1-i)}{\sqrt{2}}\left(\frac{h}{r}\right)\left(e^{-\frac{3}{2}i\phi}+e^{\frac{i}{2}\phi}\right)\ln\left(1+\left(\frac{h}{r}\right)^{2}e^{2i\phi}\right)\right)\tilde{C}', \tag{3.124}$$

$$F(\sigma_\phi)=\mathfrak{Re}\left(\frac{\nu}{(1-\nu)}\frac{1}{\pi\sqrt{\sin\phi}}\frac{(i-1)}{\sqrt{2}}\left(\frac{h}{r}\right)\left(e^{-\frac{3}{2}i\phi}+e^{\frac{i}{2}\phi}\right)\ln\left(1+\left(\frac{h}{r}\right)^{2}e^{2i\phi}\right)\right)\tilde{C}', \tag{3.125}$$

$$F(\sigma_{r\phi})=\mathfrak{Re}\left(\frac{-\nu}{(1-\nu)}\frac{1}{\pi\sqrt{\sin\phi}}\frac{(i+1)}{\sqrt{2}}\left(\frac{h}{r}\right)\left(e^{-\frac{3}{2}i\phi}+e^{\frac{i}{2}\phi}\right)\ln\left(1+\left(\frac{h}{r}\right)^{2}e^{2i\phi}\right)\right)\tilde{C}', \tag{3.126}$$

$$Q_{-1}(\sigma_r)=\mathfrak{Re}\left(\frac{(2-\nu)}{\pi\sqrt{\sin\phi}}(1-i)\sqrt{2}\left(\frac{h}{r}\right)\left(e^{-\frac{3}{2}i\phi}+e^{\frac{i}{2}\phi}\right)\ln\left(1+\left(\frac{h}{r}\right)^{2}e^{2i\phi}\right)\right)\tilde{C}', \tag{3.127}$$

$$Q_{-1}(\sigma_\phi)=\mathfrak{Re}\left(\frac{(2-\nu)}{\pi\sqrt{\sin\phi}}(i-1)\sqrt{2}\left(\frac{h}{r}\right)\left(e^{-\frac{3}{2}i\phi}+e^{\frac{i}{2}\phi}\right)\ln\left(1+\left(\frac{h}{r}\right)^{2}e^{2i\phi}\right)\right)\tilde{C}', \tag{3.128}$$

$$Q_{-1}(\sigma_{r\phi})=\mathfrak{Re}\left(-\frac{(2-\nu)}{\pi\sqrt{\sin\phi}}(i+1)\sqrt{2}\left(\frac{h}{r}\right)\left(e^{-\frac{3}{2}i\phi}+e^{\frac{i}{2}\phi}\right)\ln\left(1+\left(\frac{h}{r}\right)^{2}e^{2i\phi}\right)\right)\tilde{C}', \tag{3.129}$$

$$
\begin{aligned}
&Q_k(\sigma_r)\\
&= \mathfrak{Re}\left(\frac{(4k+5)(2k-\nu+4)}{\pi\sqrt{\sin\phi}}(i-1)\sqrt{2}\left(\frac{h}{r}\right)\left(e^{-\frac{3}{2}i\phi}+e^{\frac{i}{2}\phi}\right)\ln\left(1+\left(\frac{h}{r}\right)^2 e^{2i\phi}\right)\right)C'_k, \quad (3.130)\\
&Q_k(\sigma_\phi)\\
&= \mathfrak{Re}\left(\frac{(4k+5)(2k-\nu+4)}{\pi\sqrt{\sin\phi}}(1-i)\sqrt{2}\left(\frac{h}{r}\right)\left(e^{-\frac{3}{2}i\phi}+e^{\frac{i}{2}\phi}\right)\ln\left(1+\left(\frac{h}{r}\right)^2 e^{2i\phi}\right)\right)C'_k, \quad (3.131)\\
&Q_k(\sigma_{r\phi})\\
&= \mathfrak{Re}\left(\frac{(4k+5)(2k-\nu+4)}{\pi\sqrt{\sin\phi}}(i+1)\sqrt{2}\left(\frac{h}{r}\right)\left(e^{-\frac{3}{2}i\phi}+e^{\frac{i}{2}\phi}\right)\ln\left(1+\left(\frac{h}{r}\right)^2 e^{2i\phi}\right)\right)C'_k. \quad (3.132)
\end{aligned}
$$

We note that the terms related to σ_θ, v_r and v_ϕ grow slowly, therefore, they are not included in our acceleration technique. In the case of $\phi = \pi$ we have that

$$Q_{-1}(v_r) = 4(2-\nu)\left(\ln(2) - \ln\left(1+\sqrt{1+\left(\frac{h}{r}\right)^2}\right)\right)\tilde{C}', \quad (3.133)$$

$$Q_{-1}(\sigma_r) = 4(2-\nu)\left(\frac{h}{r}\right)^3 \frac{1}{\sqrt{1+\left(\frac{h}{r}\right)^2}+1+\left(\frac{h}{r}\right)^2}\tilde{C}', \quad (3.134)$$

$$Q_{-1}(\sigma_\phi) = -2(2-\nu)\left(\frac{h}{r}\right)^3 \frac{1}{\sqrt{1+\left(\frac{h}{r}\right)^2}+1+\left(\frac{h}{r}\right)^2}\tilde{C}', \quad (3.135)$$

$$Q_{-1}(\sigma_\theta) = -2(2-\nu)\left(\frac{h}{r}\right)^3 \frac{1}{\sqrt{1+\left(\frac{h}{r}\right)^2}+1+\left(\frac{h}{r}\right)^2}\tilde{C}', \quad (3.136)$$

$$Q_k(v_r) = -4(4k+5)(2k-\nu+4)\left(\ln(2) - \ln\left(1+\sqrt{1+\left(\frac{h}{r}\right)^2}\right)\right)C'_k, \quad (3.137)$$

$$Q_k(\sigma_r) = -4(4k+5)(2k-\nu+4)\left(\frac{h}{r}\right)^3 \frac{1}{\sqrt{1+\left(\frac{h}{r}\right)^2}+1+\left(\frac{h}{r}\right)^2}C'_k, \quad (3.138)$$

$$Q_k(\sigma_\phi) = 2(4k+5)(2k-\nu+4)\left(\frac{h}{r}\right)^3 \frac{1}{\sqrt{1+\left(\frac{h}{r}\right)^2}+1+\left(\frac{h}{r}\right)^2} C'_k, \tag{3.139}$$

$$Q_k(\sigma_\theta) = 2(4k+5)(2k-\nu+4)\left(\frac{h}{r}\right)^3 \frac{1}{\sqrt{1+\left(\frac{h}{r}\right)^2}+1+\left(\frac{h}{r}\right)^2} C'_k. \tag{3.140}$$

3.4.3. Zero displacement and prescribed displacements

The term A_{n-1} from the equation (3.65) gives us the contributions

$$F_n = \frac{\alpha_{2n}}{\Delta_n}\left[\frac{2(n+2)}{5}\left(\omega_1^{(n)} - \omega_0^{(n)}\right)\right], \tag{3.141}$$

$$\text{or } F_n = 1/4\,\frac{(4\,n+1)\,P_{2n}(0)}{(1+n)\,(2\,n-3)\,(-3\,n+4\,\nu\,n-1+\nu)\,(2\,n-1)^2}, \tag{3.142}$$

$$G_n^{(-1)} = \frac{\alpha_{2n}}{\Delta_n}\left[(2(3-4\nu)n+7-8\nu)\omega_0^{(n)} + (1-2\nu)\frac{(4n+1)}{2n}P_{2n}\right], \tag{3.143}$$

$$G_n^{(k)} = \frac{\alpha_{2n}}{\Delta_n}\Big[(2k+3)\big((2n+1)(2k-1+4\nu) - (2k+3)(2k+6-4\nu)\big)\omega_{k+1}^{(n)} + (2k-2n+1)\alpha_{2k+2}\omega_k^{(n)}\Big], \tag{3.144}$$

whose dominant terms are

$$F_n \approx -\frac{1}{8(3-4\nu)n^4}P_{2n}(0), \tag{3.145}$$

$$G_n^{(-1)} \approx -\frac{1}{2}\frac{(1-\nu)}{(3-4\nu)n^2}P_{2n}(0), \tag{3.146}$$

$$G_n^{(k)} \approx \frac{1}{2}\frac{(4k+5)(1-\nu)}{(3-4\nu)n^2}P_{2n}(0). \tag{3.147}$$

Using these expressions we can determine the dominant term. For the sake of convenience, we work in the complex plane, and subsequently we consider just the real part. For example, for σ_r we have

$$s_{n-1}(\sigma_r) = -\frac{\sqrt{2}}{4}\sqrt{\frac{1}{n\pi\sin^3\phi}}(1+i)n^3\left(\frac{h}{r}\right)^{2n+1} e^{2in\phi}\Big(-16ne^{-5/2i\phi} + 3e^{-5/2i\phi} + 2e^{-1/2i\phi} + 16ne^{3/2i\phi} - e^{3/2i\phi}\Big). \tag{3.148}$$

The asymptotic term are

$$F_n s_{n-1} = \frac{\sqrt{2}(1+i)}{32\pi(-3+4\nu)}\sqrt{\frac{1}{\sin\phi}}\left(\frac{h}{r}\right)^{2n+1}\frac{(-1)^n}{n^2}\left(1-\frac{1}{8n}\right)e^{2in\phi}\Big(e^{-\frac{5}{2}i\phi}(16n-3) -2e^{-\frac{1}{2}i\phi}-e^{\frac{3}{2}i\phi}(16n-1)\Big), \tag{3.149}$$

$$G_n^{(-1)} s_{n-1} = -\frac{\sqrt{2}(1+i)}{8\pi(-3+4\nu)}\sqrt{\frac{1}{\sin\phi}}\left(\frac{h}{r}\right)^{2n+1}(-1)^n\left(1-\frac{1}{8n}\right)e^{2in\phi}\Big(e^{-\frac{5}{2}i\phi}(16n-3) -2e^{-\frac{1}{2}i\phi}-e^{\frac{3}{2}i\phi}(16n-1)\Big), \tag{3.150}$$

$$G_n^{(k)} s_{n-1} = (4k+5)\frac{\sqrt{2}(1+i)}{8\pi(-3+4\nu)}\sqrt{\frac{1}{\sin\phi}}\left(\frac{h}{r}\right)^{2n+1}(-1)^n\left(1-\frac{1}{8n}\right)e^{2in\phi}\Big(e^{-\frac{5}{2}i\phi}(16n-3) -2e^{-\frac{1}{2}i\phi}-e^{\frac{3}{2}i\phi}(16n-1)\Big). \tag{3.151}$$

The following sums hold

$$\sum_{n=1}^{\infty}\left(\frac{h}{r}\right)^{2n+1}(-1)^n e^{2in\phi} n = -\left(\frac{h}{r}\right)^3 e^{2i\phi}\frac{1}{\left(1+\left(\frac{h}{r}\right)^2 e^{2i\phi}\right)^2}, \tag{3.152}$$

$$\sum_{n=1}^{\infty}\left(\frac{h}{r}\right)^{2n+1}(-1)^n e^{2in\phi} = -\left(\frac{h}{r}\right)^3 e^{2i\phi}\frac{1}{1+\left(\frac{h}{r}\right)^2 e^{2i\phi}}, \tag{3.153}$$

$$\sum_{n=1}^{\infty}\left(\frac{h}{r}\right)^{2n+1}(-1)^n e^{2in\phi}\frac{1}{n} = -\left(\frac{h}{r}\right)\ln\left(1+\left(\frac{h}{r}\right)^2 e^{2i\phi}\right), \tag{3.154}$$

$$\sum_{n=1}^{\infty}\left(\frac{h}{r}\right)^{2n+1}(-1)^n\frac{e^{2in\phi}}{n(n+1)} = \frac{e^{2i\phi}\left(\frac{h}{r}\right)^2-\left(1+\left(\frac{h}{r}\right)^2 e^{2i\phi}\right)\ln\left(1+\left(\frac{h}{r}\right)^2 e^{2i\phi}\right)}{\left(\frac{h}{r}\right)}. \tag{3.155}$$

3.5. Some clues about the programming

Once we have computed all the expressions for the displacements and the stresses, we face the challenge of putting them in a computer code, in order to evaluate each expression and plot the results. The way to do so is tricky, so we present next some of the solutions we have used to solve those problems that every implementation usually has.

One of our biggest concerns was the implementation of the coefficients $l_{2n},\ m_{2n}$ from (3.3.2), (3.3.4), because we need to calculate the integrals for the Legendre polynomials of

degree from 0 to N, where N could take values up to 500, so we need a suitable method to compute these integrals.

The first step is to determine the most general form that these integrals could have. We use the following recurrence relation for the Legendre polynomials,

$$(1-x^2)P_n'(x) = n(P_{n-1}(x) - xP_n(x)), \tag{3.156}$$

so we can write any of the integrals that will arise in the following way

$$\int_{-1}^{0} g(x)P_{2n}(x)\mathrm{d}x. \tag{3.157}$$

We use a partition of the interval $[-1,0]$ defined as $x_1 = -1 < x_2 < \ldots < x_{N+1} = 0$, and we take the Lagrange interpolation functions, that is

$$\phi_1(x) = \begin{cases} \dfrac{x_2 - \phi}{x_2 - x_1} & [x_1, x_2] \\ 0 & [x_3, x_{N+1}] \end{cases} \tag{3.158}$$

$$\phi_j(x) = \begin{cases} \dfrac{\phi - x_{j-1}}{x_j - x_{j-1}} & [x_{j-1}, x_j] \\ \dfrac{x_{j+1} - \phi}{x_{j+1} - x_j} & [x_j, x_{j+1}] \end{cases} \qquad j = 2, \ldots, N \tag{3.159}$$

$$\phi_{N+1}(x) = \begin{cases} 0 & [x_1, x_{N-1}] \\ \dfrac{\phi - x_N}{x_{N+1} - x_N} & [x_N, x_{N+1}] \end{cases} \tag{3.160}$$

With this particular partition, we use the approximation

$$g(x) \approx \sum_{j=1}^{N+1} g(x_j)\phi_j(x), \tag{3.161}$$

$$\int_{-1}^{0} g(x)P_{2n}(x)\mathrm{d}x \approx \int_{-1}^{0} \left(\sum_{j=1}^{N+1} g(x_j)\phi_j(x)P_{2n}(x) \right) \mathrm{d}x, \tag{3.162}$$

$$\approx \sum_{j=1}^{N+1} g(x_j) \int_{-1}^{0} \big(\phi_j(x)P_{2n}(x)\big)\mathrm{d}x. \tag{3.163}$$

So, we express the integrals in the following ways

$$\int_{x_j}^{x_{j+1}} xP_{2n}(x)\mathrm{d}x = \frac{x_{j+1}P_{2n+1}(x_{j+1}) - x_jP_{2n+1}(x_j)}{4n+1} - \frac{x_{j+1}P_{2n-1}(x_{j+1}) - x_jP_{2n-1}(x_j)}{4n+1}$$
$$- \frac{P_{2n+2}(x_{j+1}) - P_{2n+2}(x_j)}{(4n+1)(4n+3)} + 2\frac{P_{2n}(x_{j+1}) - P_{2n}(x_j)}{(4n-1)(4n+3)}$$
$$- \frac{P_{2n-2}(x_{j+1}) - P_{2n-2}(x_j)}{(4n-1)(4n+1)}, \tag{3.164}$$

$$\int_{x_j}^{x_{j+1}} P_{2n}(x)\mathrm{d}x = \frac{P_{2n+1}(x_{j+1}) - P_{2n+1}(x_j)}{4n+1} - \frac{P_{2n-1}(x_{j+1}) - P_{2n-1}(x_j)}{4n+1}. \tag{3.165}$$

3.6. Numerical results

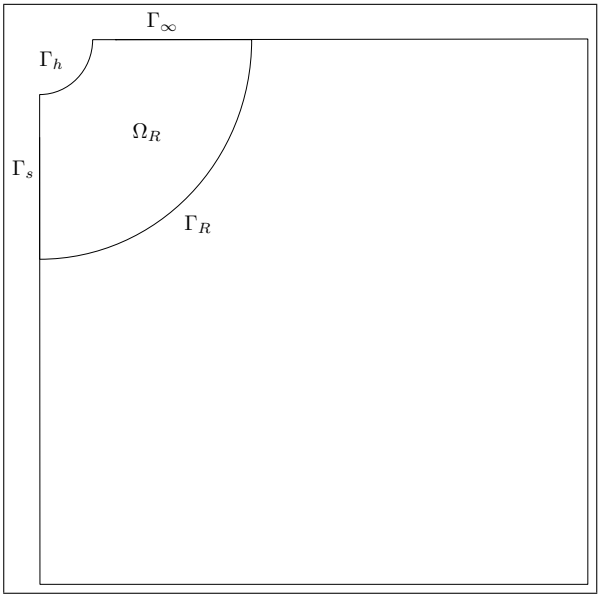

Figure 3.1. Boundaries.

We need a proper benchmark to test our results. For this purpose we choose the recognized comercial software, COMSOL (see (Multiphysics, 1994)). We first need to evaluate wheter the results given by COMSOL for our semi-infinite problem are trustable, because it is necessary to use artificial boundaries in order to limit the domain. We use an axisymmetric domain, with a hemispherical perturbation of radius h in the presence of the gravity force. In order to determine a suitable size for the domain, we make the following experiment: We consider domains consisting of squares of different sizes with a hemispherical

perturbation of radius $h = 600$ m, and we solve our semi-infinite problem using COMSOL in each one of these domains. The radii vary from a minimum value of 1000 m to a maximum value of 13000 m, in increments of 1000 m. The results obtained with the maximum radius are taken as a reference. Let us call XY the results yielded by Comsol, and xy the results yielded by our methodology. We use an interpolation between this sets of points in order to measure the point by point error, this is

$$E_{boundary} = \frac{\sqrt{\sum_i (Y_i - y_i)^2}}{\sqrt{\sum_i (Y_i)^2}}. \tag{3.166}$$

The results in the important boundaries (see Figure 3.1) for both displacements are shown

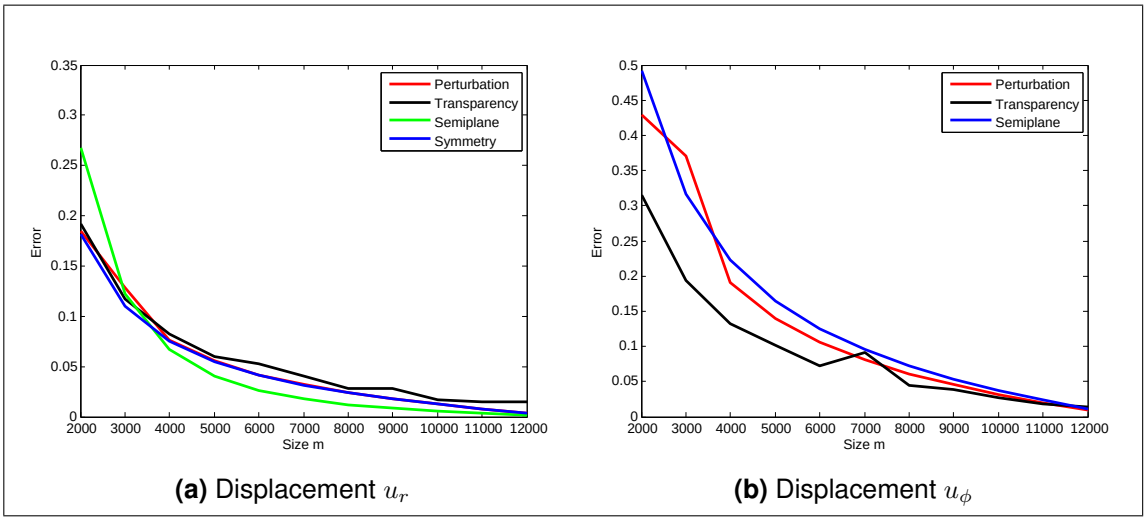

(a) Displacement u_r **(b)** Displacement u_ϕ

Figure 3.2. Displacement relative error between our method and the results yielded by COMSOL in a square of size 13000 m.

in 3.2a and 3.2b. According to these results, we choose a square of size 10000 m as benchmark.

3.6.1. Traction-free boundary

The Figures 3.3a to 3.4h show the results provided by our method and the benchmark for the case of traction-free boundary condition on the hemisphere.

The numerical error associated with the traction-free boundary condition on each boundary (see Figure 3.1) are shown in Table 3.1. These results allow us to validate our methodology.

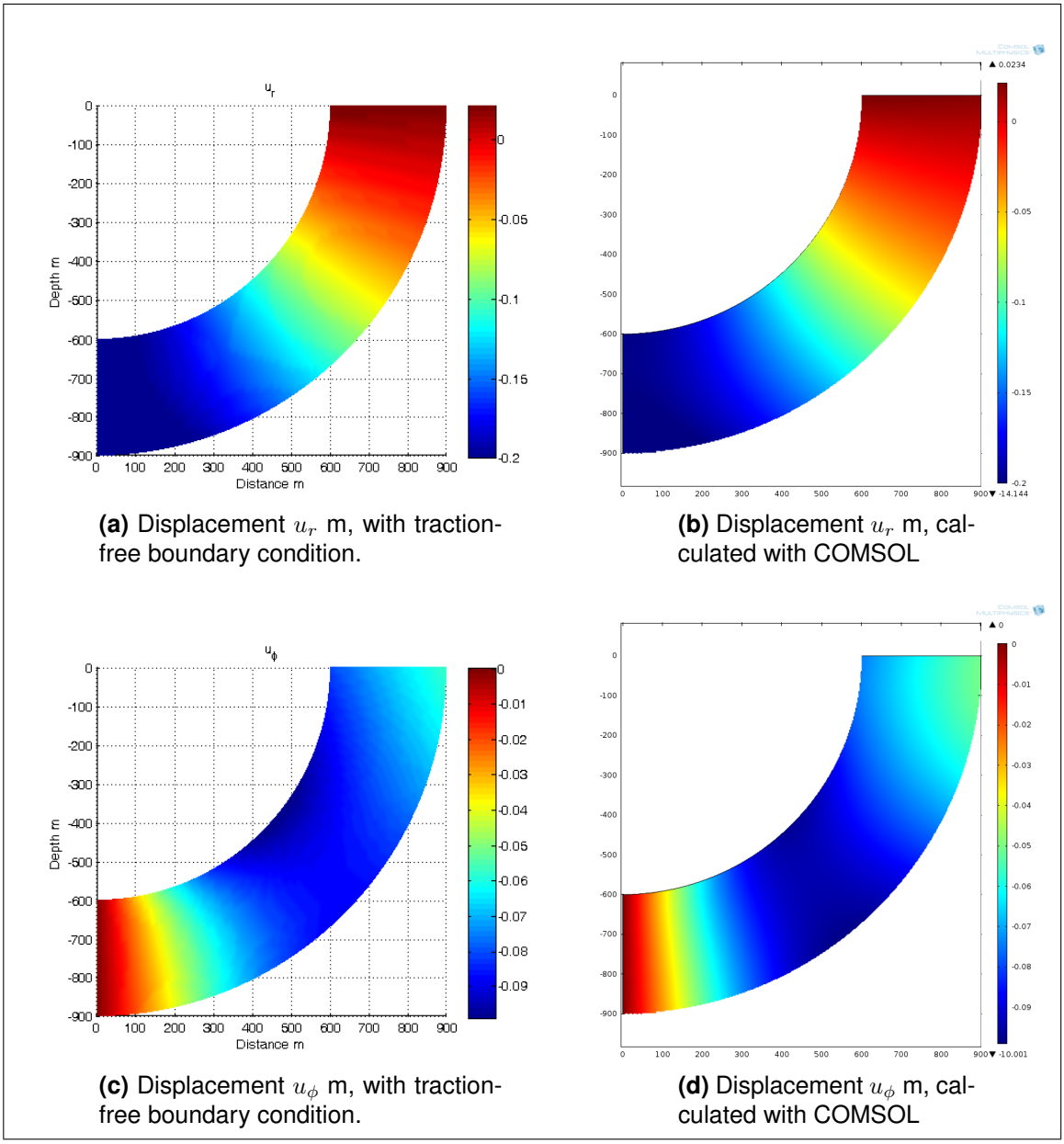

(a) Displacement u_r m, with traction-free boundary condition.

(b) Displacement u_r m, calculated with COMSOL

(c) Displacement u_ϕ m, with traction-free boundary condition.

(d) Displacement u_ϕ m, calculated with COMSOL

Figure 3.3. Displacement for traction-free boundary condition with $\nu = 0.3$, $\lambda = 40.5$ GPa, $\mu = 27$ GPa, $\varrho = 2725\ \mathrm{kg/m^3}$.

3.6.2. Loaded boundary

In this case we can obtain again the results presented in Figures 3.3a to 3.6h if we use (3.30) and (3.31) as our boundary condition.

Table 3.1. Comparison of the absolute error between the semi-analytical solution and the model implemented in COMSOL in a square of side 10000 m.

Boundarie	u_r	u_ϕ
Plane Γ_∞	0.0092	0.0924
Perturbation Γ_h	0.0314	0.0789
Transparency Γ_R	0.0348	0.1485
Axisymmetric Γ_s	0.0311	0

3.6.3. Zero displacement

The Figures 3.5a to 3.6h show the results provided by our method and the benchmark in the case of zero displacement on the hemisphere.

Table 3.2. Comparison of the absolute error between the semi-analytical solution and the model implemented in COMSOL in a square of side 10000 m.

	u_r	u_ϕ
Plane Γ_∞	0.3290	0.1080
Transparency Γ_R	0.0114	0.1823
Axisymmetry Γ_s	0.0065	0

The relative error associated with the zero displacement boundary condition in each of the boundaries (see 3.1) are shown in Table 3.2. These results allow us to validate our methodology.

3.6.4. Prescribed displacements

In this case we obtain again the results of Figures 3.5a to 3.6g if we use (3.55) and (3.56) as our boundary condition.

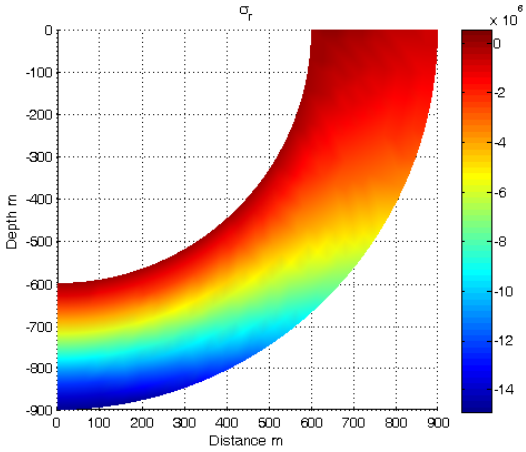

(a) Stress σ_r Pa, with traction-free boundary condition

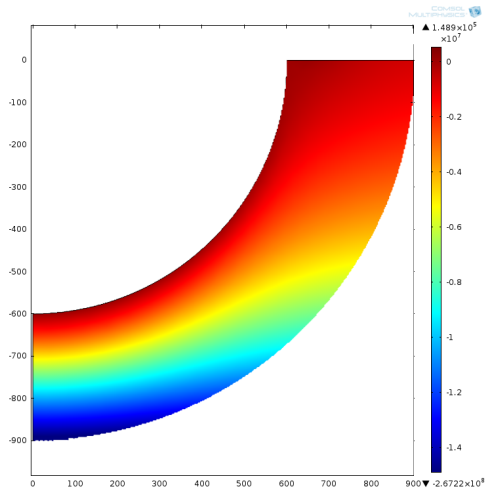

(b) Stress σ_r Pa, calculated with COMSOL

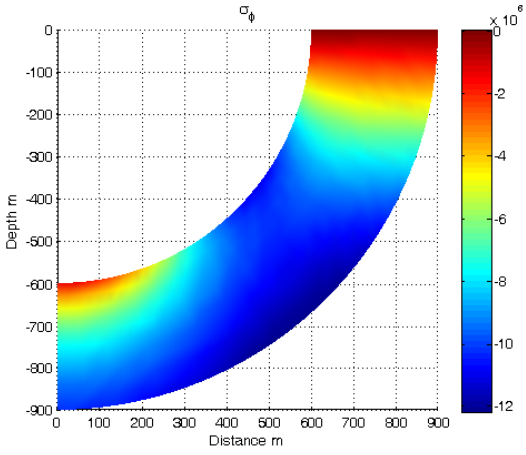

(c) Stress σ_ϕ Pa, with traction-free boundary condition

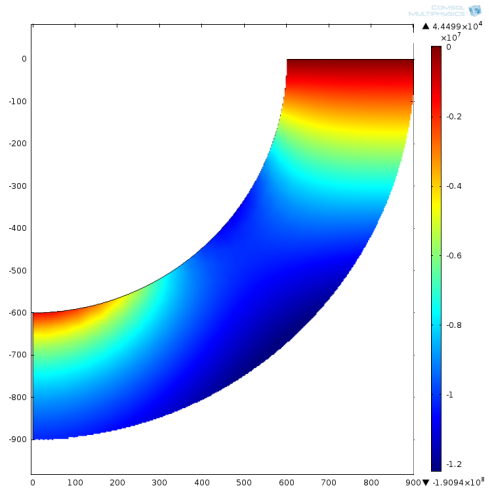

(d) Stress σ_ϕ Pa, calculated with COMSOL

Figure 3.4. Stresses for traction-free boundary condition with $\nu = 0.3$, $\lambda = 40.5$ GPa, $\mu = 27$ GPa, $\varrho = 2725\ \mathrm{kg/m^3}$.

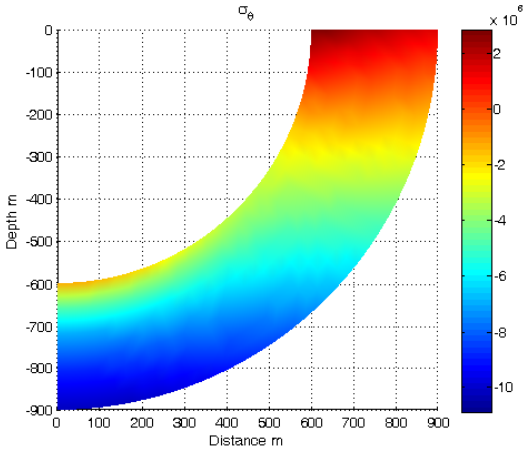

(e) Stress σ_θ Pa, with traction-free boundary condition

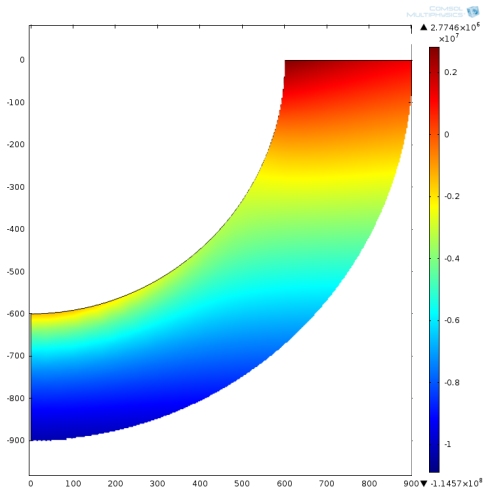

(f) Stress σ_θ Pa, calculated with COMSOL

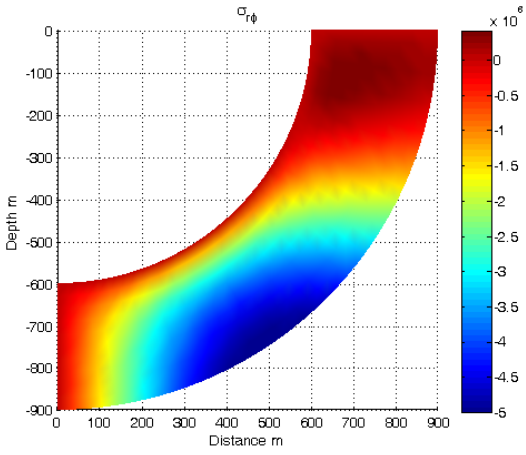

(g) Stress $\sigma_{r\phi}$ Pa, with traction-free boundary condition

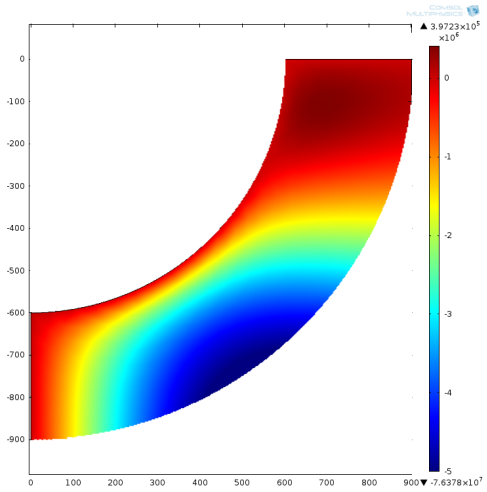

(h) Stress $\sigma_{r\phi}$ Pa, calculated with COMSOL

Figure 3.4. Stresses for traction-free boundary condition with $\nu = 0.3$, $\lambda = 40.5$ GPa, $\mu = 27$ GPa, $\varrho = 2725\ \mathrm{kg/m^3}$.

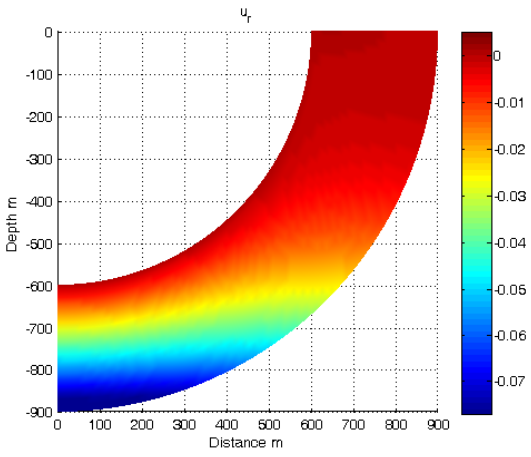

(a) Displacement u_r m, with zero displacement boundary condition.

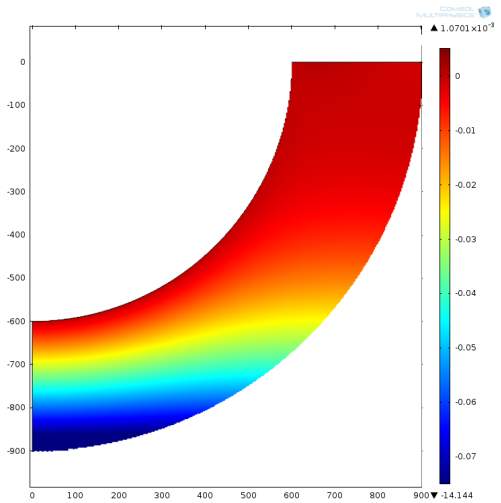

(b) Displacement u_r m, calculated with COMSOL

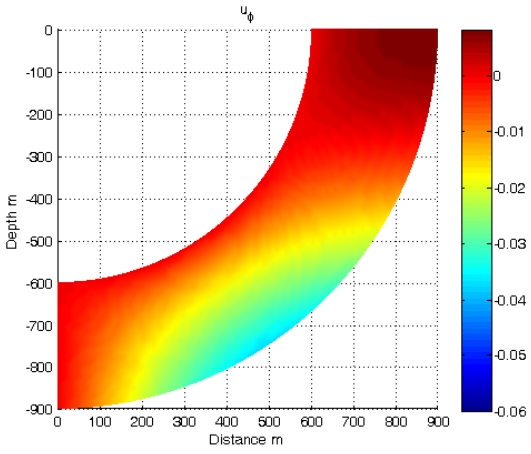

(c) Displacement u_ϕ m, with zero displacement boundary condition.

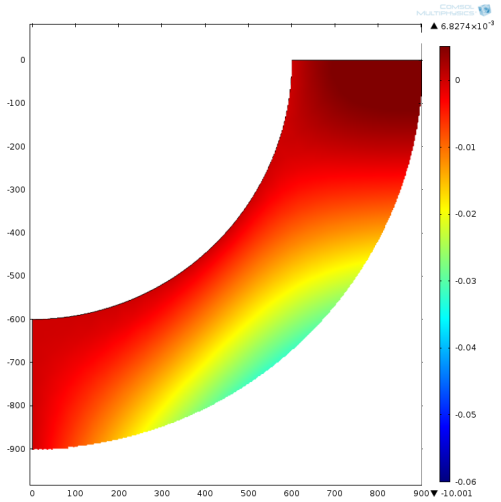

(d) Displacement u_ϕ m, calculated with COMSOL

Figure 3.5. Displacement for zero displacement boundary condition with $\nu = 0.3$, $\lambda = 40.5$ GPa, $\mu = 27$ GPa, $\varrho = 2725\ \mathrm{kg/m^3}$.

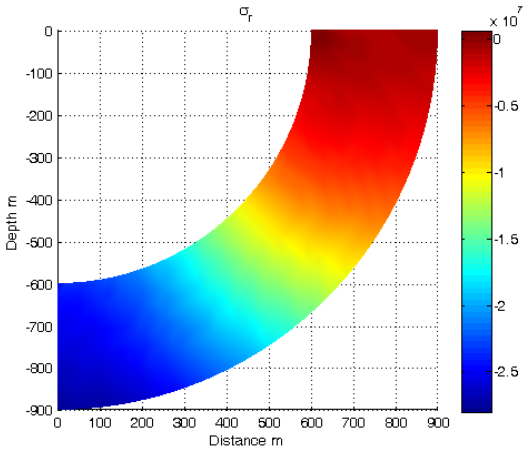

(a) Stress σ_r Pa, with zero displacement boundary condition

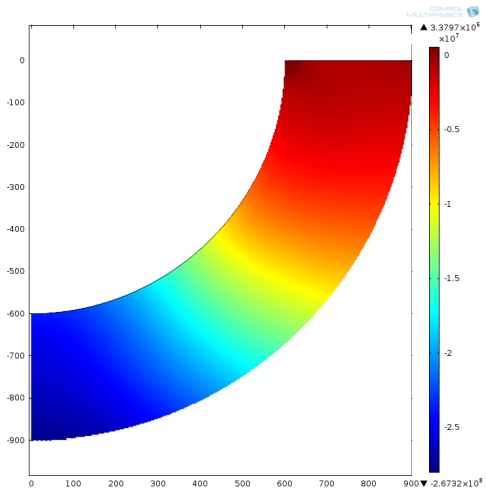

(b) Stress σ_r Pa, calculated with COMSOL

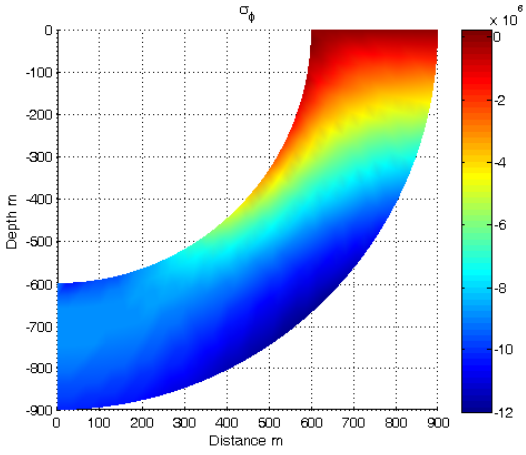

(c) Stress σ_ϕ Pa, with zero displacement boundary condition

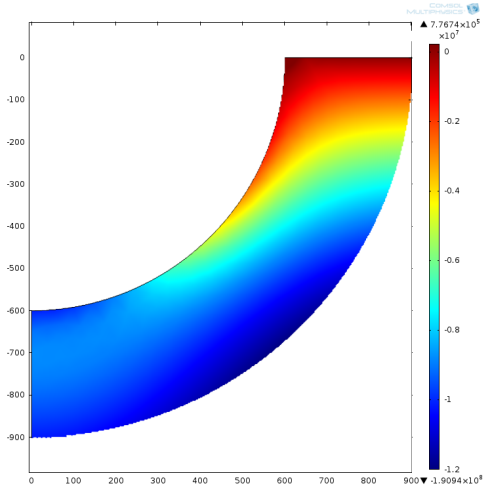

(d) Stress σ_ϕ Pa, calculated with COMSOL

Figure 3.6. Stresses for zero displacement boundary condition with $\nu = 0.3$, $\lambda = 40.5$ GPa, $\mu = 27$ GPa, $\varrho = 2725\ \mathrm{kg/m^3}$.

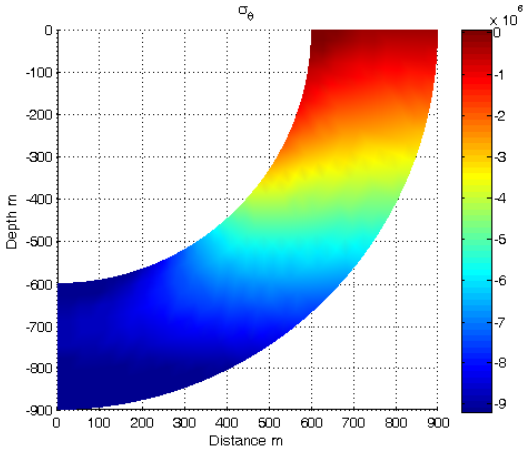

(e) Stress σ_θ Pa, with zero displacement boundary condition

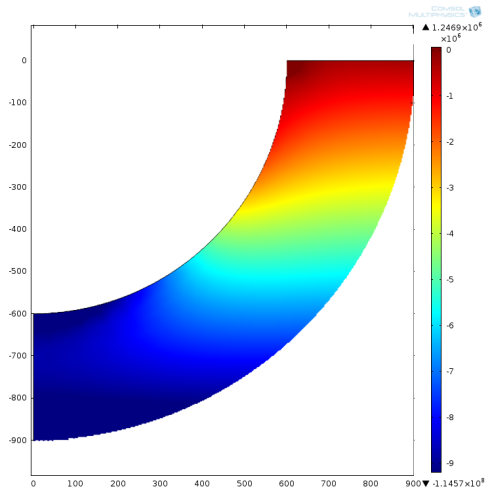

(f) Stress σ_θ Pa, calculated with COMSOL

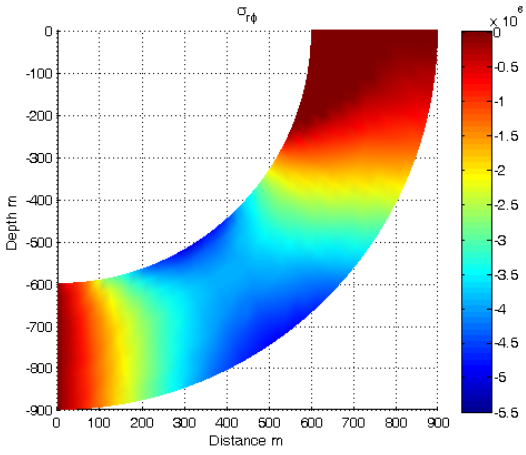

(g) Stress $\sigma_{r\phi}$ Pa, with zero displacement boundary condition

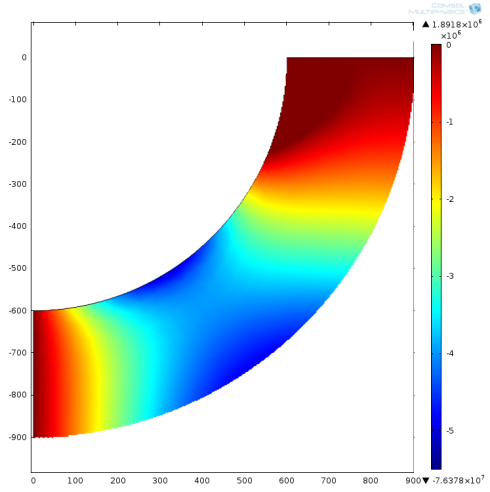

(h) Stress $\sigma_{r\phi}$ Pa, calculated with COMSOL

Figure 3.6. Stresses for zero displacement boundary condition with $\nu = 0.3$, $\lambda = 40.5$ GPa, $\mu = 27$ GPa, $\varrho = 2725\ \mathrm{kg/m^3}$.

4. AN EFFICIENT SEMI-ANALYTICAL METHOD TO COMPUTE DISPLACEMENTS

Throughout this chapter, we consider the same half-space with a hemispherical pit used in the previous chapter. In what follows, we are going to impose the boundary conditions on the pit by minimising a quadratic functional which represents the surface elastic energy. Even though this approach does not eliminate the problem of an infinite number of equations and coefficients, it provides a systematic method to deal with it. The minimisation of the functional leads to a linear system of equations for a finite number of coefficients of the series. The associated matrix is symmetric, positive definite and possesses a particular block structure that allows us to solve it in an efficient and robust way, thus avoiding to have to deal with cumbersome equations and slowly convergent double series.

Furthermore, in order to simplify the calculations, we re-define the notation for the displacements and stresses.

4.1. Series solution

Having already solved (2.27) and (2.28), we now resume the calculation of a solution to (2.12) in series form. We have obtained potentials Φ_n, given in (2.31) for $n \geq 0$ and in (2.32) for $n = -1$, and potentials Ψ_n, given in (2.30) for $n \geq 0$. Both kinds of potentials may be combined in different ways in (2.25) or (2.26), giving rise to displacement fields $\boldsymbol{v}$ satisfying (2.12a) and (2.12e). We shall consider two sets of such displacement fields. The first set will consist of displacement fields $\boldsymbol{v}_n^{(1)}$, obtained by setting $\Phi = \Phi_n$ and $\Psi = 0$ in (2.25) for $n \geq -1$, that is,

$$2\mu \boldsymbol{v}_n^{(1)} = \nabla \Phi_n, \tag{4.1}$$

whereas the second set will consist of displacement fields $\boldsymbol{v}_n^{(2)}$, obtained by setting $\Psi = (2n+1)\Psi_n$ and $\Phi = -(n - 4 + 4\nu)\Phi_{n-1}$ in (2.25) for $n \geq 0$, that is,

$$2\mu \boldsymbol{v}_n^{(2)} = -(n - 4 + 4\nu)\nabla \Phi_{n-1} + (2n+1)\big[\nabla(z\Psi_n) - 4(1-\nu)\Psi_n \hat{\boldsymbol{k}}\big]. \tag{4.2}$$

The reason for considering this particular combination of potentials Φ_n and Ψ_n is that, as stated in (R. A. Eubanks, 1954), the forthcoming calculations are considerably simplified. The general solution to Navier's equation (2.11) corresponds to an infinite linear combination of displacement fields $\boldsymbol{v}_n^{(1)}$ and $\boldsymbol{v}_n^{(2)}$, that is,

$$\boldsymbol{v}(r,\phi) = \sum_{n=-1}^{\infty} a_n^{(1)} \boldsymbol{v}_n^{(1)}(r,\phi) + \sum_{n=0}^{\infty} a_n^{(2)} \boldsymbol{v}_n^{(2)}(r,\phi), \tag{4.3}$$

where $a_{-1}^{(1)}, a_0^{(1)}, a_1^{(1)}, \ldots$ and $a_0^{(2)}, a_1^{(2)}, a_2^{(2)}, \ldots$ are unknown real coefficients. Displacement fields $\boldsymbol{v}_n^{(1)}$ and $\boldsymbol{v}_n^{(2)}$ are also expressed in terms of their components in r and ϕ by employing (2.26). Substituting these components in the Hooke's law yields the components of the stress fields associated with $\boldsymbol{v}_n^{(1)}$ and $\boldsymbol{v}_n^{(2)}$, which we denote respectively by $\boldsymbol{\sigma}_n^{(1)}$ and $\boldsymbol{\sigma}_n^{(2)}$. The stress tensor $\boldsymbol{\sigma}$ associated with $\boldsymbol{v}$ in (4.3) is thus expressed as

$$\boldsymbol{\sigma}(r,\phi) = \sum_{n=-1}^{\infty} a_n^{(1)} \boldsymbol{\sigma}_n^{(1)}(r,\phi) + \sum_{n=0}^{\infty} a_n^{(2)} \boldsymbol{\sigma}_n^{(2)}(r,\phi). \tag{4.4}$$

Making all the necessary substitutions and rearranging the resulting expressions in each case, we obtain that the displacement fields $\boldsymbol{v}_n^{(1)}$ and $\boldsymbol{v}_n^{(2)}$, together with their associated respective stress fields $\boldsymbol{\sigma}_n^{(1)}$ and $\boldsymbol{\sigma}_n^{(2)}$, can be expressed as

$$\boldsymbol{v}_n^{(1)}(r,\phi) = \frac{1}{r^{n+2}}\, \boldsymbol{w}_n^{(1)}(\phi), \qquad \boldsymbol{\sigma}_n^{(1)}(r,\phi) = \frac{1}{r^{n+3}}\, \boldsymbol{\tau}_n^{(1)}(\phi), \qquad n = -1, 0, 1, \ldots \tag{4.5a}$$

$$\boldsymbol{v}_n^{(2)}(r,\phi) = \frac{1}{r^{n+1}}\, \boldsymbol{w}_n^{(2)}(\phi), \qquad \boldsymbol{\sigma}_n^{(2)}(r,\phi) = \frac{1}{r^{n+2}}\, \boldsymbol{\tau}_n^{(2)}(\phi), \qquad n = 0, 1, 2, \ldots \tag{4.5b}$$

where $\boldsymbol{w}_n^{(1)}$, $\boldsymbol{w}_n^{(2)}$ are vector functions, and $\boldsymbol{\tau}_n^{(1)}$, $\boldsymbol{\tau}_n^{(2)}$ are tensor functions, all of them depending only on the angle ϕ. This is a convenient form of expressing the displacement and stress fields, since it allows us to make explicit the dependence on r, separating it from the dependence on ϕ. The components of functions $\boldsymbol{w}_n^{(1)}$ and $\boldsymbol{\tau}_n^{(1)}$ for $n = -1$ are

$$2\mu[w_{-1}^{(1)}]_r(\phi) = 1, \tag{4.6a}$$

$$2\mu[w_{-1}^{(1)}]_\phi(\phi) = q(\phi)\sin\phi, \tag{4.6b}$$

$$[\tau_{-1}^{(1)}]_r(\phi) = -1, \tag{4.6c}$$

$$[\tau_{-1}^{(1)}]_{\phi}(\phi) = -q(\phi)\cos\phi, \tag{4.6d}$$

$$[\tau_{-1}^{(1)}]_{\theta}(\phi) = q(\phi), \tag{4.6e}$$

$$[\tau_{-1}^{(1)}]_{r\phi}(\phi) = -q(\phi)\sin\phi, \tag{4.6f}$$

where the function $q(\cdot)$ is defined as

$$q(\phi) = \frac{1}{1-\cos\phi}, \qquad \frac{\pi}{2} \le \phi \le \pi. \tag{4.7}$$

The components of functions $\boldsymbol{w}_n^{(1)}$ and $\boldsymbol{\tau}_n^{(1)}$ for $n \ge 0$ are

$$2\mu[w_n^{(1)}]_r(\phi) = -(n+1)P_n(\cos\phi), \tag{4.8a}$$

$$2\mu[w_n^{(1)}]_{\phi}(\phi) = -\sin\phi\, P_n'(\cos\phi), \tag{4.8b}$$

$$[\tau_n^{(1)}]_r(\phi) = (n+1)(n+2)P_n(\cos\phi), \tag{4.8c}$$

$$[\tau_n^{(1)}]_{\phi}(\phi) = P_{n+1}'(\cos\phi) - (n+1)(n+2)P_n(\cos\phi), \tag{4.8d}$$

$$[\tau_n^{(1)}]_{\theta}(\phi) = -P_{n+1}'(\cos\phi), \tag{4.8e}$$

$$[\tau_n^{(1)}]_{r\phi}(\phi) = (n+2)\sin\phi\, P_n'(\cos\phi). \tag{4.8f}$$

The components of functions $\boldsymbol{w}_n^{(2)}$ and $\boldsymbol{\tau}_n^{(2)}$ for $n = 0$ are

$$2\mu[w_0^{(2)}]_r(\phi) = -4(1-\nu)(1+\cos\phi), \tag{4.9a}$$

$$2\mu[w_0^{(2)}]_{\phi}(\phi) = -\big(4(1-\nu)q(\phi) - 3 + 4\nu\big)\sin\phi, \tag{4.9b}$$

$$[\tau_0^{(2)}]_r(\phi) = 2\big(2 - 2\nu + (2-\nu)\cos\phi\big), \tag{4.9c}$$

$$[\tau_0^{(2)}]_{\phi}(\phi) = (4(1-\nu)q(\phi) - 1 + 2\nu)\cos\phi, \tag{4.9d}$$

$$[\tau_0^{(2)}]_{\theta}(\phi) = -4(1-\nu)q(\phi) - (1-2\nu)\cos\phi, \tag{4.9e}$$

$$[\tau_0^{(2)}]_{r\phi}(\phi) = \big(4(1-\nu)q(\phi) - 1 + 2\nu\big)\sin\phi, \tag{4.9f}$$

and for $n \ge 1$ are

$$2\mu[w_n^{(2)}]_r(\phi) = -(n+1)(n+4-4\nu)P_{n+1}(\cos\phi), \tag{4.10a}$$

$$2\mu[w_n^{(2)}]_\phi(\phi) = -(n-3+4\nu)\sin\phi\, P'_{n+1}(\cos\phi), \tag{4.10b}$$

$$[\tau_n^{(2)}]_r(\phi) = (n+1)\big((n+1)(n+4)-2\nu\big)P_{n+1}(\cos\phi), \tag{4.10c}$$

$$\begin{aligned}[\tau_n^{(2)}]_\phi(\phi) = &-(n+1)(n^2-n+1-2\nu)P_{n+1}(\cos\phi)\\ &+(n-3+4\nu)P'_n(\cos\phi),\end{aligned} \tag{4.10d}$$

$$\begin{aligned}[\tau_n^{(2)}]_\theta(\phi) = &-(1-2\nu)(n+1)(2n+1)P_{n+1}(\cos\phi)\\ &-(n-3+4\nu)P'_n(\cos\phi),\end{aligned} \tag{4.10e}$$

$$[\tau_n^{(2)}]_{r\phi}(\phi) = (n^2+2n-1+2\nu)\sin\phi\, P'_{n+1}(\cos\phi). \tag{4.10f}$$

Substituting (4.5) in (4.3) and (4.4), and grouping terms with the same power of r, we obtain that $\boldsymbol{v}$ and $\boldsymbol{\sigma}$ are also expressed as

$$\boldsymbol{v}(r,\phi) = \sum_{n=-1}^{\infty} \frac{1}{r^{n+2}}\Big(a_n^{(1)}\boldsymbol{w}_n^{(1)}(\phi) + a_{n+1}^{(2)}\boldsymbol{w}_{n+1}^{(2)}(\phi)\Big), \tag{4.11}$$

$$\boldsymbol{\sigma}(r,\phi) = \sum_{n=-1}^{\infty} \frac{1}{r^{n+3}}\Big(a_n^{(1)}\boldsymbol{\tau}_n^{(1)}(\phi) + a_{n+1}^{(2)}\boldsymbol{\tau}_{n+1}^{(2)}(\phi)\Big). \tag{4.12}$$

4.1.1. Traction-free boundary on Γ_∞

As done in the previous chapter, we need to impose the traction-free boundary condition on the plane boundary (which is $\sigma_\phi(\boldsymbol{v}) = \sigma_{r\phi}(\boldsymbol{v}) = 0$), that is

$$\sigma_\phi(\boldsymbol{v}) = \sum_{n=-1}^{\infty} \frac{1}{r^{n+3}}\left(a_n^{(1)}[\tau_n^{(1)}]_\phi\left(\frac{\pi}{2}\right) + a_{n+1}^{(2)}[\tau_{n+1}^{(2)}]_\phi\left(\frac{\pi}{2}\right)\right) = 0, \tag{4.13a}$$

$$\sigma_{r\phi}(\boldsymbol{v}) = \sum_{n=-1}^{\infty} \frac{1}{r^{n+3}}\left(a_n^{(1)}[\tau_n^{(1)}]_{r\phi}\left(\frac{\pi}{2}\right) + a_{n+1}^{(2)}[\tau_{n+1}^{(2)}]_{r\phi}\left(\frac{\pi}{2}\right)\right) = 0. \tag{4.13b}$$

In order to find out under which conditions (4.13a) and (4.13b) hold, we evaluate (4.6d), (4.6f), (4.8d), (4.8f), (4.9d), (4.9f), (4.10d) and (4.10f) at $\phi = \pi/2$. The result varies depending on whether n is even or odd, so we discriminate between these two cases before

evaluating the expressions. In the even case, we arrive at

$$[\tau_{2n}^{(1)}]_{\phi}\Big(\frac{\pi}{2}\Big) = -(2n+1)^2 P_{2n}(0) \quad n \geq 0, \tag{4.14a}$$

$$[\tau_{2n}^{(1)}]_{r\phi}\Big(\frac{\pi}{2}\Big) = 0 \quad n \geq 0, \tag{4.14b}$$

$$[\tau_{2n}^{(2)}]_{\phi}\Big(\frac{\pi}{2}\Big) = 0 \quad n \geq 0, \tag{4.14c}$$

$$[\tau_{2n}^{(2)}]_{r\phi}\Big(\frac{\pi}{2}\Big) = \begin{cases} 3-2\nu & n=0, \\ (2n+1)\alpha_{2n} P_{2n}(0) & n \geq 1, \end{cases} \tag{4.14d}$$

and in the odd case, we obtain

$$[\tau_{2n+1}^{(1)}]_{\phi}\Big(\frac{\pi}{2}\Big) = 0 \quad n \geq -1, \tag{4.15a}$$

$$[\tau_{2n+1}^{(1)}]_{r\phi}\Big(\frac{\pi}{2}\Big) = \begin{cases} -1 & n=-1, \\ (2n+1)(2n+3) P_{2n}(0) & n \geq 0, \end{cases} \tag{4.15b}$$

$$[\tau_{2n+1}^{(2)}]_{\phi}\Big(\frac{\pi}{2}\Big) = (2n+1)\alpha_{2n} P_{2n}(0) \quad n \geq 0, \tag{4.15c}$$

$$[\tau_{2n+1}^{(2)}]_{r\phi}\Big(\frac{\pi}{2}\Big) = 0 \quad n \geq 0, \tag{4.15d}$$

where

$$\alpha_{2n} = (2n+1)^2 - 2(1-\nu),$$

and having combined with the recurrence relations (6.17) as appropriate. It is easy to verify that by virtue of (4.14) and (4.15), identities (4.13a) and (4.13b) hold, provided that the coefficients $a_n^{(1)}$ and $a_n^{(2)}$ satisfy the relations

$$a_{-1}^{(1)} = (3-2\nu) a_0^{(2)}, \tag{4.16a}$$

$$(2n+1) a_{2n}^{(1)} = \alpha_{2n}\, a_{2n+1}^{(2)} \qquad n \geq 0, \tag{4.16b}$$

$$(2n+2) a_{2n+1}^{(1)} = \alpha_{2n+2}\, a_{2n+2}^{(2)} \quad n \geq 0. \tag{4.16c}$$

Thus, separating the infinite sums in (4.11) and (4.12) into even and odd terms, and combining with (4.16), we arrive at the following expressions for $\boldsymbol{v}$ and $\boldsymbol{\sigma}$:

$$\begin{aligned}\boldsymbol{v}(r,\phi) = {} & \frac{a_0^{(2)}}{r}\Big((3-2\nu)\boldsymbol{w}_{-1}^{(1)}(\phi) + \boldsymbol{w}_0^{(2)}(\phi)\Big) \\ & + \sum_{n=0}^{\infty} \frac{a_{2n+2}^{(2)}}{(2n+2)r^{2n+3}}\Big(\alpha_{2n+2}\boldsymbol{w}_{2n+1}^{(1)}(\phi) + (2n+2)\boldsymbol{w}_{2n+2}^{(2)}(\phi)\Big) \\ & + \sum_{n=0}^{\infty} \frac{a_{2n+1}^{(2)}}{(2n+1)r^{2n+2}}\Big(\alpha_{2n}\boldsymbol{w}_{2n}^{(1)}(\phi) + (2n+1)\boldsymbol{w}_{2n+1}^{(2)}(\phi)\Big),\end{aligned} \tag{4.17a}$$

$$\begin{aligned}\boldsymbol{\sigma}(r,\phi) = {} & \frac{a_0^{(2)}}{r^2}\Big((3-2\nu)\boldsymbol{\tau}_{-1}^{(1)}(\phi) + \boldsymbol{\tau}_0^{(2)}(\phi)\Big) \\ & + \sum_{n=0}^{\infty} \frac{a_{2n+2}^{(2)}}{(2n+2)r^{2n+4}}\Big(\alpha_{2n+2}\boldsymbol{\tau}_{2n+1}^{(1)}(\phi) + (2n+2)\boldsymbol{\tau}_{2n+2}^{(2)}(\phi)\Big) \\ & + \sum_{n=0}^{\infty} \frac{a_{2n+1}^{(2)}}{(2n+1)r^{2n+3}}\Big(\alpha_{2n}\boldsymbol{\tau}_{2n}^{(1)}(\phi) + (2n+1)\boldsymbol{\tau}_{2n+1}^{(2)}(\phi)\Big).\end{aligned} \tag{4.17b}$$

This solution satisfies (2.12b), as well as (2.12a) and (2.12e). Defining the vector functions

$$\boldsymbol{w}_n^{(A)}(\phi) = \alpha_{2n}\boldsymbol{w}_{2n}^{(1)}(\phi) + (2n+1)\boldsymbol{w}_{2n+1}^{(2)}(\phi) \qquad n \geq 0, \tag{4.18a}$$

$$\boldsymbol{w}_n^{(B)}(\phi) = \begin{cases} (3-2\nu)\boldsymbol{w}_{-1}^{(1)}(\phi) + \boldsymbol{w}_0^{(2)}(\phi) & n = -1, \\ \alpha_{2n+2}\boldsymbol{w}_{2n+1}^{(1)}(\phi) + (2n+2)\boldsymbol{w}_{2n+2}^{(2)}(\phi) & n \geq 0, \end{cases} \tag{4.18b}$$

and the tensor functions

$$\boldsymbol{\tau}_n^{(A)}(\phi) = \alpha_{2n}\boldsymbol{\tau}_{2n}^{(1)}(\phi) + (2n+1)\boldsymbol{\tau}_{2n+1}^{(2)}(\phi) \qquad n \geq 0, \tag{4.19a}$$

$$\boldsymbol{\tau}_n^{(B)}(\phi) = \begin{cases} (3-2\nu)\boldsymbol{\tau}_{-1}^{(1)}(\phi) + \boldsymbol{\tau}_0^{(2)}(\phi) & n = -1, \\ \alpha_{2n+2}\boldsymbol{\tau}_{2n+1}^{(1)}(\phi) + (2n+2)\boldsymbol{\tau}_{2n+2}^{(2)}(\phi) & n \geq 0, \end{cases} \tag{4.19b}$$

and using the fact that the coefficients $a_n^{(2)}$ are arbitrary, it is possible to reexpress (4.17a) and (4.17b) as

$$\boldsymbol{v}(r,\phi) = \sum_{n=0}^{\infty} A_n \Big(\frac{h}{r}\Big)^{2n+2} \boldsymbol{w}_n^{(A)}(\phi) + \sum_{n=-1}^{\infty} B_n \Big(\frac{h}{r}\Big)^{2n+3} \boldsymbol{w}_n^{(B)}(\phi), \tag{4.20a}$$

$$\boldsymbol{\sigma}(r,\phi) = \frac{1}{h}\Bigg[\sum_{n=0}^{\infty} A_n \Big(\frac{h}{r}\Big)^{2n+3} \boldsymbol{\tau}_n^{(A)}(\phi) + \sum_{n=-1}^{\infty} B_n \Big(\frac{h}{r}\Big)^{2n+4} \boldsymbol{\tau}_n^{(B)}(\phi)\Bigg], \tag{4.20b}$$

where A_n and B_n are unknown real coefficients. The components of functions $\boldsymbol{w}_n^{(A)}$, $\boldsymbol{\tau}_n^{(A)}$ for $n = 0, 1, 2, \ldots$ are

$$2\mu[w_n^{(A)}]_r(\phi) = -(2n+1)\big(\alpha_{2n} P_{2n}(\cos\phi) + \gamma_{2n} P_{2n+2}(\cos\phi)\big), \tag{4.21a}$$

$$2\mu[w_n^{(A)}]_\phi(\phi) = -\sin\phi\big(\alpha_{2n} P'_{2n}(\cos\phi) + \epsilon_{2n} P'_{2n+2}(\cos\phi)\big), \tag{4.21b}$$

$$[\tau_n^{(A)}]_r(\phi) = (2n+1)(2n+2)\big(\alpha_{2n} P_{2n}(\cos\phi) + \beta_{2n} P_{2n+2}(\cos\phi)\big), \tag{4.21c}$$

$$\begin{aligned}[\tau_n^{(A)}]_\phi(\phi) &= (\alpha_{2n} + \epsilon_{2n}) P'_{2n+1}(\cos\phi) - (2n+1)(2n+2) \\ &\quad \times \big(\alpha_{2n} P_{2n}(\cos\phi) + (\alpha_{2n} - 2n + 2 - 4\nu) P_{2n+2}(\cos\phi)\big),\end{aligned} \tag{4.21d}$$

$$\begin{aligned}[\tau_n^{(A)}]_\theta(\phi) &= -(4n+3)\big((2n+1)(2n+2)(1-2\nu) P_{2n+2}(\cos\phi) \\ &\quad + (2n - 1 + 2\nu) P'_{2n+1}(\cos\phi)\big),\end{aligned} \tag{4.21e}$$

$$[\tau_n^{(A)}]_{r\phi}(\phi) = \sin\phi\big((2n+2)\alpha_{2n} P'_{2n}(\cos\phi) + (2n+1)\alpha_{2n+1} P'_{2n+2}(\cos\phi)\big). \tag{4.21f}$$

In the case $n = -1$, the components of functions $\boldsymbol{w}_n^{(B)}$, $\boldsymbol{\tau}_n^{(B)}$ are

$$2\mu[w_{-1}^{(B)}]_r(\phi) = -\big(1 - 2\nu + 4(1-\nu)\cos\phi\big), \tag{4.22a}$$

$$2\mu[w_{-1}^{(B)}]_\phi(\phi) = \sin\phi\big(3 - 4\nu - (1-2\nu) q(\phi)\big), \tag{4.22b}$$

$$[\tau_{-1}^{(B)}]_r(\phi) = 1 - 2\nu + 2(2-\nu)\cos\phi, \tag{4.22c}$$

$$[\tau_{-1}^{(B)}]_\phi(\phi) = -(1-2\nu)\big(1 + \cos\phi - q(\phi)\big), \tag{4.22d}$$

$$[\tau_{-1}^{(B)}]_\theta(\phi) = -(1-2\nu)\big(\cos\phi + q(\phi)\big), \tag{4.22e}$$

$$[\tau_{-1}^{(B)}]_{r\phi}(\phi) = -(1-2\nu)\sin\phi\big(1 - q(\phi)\big), \tag{4.22f}$$

whereas in the case $n = 0, 1, 2, \ldots$, they are

$$2\mu[w_n^{(B)}]_r(\phi) = -(2n+2)\big(\alpha_{2n+2}P_{2n+1}(\cos\phi) + \gamma_{2n+1}P_{2n+3}(\cos\phi)\big), \tag{4.23a}$$

$$2\mu[w_n^{(B)}]_\phi(\phi) = -\sin\phi\big(\alpha_{2n+2}P'_{2n+1}(\cos\phi) + \epsilon_{2n+1}P'_{2n+3}(\cos\phi)\big), \tag{4.23b}$$

$$[\tau_n^{(B)}]_r(\phi) = (2n+2)(2n+3)\big(\alpha_{2n+2}P_{2n+1}(\cos\phi) + \beta_{2n+1}P_{2n+3}(\cos\phi)\big), \tag{4.23c}$$

$$\begin{aligned}[\tau_n^{(B)}]_\phi(\phi) = {}& \big(\alpha_{2n+2} + \epsilon_{2n+1}\big)P'_{2n+2}(\cos\phi) - (2n+2)(2n+3) \\ & \times \big(\alpha_{2n+2}P_{2n+1}(\cos\phi) + (\alpha_{2n+1} - 2n + 1 - 4\nu)P_{2n+3}(\cos\phi)\big),\end{aligned} \tag{4.23d}$$

$$\begin{aligned}[\tau_n^{(B)}]_\theta(\phi) = {}& -(4n+5)\big((2n+2)(2n+3)(1-2\nu)P_{2n+3}(\cos\phi) \\ & + (2n+1+2\nu)P'_{2n+2}(\cos\phi)\big),\end{aligned} \tag{4.23e}$$

$$[\tau_n^{(B)}]_{r\phi}(\phi) = \sin\phi\,\alpha_{2n+2}\big((2n+3)P'_{2n+1}(\cos\phi) + (2n+2)P'_{2n+3}(\cos\phi)\big), \tag{4.23f}$$

where the coefficients β_{2n}, γ_{2n} and ϵ_{2n} are defined as

$$\begin{aligned}\beta_{2n} &= (2n+2)(2n+5) - 2\nu, \\ \gamma_{2n} &= (2n+2)(2n+5-4\nu), \\ \epsilon_{2n} &= (2n+1)(2n-2+4\nu).\end{aligned}$$

4.1.2. Axisymmetric boundary conditions

Let us briefly analyse the fulfilment of the axisymmetric boundary conditions on Γ_s, given in (2.12d). We have that

$$\boldsymbol{\sigma}(\boldsymbol{v})\hat{\boldsymbol{\phi}}\cdot\hat{\boldsymbol{r}} = (\sigma_{r\phi}(\boldsymbol{v})\hat{\boldsymbol{r}} + \sigma_\phi(\boldsymbol{v})\hat{\boldsymbol{\phi}})\cdot\hat{\boldsymbol{r}} = \sigma_{r\phi}(\boldsymbol{v}), \tag{4.24}$$

and

$$\boldsymbol{v}\cdot\hat{\boldsymbol{\phi}} = v_\phi, \tag{4.25}$$

so we need that the component v_ϕ of (4.20a) and the component $\sigma_{r\phi}$ of (4.20b) vanish on Γ_∞, that is, for $\phi = \pi$ (cf. (2.6b)). Actually, these conditions are already fulfilled due to the factor $\sin\phi$ existing in (4.21b), (4.21f), (4.22b), (4.22f), (4.23b) and (4.23f). Consequently,

the analytical solution given in (4.20a)-(4.20b) satisfies also (2.12d). In the next section, we impose the boundary conditions on Γ_h, given in (2.12c).

4.2. Numerical enforcement of boundary conditions on the hemispherical pit

Up to now, we have obtained a solution in series form, given in (4.20a)-(4.20b), which satisfies the elasticity equation (2.12a), the traction-free boundary conditions on the infinite plane surface (2.12b), the axisymmetric boundary conditions on the vertical surface (2.12d), and the decaying condition at infinity (2.12e). It is a fully analytical solution, since no numerical approximation has been introduced yet. In the present section, we enforce this solution to satisfy the boundary conditions on the hemispherical surface (2.12c), which is only possible in numerical form, so the sought solution becomes semi-analytical. This numerical enforcement is done by means of minimising a quadratic functional, as described below.

4.2.1. Truncation of the series

The fulfilment of the boundary conditions on the pit (2.12c) is directly related to the coefficients A_n and B_n in (4.20a)-(4.20b), which have to be chosen in such a way that (2.12c) is satisfied. However, there is an infinite number of coefficients A_n and B_n, which are determined by an infinite set of simultaneous linear equations. Hence, it is not possible to calculate them exactly, keeping the analytical nature of the solution. This drawback is overcome by truncating the infinite series in (4.20a)-(4.20b) at a finite order N, which introduces the first numerical approximation to our procedure and gives rise to a semi-analytical solution of (2.12). The truncated solution is given by

$$\boldsymbol{v}_N(r,\phi) = \sum_{n=0}^{N} A_n \Big(\frac{h}{r}\Big)^{2n+2} \boldsymbol{w}_n^{(A)}(\phi) + \sum_{n=-1}^{N} B_n \Big(\frac{h}{r}\Big)^{2n+3} \boldsymbol{w}_n^{(B)}(\phi), \tag{4.26a}$$

$$\boldsymbol{\sigma}_N(r,\phi) = \frac{1}{h}\Bigg[\sum_{n=0}^{N} A_n \Big(\frac{h}{r}\Big)^{2n+3} \boldsymbol{\tau}_n^{(A)}(\phi) + \sum_{n=-1}^{N} B_n \Big(\frac{h}{r}\Big)^{2n+4} \boldsymbol{\tau}_n^{(B)}(\phi)\Bigg]. \tag{4.26b}$$

This approximation fixes a finite number of coefficients A_n and B_n that are to be calculated. This is done by solving a finite linear system of equations for the coefficients A_n and B_n, which is obtained next.

4.2.2. Quadratic functional and its matrix form

The method to determine a linear system of equations satisfied by the coefficients A_n and B_n is based upon the minimisation of a quadratic functional, which we define as

$$\mathcal{J}(\boldsymbol{v}_N) = \frac{1}{2h}\int_{\Gamma_h} \boldsymbol{\sigma}_N\,\hat{\boldsymbol{r}}\cdot\boldsymbol{v}_N\,\mathrm{d}s - \frac{1}{h}\int_{\Gamma_h}\boldsymbol{f}\cdot\boldsymbol{v}_N\,\mathrm{d}s, \tag{4.27}$$

where $\boldsymbol{v}_N$ and $\boldsymbol{\sigma}_N$ are given in (4.26a) and (4.26b), respectively, and $\boldsymbol{f}$ is the vector function that arises at the right-hand side of (2.12c), whose components in r and ϕ were defined in (2.14a) and (2.14b), respectively. The first term in the right-hand side of (4.27) is quadratic in $\boldsymbol{v}_N$ and represents the surface elastic potential energy on Γ_h. The minus sign has been chosen in order to obtain a strictly convex functional. The second term is linear in $\boldsymbol{v}_N$ and is related to the right-hand side vector function $\boldsymbol{f}$. Although we have assumed a particular function $\boldsymbol{f}$, the subsequent analysis is valid for any piecewise continuous function $\boldsymbol{f}:\Gamma_h\to\mathbb{R}^2$ satisfying $f_\phi(\pi)=0$. Moreover, $\boldsymbol{v}_N$ and $\boldsymbol{\sigma}_N$ are regarded in (4.27) as generic functions depending on the arbitrary coefficients $A_0, A_1, A_2, \ldots, A_N$ and $B_{-1}, B_0, B_1, \ldots, B_N$, respectively, which are to be determined in order to minimise the functional J. Expressing $\boldsymbol{v}_N$, $\boldsymbol{\sigma}_N$ $\boldsymbol{f}$ in terms of their respective components in r and ϕ, making explicit the integrals and rearranging terms, (4.27) is rewritten as

$$\begin{aligned}\mathcal{J}(\boldsymbol{v}_N) = \frac{h}{2}\int_{\pi/2}^{\pi}\big([\sigma_N]_r(h,\phi)[v_N]_r(h,\phi) + [\sigma_N]_{r\phi}(h,\phi)[v_N]_\phi(h,\phi)\big)\sin\phi\,\mathrm{d}\phi \\ -h\int_{\pi/2}^{\pi}\big(f_r(h,\phi)[v_N]_r(h,\phi) + f_\phi(h,\phi)[v_N]_\phi(h,\phi)\big)\sin\phi\,\mathrm{d}\phi,\end{aligned} \tag{4.28}$$

and next, the components of $\boldsymbol{v}_N$ and $\boldsymbol{\sigma}_N$ in (4.26a) and (4.26b) are evaluated at $r=h$ and substituted in (4.28). Expanding the resulting terms and collecting the products A_nA_k,

A_nB_k, B_nA_k and B_nB_k, the functional J is reexpressed as

$$\begin{aligned}\mathcal{J}(\boldsymbol{v}_N) = &\frac{1}{2}\sum_{n=0}^{N}\sum_{k=0}^{N} Q_{nk}^{(AA)} A_nA_k + \frac{1}{2}\sum_{n=0}^{N}\sum_{k=-1}^{N} Q_{nk}^{(AB)} A_nB_k \\ &+ \frac{1}{2}\sum_{n=-1}^{N}\sum_{k=0}^{N} Q_{nk}^{(BA)} B_nA_k + \frac{1}{2}\sum_{n=-1}^{N}\sum_{k=-1}^{N} Q_{nk}^{(BB)} B_nB_k \\ &- \sum_{n=0}^{N} y_n^{(A)} A_n - \sum_{n=-1}^{N} y_n^{(B)} B_n,\end{aligned} \tag{4.29}$$

where the terms $Q_{nk}^{(AA)}$, $Q_{nk}^{(AB)}$, $Q_{nk}^{(BA)}$, $Q_{nk}^{(BB)}$, $y_n^{(A)}$ and $y_n^{(B)}$ correspond to the entries of matrices $\boldsymbol{Q}^{(AA)} \in \mathbf{M}_{N+1}(\mathbb{R})$, $\boldsymbol{Q}^{(AB)} \in \mathbf{M}_{(N+1)\times(N+2)}(\mathbb{R})$, $\boldsymbol{Q}^{(BA)} \in \mathbf{M}_{(N+2)\times(N+1)}(\mathbb{R})$, $\boldsymbol{Q}^{(BB)} \in \mathbf{M}_{N+2}(\mathbb{R})$ and vectors $\boldsymbol{y}^{(A)} \in \mathbb{R}^{N+1}$ and $\boldsymbol{y}^{(B)} \in \mathbb{R}^{N+2}$, respectively. These entries are defined as the following integrals:

$$Q_{nk}^{(\alpha\beta)} = -\int_{\pi/2}^{\pi} \Big([w_n^{(\alpha)}]_r(\phi)[\tau_k^{(\beta)}]_r(\phi) + [w_n^{(\alpha)}]_\phi(\phi)[\tau_k^{(\beta)}]_{r\phi}(\phi) \Big) \sin\phi \, \mathrm{d}\phi, \tag{4.30a}$$

$$y_n^{(\alpha)} = -h\int_{\pi/2}^{\pi} \Big([w_n^{(\alpha)}]_r(\phi) f_r(\phi) + [w_n^{(\alpha)}]_\phi(\phi) f_\phi(\phi) \Big) \sin\phi \, \mathrm{d}\phi, \tag{4.30b}$$

where $\alpha, \beta = A, B$. Substituting (2.14a), (2.14b), (4.21a), (4.21b), (4.21c), (4.21f), (4.22a), (4.22b), (4.22c), (4.22f), (4.23a), (4.23b), (4.23c), (4.23f) in (4.30a) and (4.30b) as appropriate leads us to obtain expressions for the quantities $Q_{nk}^{(\alpha\beta)}$ and $y_n^{(\alpha)}$ in terms of explicit integrals. These expressions are too cumbersome to be reproduced here. However, with the aid of the integral formulae provided in the Appendix 6.1, all the involved integrals are calculated exactly, yielding explicit expressions for the entries of matrices $\boldsymbol{Q}^{(\alpha\beta)}$ and vectors $\boldsymbol{y}^{(\alpha)}$ which we reproduce next for $\alpha, \beta = A, B$. The entries of the matrix $\boldsymbol{Q}^{(AA)}$ are computed by using (6.4a) and (6.4d), corresponding to a tridiagonal symmetric matrix with main diagonal entries

$$\begin{aligned}2\mu Q_{nn}^{(AA)} = &\frac{(2n+1)(2n+2)(4n+3)}{(4n+5)} \\ &\times \big((2n+3)(16n^3 + 32n^2 + 22n + 8\nu^2 - 12\nu + 9) + 4(1-\nu^2) \big),\end{aligned} \tag{4.31a}$$

where $0 \leq n \leq N$, and sub-diagonal and super-diagonal entries

$$\begin{aligned} 2\mu Q^{(AA)}_{n,n+1} = Q^{(AA)}_{n+1,n} &= \frac{(2n+1)(2n+2)(2n+3)(2n+4)(4n+3)}{(4n+5)} \\ &\times \big((2n+2)(2n+4) - 1 + 2\nu\big), \end{aligned} \tag{4.31b}$$

where $0 \leq n \leq N-1$. The entries of matrices $\boldsymbol{Q}^{(AB)}$ and $\boldsymbol{Q}^{(BA)}$ are calculated by using (6.4a), (6.4c), (6.4f) and (6.5a). It is obtained that they correspond to full matrices satisfying $\boldsymbol{Q}^{(BA)} = [\boldsymbol{Q}^{(AB)}]^T$. The entries of $\boldsymbol{Q}^{(AB)}$ in the case $k = -1$ are given by

$$2\mu Q^{(AB)}_{n,-1} = -\frac{4(4n+3)(2n(2n+3)\nu(\nu-2) - 3 + 5\nu - 4\nu^2)P_{2n}(0)}{(2n-1)(2n+2)(2n+4)}, \tag{4.32a}$$

and in the case $0 \leq k \leq N+1$ are given by

$$2\mu Q^{(AB)}_{nk} = \frac{4(2k+1)(2k+3)(4k+5)(2n+1)(4n+3)\eta_{nk}\, P_{2n}(0)P_{2k}(0)}{(2k+6+2n)(2k+3-2n)(2k+4+2n)(2k-1-2n)(2k+1-2n)}, \tag{4.32b}$$

where

$$\begin{aligned} \eta_{nk} &= 51 + 58k + 32k^2n^2 + 188kn + 138n + 56k^2n + 72n^2 + 16k^2 + 104kn^2 \\ &- \big((2k-1-2n)\big(4n^2(2k+4) - 4k((2k+5)n + 2k + 6) - 21\big) - 8k(2k+2)\big)\nu \\ &- (2k+3-2n)(2k+6+2n)(2k-1-2n)\nu^2, \end{aligned}$$

and $0 \leq n \leq N$. The entries of matrix $\boldsymbol{Q}^{(BB)}$ are calculated by using (6.4b), (6.4c), (6.4e), and (6.5b), together with some elementary primitives of trigonometric functions. It is obtained that $\boldsymbol{Q}^{(BB)}$ corresponds to a symmetric matrix that is almost tridiagonal, except for its first row and its first column, which are full. The entries associated with the first row and column of $\boldsymbol{Q}^{(BB)}$ are

$$2\mu Q^{(BB)}_{-1,-1} = 2(1-2\nu)^2 \ln 2 + \frac{2}{3}(2 + 5\nu - 6\nu^2), \tag{4.33a}$$

$$\begin{aligned} 2\mu Q^{(BB)}_{n,-1} = Q^{(BB)}_{-1,n} &= -\frac{2(1-2\nu)(4n+5)(2n+1)\big((2n+4)\nu - 1\big)P_{2n}(0)}{(2n+2)(2n+4)} \\ &+ 2(7+2\nu)\delta_{n0}, \end{aligned} \tag{4.33b}$$

where $0 \leq n \leq N$ and δ_{nk} stands for the Kronecker delta. The entries associated with the tridiagonal part of $\boldsymbol{Q}^{(BB)}$ are the main diagonal entries

$$\begin{aligned} 2\mu Q_{nn}^{(BB)} &= \frac{(4n+5)(2n+2)(2n+3)}{(4n+7)} \\ &\times (32n^4+208n^3+492n^2+4(125-2\nu+4\nu^2)n+187-20\nu+28\nu^2), \end{aligned} \tag{4.33c}$$

where $0 \leq n \leq N$, and the and sub-diagonal and super-diagonal entries

$$\begin{aligned} 2\mu Q_{n+1,n}^{(BB)} = Q_{n,n+1}^{(BB)} &= \frac{(4n+5)(2n+2)(2n+3)(2n+4)(2n+5)}{(4n+7)} \\ &\times ((2n+4)(2n+6)-1+2\nu), \end{aligned} \tag{4.33d}$$

where $0 \leq n \leq N-1$. The entries of vector $\boldsymbol{y}^{(A)}$ are computed by using (6.4c) and (6.4f), yielding

$$\begin{aligned} y_n^{(A)} &= \frac{2\varrho g h^2(4n+3)(2n+1)P_{2n}(0)}{(1-\nu)(2n-1)(2n+2)(2n+4)(2n+6)} \\ &\times (4(2n+3)-6\nu(3n+5)+\nu^2(2n+4)(2n+6)), \end{aligned} \tag{4.34}$$

where $0 \leq n \leq N$. Fig. 4.1 shows schematically the structure of matrices $\boldsymbol{Q}$. The entries of vector $\boldsymbol{y}^{(B)}$ are computed by using (6.4b), (6.4c), (6.4e) and (6.5b). It is obtained that only the first two entries of $\boldsymbol{y}^{(B)}$ are different from zero. These entries are given by

$$y_{-1}^{(B)} = \frac{\varrho g h^2(26-47\nu+30\nu^2)}{30(1-\nu)}, \tag{4.35a}$$

$$y_0^{(B)} = \frac{2\varrho g h^2(46-71\nu+70\nu^2)}{21(1-\nu)}. \tag{4.35b}$$

We define also the vectors $\boldsymbol{A} \in \mathbb{R}^{N+1}$ and $\boldsymbol{B} \in \mathbb{R}^{N+2}$ as those whose entries correspond to the coefficients A_n and B_n to be computed. From the above matrices and vectors, we also define the square matrix $\boldsymbol{Q} \in \mathbf{M}_{2N+3}(\mathbb{R})$ and the vectors $\boldsymbol{x}, \boldsymbol{y} \in \mathbb{R}^{2N+3}$ by blocks as

$$\boldsymbol{Q} = \begin{bmatrix} \boldsymbol{Q}^{(AA)} & \boldsymbol{Q}^{(AB)} \\ [\boldsymbol{Q}^{(AB)}]^T & \boldsymbol{Q}^{(BB)} \end{bmatrix}, \qquad \boldsymbol{x} = \begin{bmatrix} \boldsymbol{A} \\ \boldsymbol{B} \end{bmatrix}, \qquad \boldsymbol{y} = \begin{bmatrix} \boldsymbol{y}^{(A)} \\ \boldsymbol{y}^{(B)} \end{bmatrix}, \tag{4.36}$$

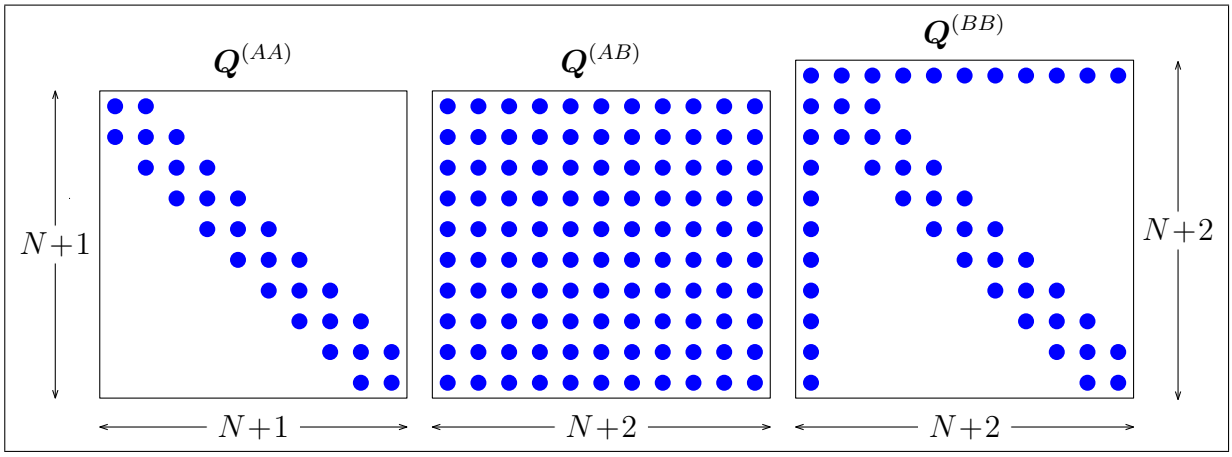

Figure 4.1. Structure of matrices $\boldsymbol{Q}^{(AA)}$,$\boldsymbol{Q}^{(AB)}$ and $\boldsymbol{Q}^{(BB)}$.

which allow us to reexpress the functional $\mathcal{J}$ given in (4.29) as the following quadratic form in $\boldsymbol{x}$:

$$\mathcal{J}(\boldsymbol{x}) = \frac{1}{2}\boldsymbol{x}^T\boldsymbol{Q}\boldsymbol{x} - \boldsymbol{x}^T\boldsymbol{y}. \tag{4.37}$$

4.2.3. Linear system and method of inversion

A linear system for the coefficients A_n and B_n is obtained by minimisation of the functional J. It holds that $\boldsymbol{Q}$ is a symmetric matrix, due to the properties of its blocks $\boldsymbol{Q}^{(ij)}$, and it is also positive definite, thanks to the elliptic nature of the elastostatic boundary-value problem. Therefore, J has a global minimum, which is reached when $\nabla\mathcal{J}(\boldsymbol{x}) = \boldsymbol{Q}\boldsymbol{x}-\boldsymbol{y} = \boldsymbol{0}$, or equivalently, when

$$\boldsymbol{Q}\boldsymbol{x} = \boldsymbol{y}. \tag{4.38}$$

Eq. (4.38) corresponds to the sought linear system of equations for the coefficients A_n and B_n. We take advantage of the symmetry and positive definiteness of $\boldsymbol{Q}$ in solving (4.38). Expressing $\boldsymbol{Q}$, $\boldsymbol{x}$ and $\boldsymbol{y}$ by blocks in (4.38) yields

$$\begin{bmatrix} \boldsymbol{Q}^{(AA)} & \boldsymbol{Q}^{(AB)} \\ [\boldsymbol{Q}^{(AB)}]^T & \boldsymbol{Q}^{(BB)} \end{bmatrix} \begin{bmatrix} \boldsymbol{A} \\ \boldsymbol{B} \end{bmatrix} = \begin{bmatrix} \boldsymbol{y}^{(A)} \\ \boldsymbol{y}^{(B)} \end{bmatrix}, \tag{4.39}$$

and this system is inverted with the aid of the so-called Schur-Banachiewicz blockwise inversion formula (cf. (Björck, 1996)), which is given by

$$\begin{aligned}\boldsymbol{A} = &\big([\boldsymbol{Q}^{(AA)}]^{-1} + [\boldsymbol{Q}^{(AA)}]^{-1}\boldsymbol{Q}^{(AB)}[\widetilde{\boldsymbol{Q}}^{(BB)}]^{-1}[\boldsymbol{Q}^{(AB)}]^{T}[\boldsymbol{Q}^{(AA)}]^{-1}\big)\boldsymbol{y}^{(A)} \\ &- [\boldsymbol{Q}^{(AA)}]^{-1}\boldsymbol{Q}^{(AB)}[\widetilde{\boldsymbol{Q}}^{(BB)}]^{-1}\boldsymbol{y}^{(B)},\end{aligned} \tag{4.40a}$$

$$\boldsymbol{B} = -[\widetilde{\boldsymbol{Q}}^{(BB)}]^{-1}[\boldsymbol{Q}^{(AB)}]^{T}[\boldsymbol{Q}^{(AA)}]^{-1}\boldsymbol{y}^{(A)} + [\widetilde{\boldsymbol{Q}}^{(BB)}]^{-1}\boldsymbol{y}^{(B)}, \tag{4.40b}$$

where $\widetilde{\boldsymbol{Q}}^{(BB)}$ denotes the Schur complement of $\boldsymbol{Q}^{(BB)}$ in $\boldsymbol{Q}$, defined as

$$\widetilde{\boldsymbol{Q}}^{(BB)} = \boldsymbol{Q}^{(BB)} - [\boldsymbol{Q}^{(AB)}]^{T}[\boldsymbol{Q}^{(AA)}]^{-1}\boldsymbol{Q}^{(AB)}. \tag{4.41}$$

To evaluate (4.40a) and (4.40b), it suffices to inverse the symmetric and positive definite matrices $\boldsymbol{Q}^{(AA)}$ and $\widetilde{\boldsymbol{Q}}^{(BB)}$. As $\boldsymbol{Q}^{(AA)}$ is in addition a tridiagonal matrix, it is efficiently inverted by using the Thomas algorithm for tridiagonal systems (cf. (Golub & Loan, 1996), Algorithm 4.3.6). To invert $\widetilde{\boldsymbol{Q}}^{(BB)}$, we employ its Cholesky factorisation, which is quickly obtained with the aid of a suitable algorithm (cf. (Golub & Loan, 1996), Algorithm 4.2.1). We thus establish the following algorithm to compute the coefficients A_n and B_n:

(i) Compute the coefficients for tridiagonal inversion of $\boldsymbol{Q}^{(AA)}$.

(ii) Use the coefficients to evaluate $[\boldsymbol{Q}^{(AA)}]^{-1}\boldsymbol{y}^{(A)}$ and $[\boldsymbol{Q}^{(AA)}]^{-1}\boldsymbol{Q}^{(AB)}$.

(iii) Calculate the Schur complement $\widetilde{\boldsymbol{Q}}^{(BB)}$ using (4.41).

(iv) Obtain the Cholesky factorisation of $\widetilde{\boldsymbol{Q}}^{(BB)}$.

(v) Use the Cholesky factorisation to evaluate $[\widetilde{\boldsymbol{Q}}^{(BB)}]^{-1}\boldsymbol{y}^{(B)}$ and $[\widetilde{\boldsymbol{Q}}^{(BB)}]^{-1}[\boldsymbol{Q}^{(AB)}]^{T}$.

(vi) Assemble $\boldsymbol{A}$ and $\boldsymbol{B}$ as indicated in (4.40a) and (4.40b).

This algorithm yields approximate values for the two series of coefficients $A_0, A_1, A_2, \ldots, A_N$ and $B_{-1}, B_0, B_1, \ldots, B_N$. By substituting these values in (4.26a) and (4.26b), we obtain the desired semi-analytical solution of the boundary-value problem (2.12) in explicit way.

4.3. Numerical results and validation

In this section, we present numerical results obtained with the semi-analytical method described throughout Chapter 4. Prior to this, the convergence of the series is numerically

verified and a convergence criterion is established in order to determine a suitable value for the truncation parameter N. Furthermore, the procedure is validated by comparing our semi-analytical solution with results obtained numerically using the commercial software COMSOL Multiphysics. The unbounded domain Ω is truncated by means of an artificial square box.

4.3.1. Numerical results

The semi-analytical method described in Chapter 3 and Section 4.2 was implemented in its entirety, and the obtained solution was numerically evaluated for different values of N. The considered numerical values of the gravity acceleration g, the radius of the pit h, the density ϱ, the Young's modulus E and the Poisson's ratio ν are shown in Table **??**.To

Table 4.1. Numerical values of the physical parameters.

Parameter	h	g	ϱ	E	ν
Value	600 m	9.81 m/s^2	2725 kg/m^3	70.2 GPa	0.3

evaluate numerically the semi-analytical solution of (2.12) and analyse its convergence as the truncation parameter N tends to infinity, we consider a bounded subregion of Ω, defined in axisymmetric spherical coordinates by the points (r, ϕ) satisfying $h \leq r \leq 2000$ m and $\pi/2 \leq \phi \leq \pi$. The evaluations are performed at the points (r_i, ϕ_j) of an equispaced rectangular grid in the (r, ϕ)-plane, defined as $r_i = h + i\Delta r$ and $\phi_j = \pi/2 + j\Delta\phi$, where $i = 0, 1, 2, \ldots, 140$, $\Delta r = 10$ m, $j = 0, 1, 2, \ldots, 500$, and $\Delta\phi = \pi/1000$. In order to test numerically the convergence of the series in terms of N, we compute the relative error between two successive solutions, considering separately the displacement field $\boldsymbol{v}$ and the stress tensor $\boldsymbol{\sigma}(\boldsymbol{v})$. The respective relative errors are defined as

$$e_N(\boldsymbol{v}) = \frac{|\boldsymbol{v}_{N+1} - \boldsymbol{v}_N|}{|\boldsymbol{v}_N|}, \qquad e_N(\boldsymbol{\sigma}) = \frac{|\boldsymbol{\sigma}_{N+1}(\boldsymbol{v}_{N+1}) - \boldsymbol{\sigma}_N(\boldsymbol{v}_N)|}{|\boldsymbol{\sigma}_N(\boldsymbol{v}_N)|}, \tag{4.42}$$

where in the latter case, $|\cdot|$ corresponds to the matrix Euclidean norm (or Frobenius norm). Successive values of the truncation parameter up to $N = 100$ were considered in the analysis. A semi-logarithmic plot with both relative errors in function of N is presented in Fig. 4.2, where it is observed that both of them decrease as N increases, exhibiting the

error associated with the stress tensor a slower decrease. We conclude from this analysis that the semi-analytical method shows an acceptable convergence. In order to set a value of N for evaluation of the semi-analytical solution, we have used as a convergence criterion that both relative errors have to be smaller than a tolerance of 0.001%, yielding the value $N = 40$ (see Fig. 4.2), which we assume from now on. Having already calculated the solution $\boldsymbol{v}$, the physical displacement field $\boldsymbol{u}$ is obtained by adding the lithostatic displacement field $\boldsymbol{u}_g$ (evaluated at the same rectangular grid), as indicated in (2.10). The physical stress tensor $\boldsymbol{\sigma}(\boldsymbol{u})$ is obtained in a similar way, by adding to $\boldsymbol{\sigma}(\boldsymbol{v})$ the lithostatic stress tensor $\boldsymbol{\sigma}(\boldsymbol{u}_g)$, whose components are explicitly obtained by substituting (2.10) in (2.7). The values of the displacement components u_r and u_ϕ, and the stress components $\sigma_r(\boldsymbol{u})$, $\sigma_\phi(\boldsymbol{u})$, $\sigma_\theta(\boldsymbol{u})$ and $\sigma_{r\phi}(\boldsymbol{u})$ are depicted in Fig. 4.3. It is observed from the plots of stress components that obtained semi-analytical solution fulfils the boundary conditions (2.9b), (2.9c) and (2.9d).

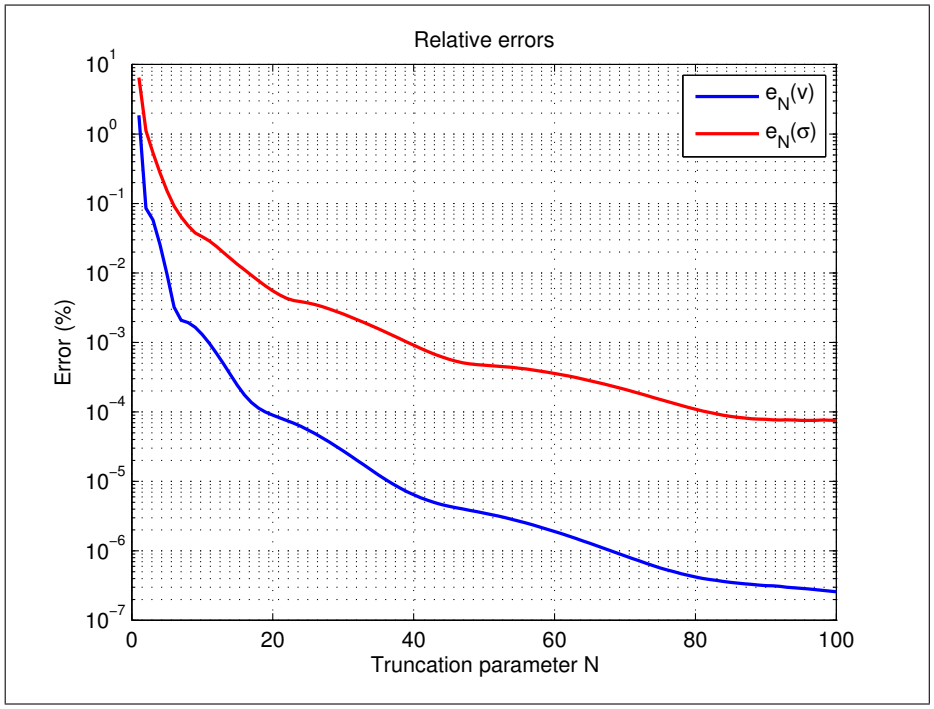

Figure 4.2. Relative error of the solution between two successive iterations in N.

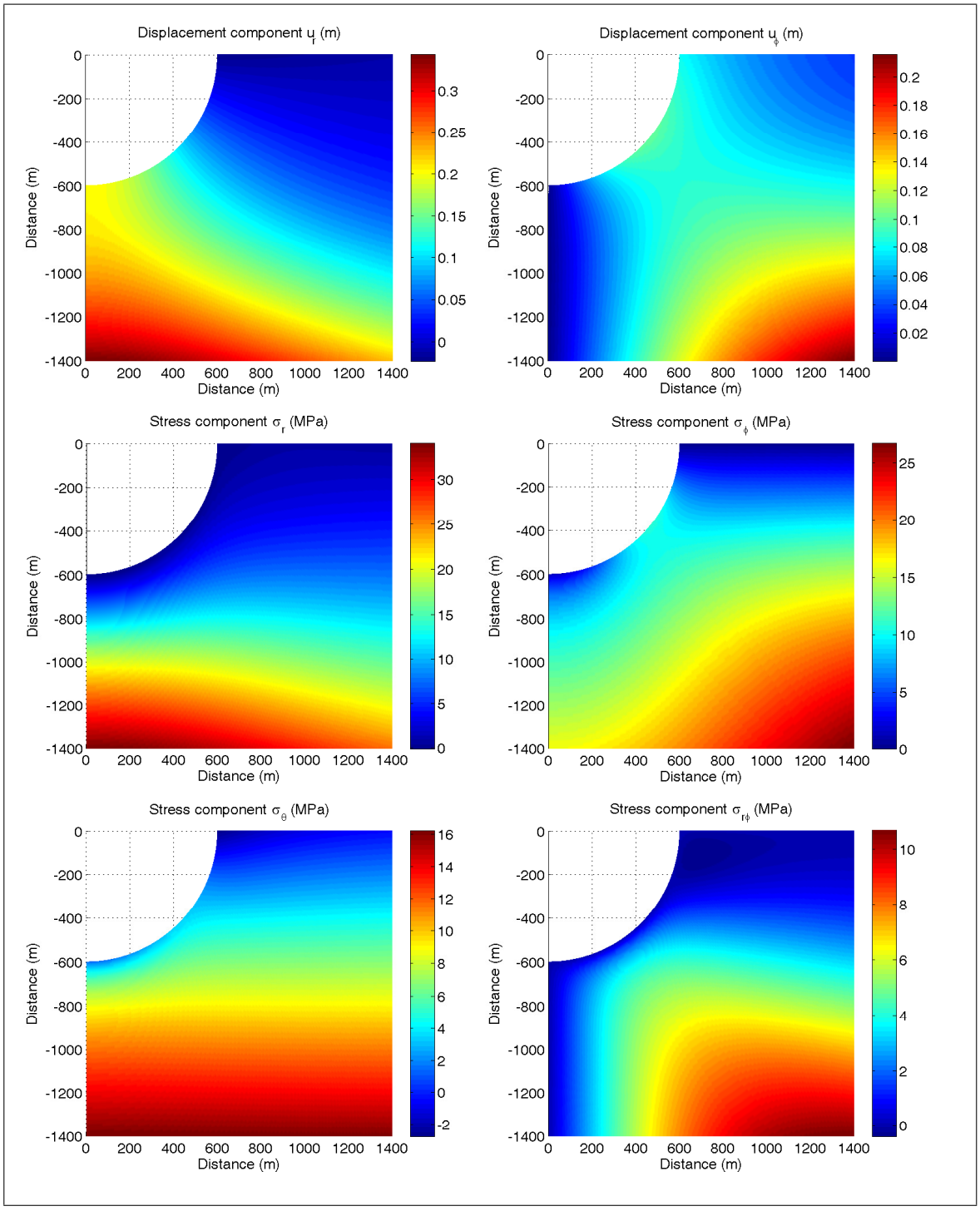

Figure 4.3. Plots of displacement and stress components obtained in Ω.

4.3.2. Validation of the procedure

In order to confirm the correctness of the semi-analytical solution, a validation test was carried out. For this, the axisymmetric boundary-value problem in $\boldsymbol{u}$ (2.9) was numerically solved using the commercial finite element software COMSOL Multiphysics, with the physical parameters of the problem fixed to the same numerical values indicated in Table **??**. The purpose of this numerical simulation is to compare the results calculated by such means with those obtained by using the semi-analytical method proposed herein. As this type of software is only able to deal with bounded regions, the unbounded domain Ω was truncated by means of an artificial square box of length L, as indicated schematically in Fig. 4.4. In order to be able to solve (2.9) in the truncated domain (denoted by Ω_{tr}), the decaying condition at infinity (2.9e) was replaced by artificial Dirichlet boundary conditions on the right and bottom boundaries, with the displacements set to the lithostatic displacement $\boldsymbol{u}_g$ field given in (2.10). Different values of the length L were considered, starting from a minimum value of $L = 1000\ \mathrm{m}$ up to a maximum value of $L = 13000\ \mathrm{m}$, with successive increases of $\Delta L = 1000\ \mathrm{m}$. For each one of these values, non-uniform tri-

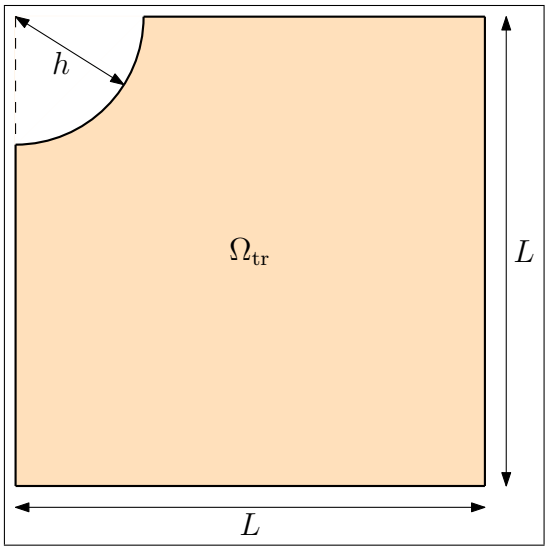

Figure 4.4. Schematic representation of the domain Ω truncated by a square box of length L.

angular meshes of the domain Ω_{tr} were generated, with the element size varying between a

minimum value of $2\ \mathrm{m}$ and a maximum value of $50\ \mathrm{m}$, and the maximum element growth rate set to 1.3. To solve numerically the boundary-value problem, standard conforming P1 finite elements in each mesh were used. Common sense indicates that as the domain size grows, the approximation of the unbounded boundary-value problem (2.9) by a bounded one becomes more accurate. Therefore, it is expected that the solution calculated numerically by finite elements approaches the semi-analytical solution as the length L increases. In order to find out whether this occurs, the displacement components u_r and u_ϕ, and the stress components σ_ϕ and σ_θ obtained by both means were compared on the surface of the pit Γ_h. The remaining stress components σ_r and $\sigma_{r\phi}$ were not considered in the comparison, since they are set to zero by the boundary condition prescribed on Γ_h (2.9c). The displacement curves obtained by the semi-analytical method, and by finite elements for some values of L, are presented separately for each displacement component in Fig. 4.5, where the horizontal axis corresponds to the angle ϕ. The stress curves for σ_ϕ and σ_θ are given in analogous way in Fig. 4.6. It is noticed from Figs. 4.5 and 4.6 that, as expected, the solution obtained by the semi-analytical method is better approximated by the solution computed numerically as the value of L increases. This behaviour is seen in the displacement as well as the stress curves, being more evident in the latter case. It is also observed from Fig. 4.5 that the component u_r obtained semi-analytically is better approximated than the component u_ϕ obtained in the same way as the value of L increases. This difference between both displacement components can be explained by the error introduced in the numerical solution by the artificial boundary conditions, particularly on the right boundary of Ω_{tr}, which affects more strongly the displacement u_ϕ near the infinite plane surface. In order to further verify the already observed tendency as L increases, the relative error of the semi-analytical solution with respect to the numerical one was evaluated on Γ_h, for all the assumed values of L, considering separately the errors associated with the displacement vector $\boldsymbol{u}$ and the stress tensor $\boldsymbol{\sigma}(\boldsymbol{u})$. Both relative error curves as functions of L are presented in a semilogarithmic plot in Fig. 4.7. These curves confirm the behaviour seen in Figs. 4.5 and 4.6: The relative error between the semi-analytical and the numerical solution decreases as L increases, both for the displacement vector and the stress tensor. In

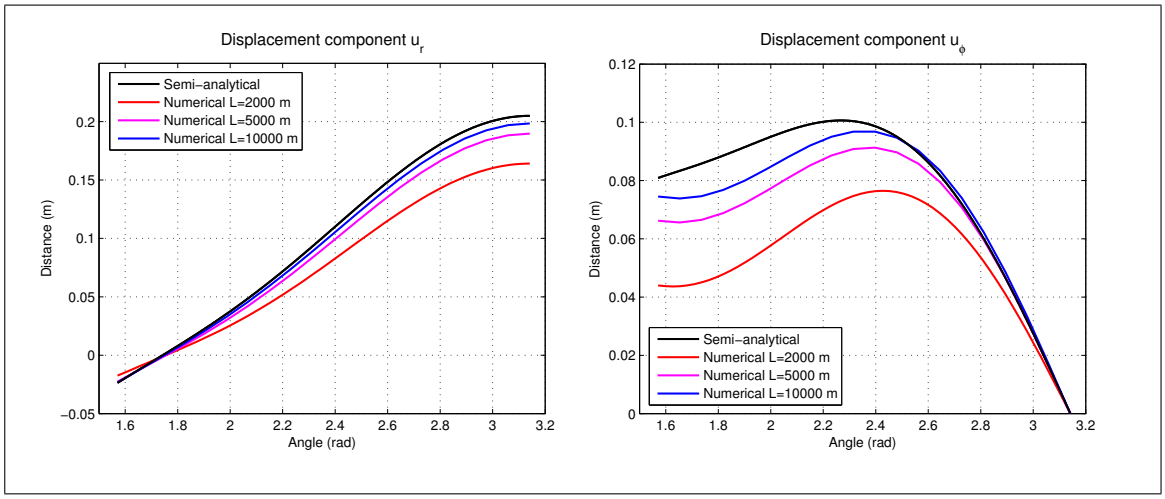

Figure 4.5. Comparison of displacement components on Γ_h.

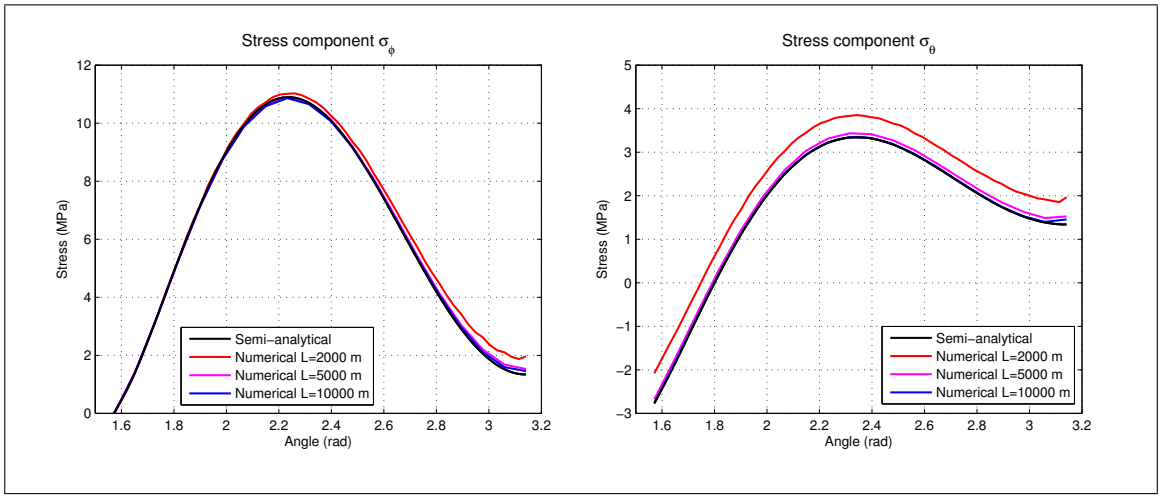

Figure 4.6. Comparison of stress components on Γ_h.

fact, both relative errors show a similar tendency, being the error in stress smaller than the error in displacement for all values of L. We confirm from this analysis the validity of the proposed semi-analytical solution.

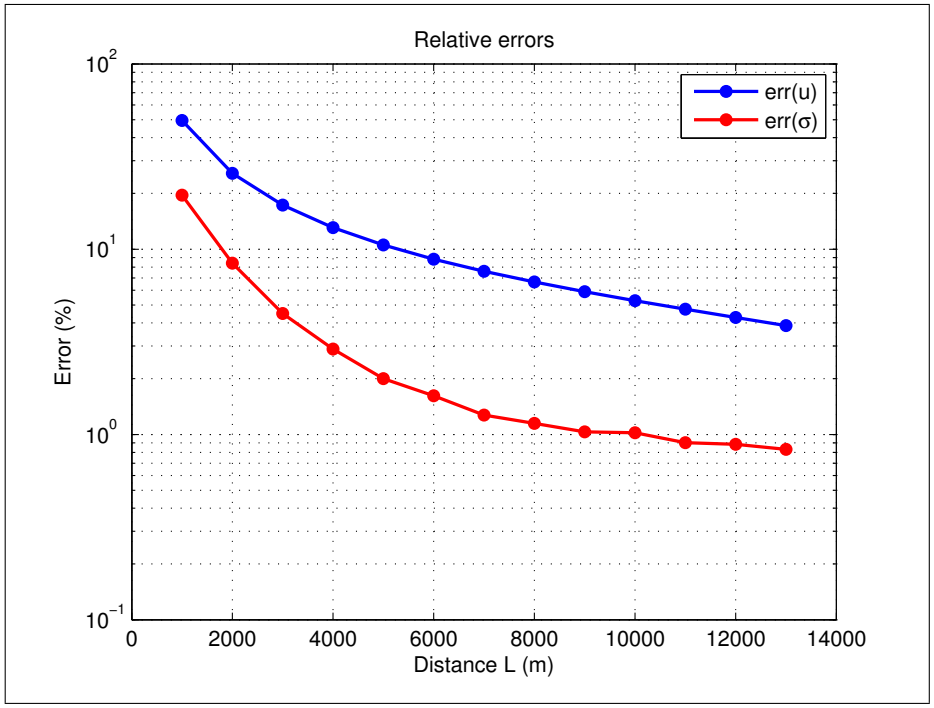

Figure 4.7. Relative errors associated with the displacement vector and the stress tensor on Γ_h.

5. A DIRICHLET-TO-NEUMANN FINITE ELEMENT METHOD FOR AXISYMMETRIC ELASTOSTATICS IN A SEMI-INFINITE DOMAIN

We present a DtN FEM procedure for boundary-value problems of elastostatics in semi-infinite domains with axisymmetry about the vertical axis. A semi-spherical artificial boundary is used to truncate the semi-infinite domain and to obtain a bounded computational domain, where a FEM scheme is employed. By using a semi-analytical procedure of solution in the unbounded residual domain lying outside the artificial boundary, the exact nonlocal boundary conditions provided by the DtN map are numerically approximated and efficiently coupled with the FEM scheme. Numerical results are provided to demonstrate the effectiveness and accuracy of the proposed method.

5.1. Mathematical formulation

5.1.1. Generalities

In this Chapter the boundary of Ω consists of three parts: A vertical boundary of axisymmetry coinciding with the axis of revolution, denoted by Γ_{s}, a horizontal unperturbed boundary coinciding with the infinite plane surface of the half-space, denoted by Γ_{∞}, and a perturbed bounded boundary which is assumed piecewise smooth, denoted by Γ_{p} (see Figure 5.1).

5.1.2. Axisymmetric elastostatic model

We consider the following elastostatic BVP in Ω: Find $\boldsymbol{u} : \Omega \to \mathbb{R}^2$ such that

$$\nabla \cdot \boldsymbol{\sigma}(\boldsymbol{u}) = \mathbf{0} \qquad \text{in } \Omega, \tag{5.1a}$$

$$\boldsymbol{\sigma}(\boldsymbol{u})\hat{\boldsymbol{z}} = \mathbf{0} \qquad \text{on } \Gamma_{\infty}, \tag{5.1b}$$

$$\boldsymbol{\sigma}(\boldsymbol{u})\hat{\boldsymbol{n}} = \boldsymbol{f} \qquad \text{on } \Gamma_{\mathrm{p}}, \tag{5.1c}$$

$$\boldsymbol{\sigma}(\boldsymbol{u})\hat{\boldsymbol{\rho}} \cdot \hat{\boldsymbol{z}} = \boldsymbol{u} \cdot \hat{\boldsymbol{\rho}} = 0 \qquad \text{on } \Gamma_{\mathrm{s}}, \tag{5.1d}$$

$$|\boldsymbol{u}| = O\big(r^{-1}\big) \qquad \text{as } r \to \infty, \tag{5.1e}$$

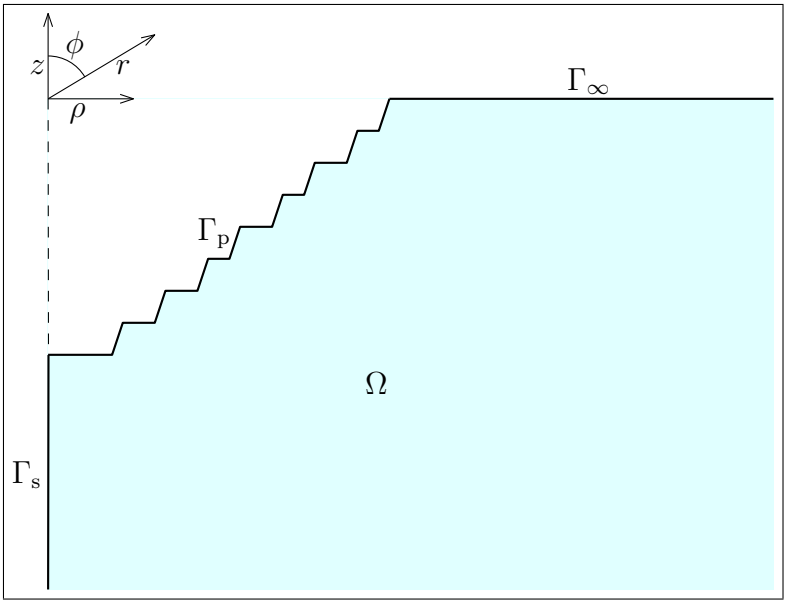

Figure 5.1. Axisymmetric semi-infinite domain.

where $\hat{\boldsymbol{n}}$ denotes the unit outward normal vector on Γ_p and $\boldsymbol{f} : \Gamma_\mathrm{p} \to \mathbb{R}^2$ is a given piecewise continuous vector function.

5.2. FEM formulation in the computational domain

5.2.1. Equivalent bounded boundary-value problem

In order to apply the DtN FEM to solve (5.1), an artificial boundary is introduced to truncate Ω, which is chosen to be a quarter circle of radius R, denoted by Γ_R (cf. Figure 5.2). Notice that if Ω is rotated about the axis of revolution to generate the 3D semi-infinite solid, Γ_R gives rise to a hemispherical surface of radius R. The bounded domain lying inside Γ_R is denoted by Ω^i, which corresponds to the computational domain. The resulting bounded parts of boundaries Γ_∞ and Γ_s are respectively denoted by Γ_∞^i and $\Gamma_\mathrm{s}^\mathrm{i}$ (cf. Figure 5.2). In order to solve (5.1), we formulate the following mathematically equivalent BVP in Ω^i: Find $\boldsymbol{u} : \Omega^\mathrm{i} \to \mathbb{R}^2$ such that

$$\nabla \cdot \boldsymbol{\sigma}(\boldsymbol{u}) = \boldsymbol{0} \qquad \text{in } \Omega^\mathrm{i}, \tag{5.2a}$$

$$\boldsymbol{\sigma}(\boldsymbol{u})\hat{\boldsymbol{z}} = \boldsymbol{0} \qquad \text{on } \Gamma_\infty^\mathrm{i}, \tag{5.2b}$$

$$\boldsymbol{\sigma}(\boldsymbol{u})\hat{\boldsymbol{n}} = \boldsymbol{f} \qquad \text{on } \Gamma_{\mathrm{p}}, \tag{5.2c}$$

$$\boldsymbol{\sigma}(\boldsymbol{u})\hat{\boldsymbol{\rho}} \cdot \hat{\boldsymbol{z}} = \boldsymbol{u} \cdot \hat{\boldsymbol{\rho}} = 0 \qquad \text{on } \Gamma_{\mathrm{s}}^{\mathrm{i}}, \tag{5.2d}$$

$$\boldsymbol{\sigma}(\boldsymbol{u})\hat{\boldsymbol{r}} = -\boldsymbol{\mathcal{M}}\boldsymbol{u} \qquad \text{on } \Gamma_R, \tag{5.2e}$$

where (5.2e) is the exact ABC on Γ_R, expressed in terms of the DtN map $\boldsymbol{\mathcal{M}}$, which we assume for the moment to be known. The definition of $\boldsymbol{\mathcal{M}}$, as well as its numerical approximation, will be discussed in detail in the next section. We have assumed that the

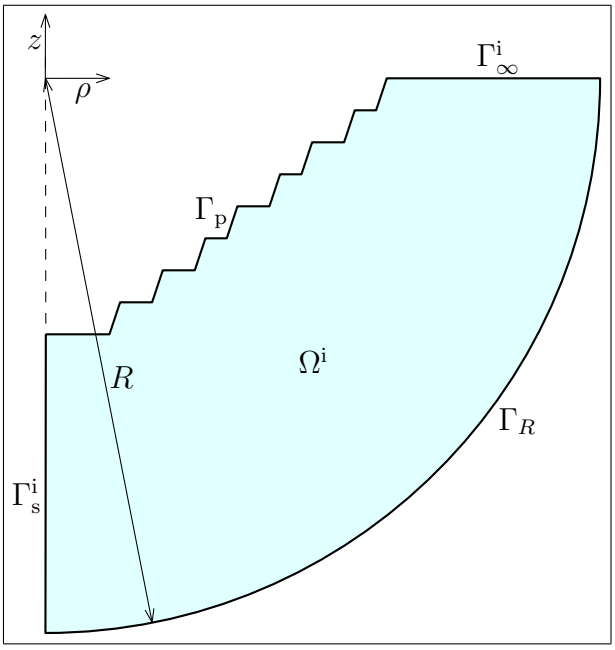

Figure 5.2. Axisymmetric computational domain.

medium occupying Ω is isotropic, homogeneous, and linear elastic. Nevertheless, the DtN FEM also applies if more general hypotheses in this regard are assumed, but restricted to the the computational domain, e.g. the medium in Ω^{i} could be inhomogeneous, anisotropic, nonlinear, and even inelastic. Moreover, nonzero right-hand sides in (5.2a) or (5.2b) are allowed as well.

5.2.2. Weak formulation

Throughout this section, we work in axisymmetric cylindrical coordinates (ρ, z). To state a weak (or variational) formulation of (5.2), we consider a Hilbert space containing

physically admissible displacement fields in Ω^{i}, defined as

$$\mathcal{V} = \left\{ \boldsymbol{v} = (v_\rho, v_z) \in [H^1(\Omega^{\mathrm{i}})]^2 : \; v_\rho = 0 \quad \text{on } \Gamma_{\mathrm{s}}^{\mathrm{i}} \right\},$$

where $H^1(\Omega^{\mathrm{i}})$ is the usual Sobolev space of L^2 functions with L^2 first derivatives. Notice that the boundary condition of zero normal displacement in Γ_{s} is included in $\mathcal{V}$. The weak formulation of (5.2) is expressed as: Find $\boldsymbol{u} \in \mathcal{V}$ such that

$$a(\boldsymbol{u}, \boldsymbol{v}) + b(\boldsymbol{u}, \boldsymbol{v}) = (\boldsymbol{f}, \boldsymbol{v})_{\Gamma_{\mathrm{p}}} \qquad \forall\, \boldsymbol{v} \in \mathcal{V}, \tag{5.3}$$

where a corresponds to the bilinear form associated with the weak formulation of the elastostatic equation, expressed in axisymmetric cylindrical coordinates (cf. (Szabo & Babuška, 1991)) as

$$a(\boldsymbol{u}, \boldsymbol{v}) = \int_{\Omega^{\mathrm{i}}} \left[\sigma_\rho(\boldsymbol{u}) \frac{\partial v_\rho}{\partial \rho} + \sigma_\theta(\boldsymbol{u}) \frac{v_\rho}{\rho} + \sigma_z(\boldsymbol{u}) \frac{\partial v_z}{\partial z} + \sigma_{\rho z}(\boldsymbol{u}) \left(\frac{\partial v_\rho}{\partial z} + \frac{\partial v_z}{\partial \rho} \right) \right] \rho \, \mathrm{d}\rho \, \mathrm{d}z, \tag{5.4}$$

whereas b is a bilinear form involving the DtN map, defined as

$$b(\boldsymbol{u}, \boldsymbol{v}) = \int_{\Gamma_R} \boldsymbol{\mathcal{M}} \boldsymbol{u} \cdot \boldsymbol{v} \, \mathrm{d}\Gamma_R, \tag{5.5}$$

and the right-hand side of (5.3) is

$$(\boldsymbol{f}, \boldsymbol{v})_{\Gamma_{\mathrm{p}}} = \int_{\Gamma_{\mathrm{p}}} \boldsymbol{f} \cdot \boldsymbol{v} \, \mathrm{d}\Gamma_{\mathrm{p}}.$$

By substituting (2.7) in (5.4), expanding terms and rearranging appropriately, a is reexpressed as

$$\begin{aligned} a(\boldsymbol{u},\boldsymbol{v}) = {} & (\lambda+2\mu)\int_{\Omega^{\mathrm{i}}}\left(\frac{\partial u_\rho}{\partial\rho}\frac{\partial v_\rho}{\partial\rho}+\frac{\partial u_z}{\partial z}\frac{\partial v_z}{\partial z}\right)\rho\,\mathrm{d}\rho\,\mathrm{d}z \\ & +\lambda\int_{\Omega^{\mathrm{i}}}\left(\frac{\partial u_\rho}{\partial\rho}\frac{\partial v_z}{\partial z}+\frac{\partial u_z}{\partial z}\frac{\partial v_\rho}{\partial\rho}\right)\rho\,\mathrm{d}\rho\,\mathrm{d}z \\ & +\mu\int_{\Omega^{\mathrm{i}}}\left(\frac{\partial u_\rho}{\partial z}+\frac{\partial u_z}{\partial\rho}\right)\left(\frac{\partial v_\rho}{\partial z}+\frac{\partial v_z}{\partial\rho}\right)\rho\,\mathrm{d}\rho\,\mathrm{d}z \\ & +\lambda\int_{\Omega^{\mathrm{i}}}\left[\left(\frac{\partial u_\rho}{\partial\rho}+\frac{\partial u_z}{\partial z}\right)v_\rho+u_\rho\left(\frac{\partial v_\rho}{\partial\rho}+\frac{\partial v_z}{\partial z}\right)\right]\mathrm{d}\rho\,\mathrm{d}z \\ & +(\lambda+2\mu)\int_{\Omega^{\mathrm{i}}}\frac{u_\rho v_\rho}{\rho}\,\mathrm{d}\rho\,\mathrm{d}z. \end{aligned} \tag{5.6}$$

The first three integrals in (5.6) are terms analogous to the 2D elastostatic case (except for the differential element), whereas the last two integrals are additional terms that arise due to the axisymmetry.

5.2.3. FEM discretisation

In what follows, the weak formulation (5.3) is discretised by using standard conforming $P1$ finite elements. Let us assume for simplicity that Γ_{p} is a polygonal line. We denote by $\mathcal{T}_h$ a family of regular triangular meshes of Ω^{i} such that $\overline{\Omega^{\mathrm{i}}} = \bigcup_{T\in\mathcal{T}_h}\overline{T}$ (the quarter circle Γ_R is approximated by a polygonal line). The indexing parameter h measures the size of each triangular element T and is defined as $h = \max\{\operatorname{diam} T : T \in \mathcal{T}_h\}$, with $\operatorname{diam} T = \sup\{\sqrt{(\rho_2-\rho_1)^2+(z_2-z_1)^2} : (\rho_1,z_1),(\rho_2,z_2) \in T\}$. For each triangular mesh $\mathcal{T}^h$, let $\mathcal{V}^h$ be a finite-dimensional vector subspace of $\mathcal{V}$ consisting of continuous piecewise linear vector functions, defined as

$$\mathcal{V}^h = \left\{\boldsymbol{v}^h \in \mathcal{V} :\ \boldsymbol{v}^h \in [\mathcal{C}^0(\Omega^{\mathrm{i}})]^2,\ \boldsymbol{v}^h\big|_T \in [\mathcal{P}_1(T)]^2 \quad \forall\, T \in \mathcal{T}^h\right\},$$

where $\mathcal{C}^0(\Omega^{\mathrm{i}})$ denotes the space of continuous functions in Ω^{i} and $\mathcal{P}_1(T)$ stands for the space of polynomials of degree at most one defined in T. The discrete version of (5.3) is

expressed as: Find $\boldsymbol{u}^h \in \mathcal{V}^h$ such that

$$a(\boldsymbol{u}^h, \boldsymbol{v}^h) + b(\boldsymbol{u}^h, \boldsymbol{v}^h) = (\boldsymbol{f}, \boldsymbol{v}^h)_{\Gamma_\mathrm{p}} \qquad \forall\, \boldsymbol{v}^h \in \mathcal{V}^h. \tag{5.7}$$

Let $\mathcal{I}$ be the set of all nodes of the triangular mesh $\mathcal{T}^h$. For each $i \in \mathcal{I}$, we introduce a nodal shape (or basis) function $\psi_i \in \mathcal{V}^h$ which has unit value at node i and zero value at all other nodes. Let also $\mathcal{I}_\mathrm{s} \subset \mathcal{I}$ be the set of nodes lying on $\Gamma_\mathrm{s}^\mathrm{i}$. A nodal basis of $\mathcal{V}^h$ is thus built by considering vector functions $\psi_i \hat{\boldsymbol{\rho}}$ for nodes $i \in \mathcal{I} \setminus \mathcal{I}_\mathrm{s}$, to allow for the condition of zero normal displacement given by (5.2d), and vector functions $\psi_i \hat{\boldsymbol{z}}$ for all nodes $i \in \mathcal{I}$. Consequently, the solution of (5.7) is expressed as a linear combination of the nodal basis functions as

$$\boldsymbol{u}^h(\rho, z) = \sum_{i \in \mathcal{I} \setminus \mathcal{I}_\mathrm{s}} d_{\rho i}\, \psi_i(\rho, z) \hat{\boldsymbol{\rho}} + \sum_{i \in \mathcal{I}} d_{zi}\, \psi_i(\rho, z) \hat{\boldsymbol{z}}, \tag{5.8}$$

where $d_{\rho i}$ and d_{zi} are respectively the unknown nodal values of components u_ρ^h and u_z^h of the solution $\boldsymbol{u}^h$. Replacing (5.8) in (5.7) and substituting $\boldsymbol{v}^h$ by each one of the nodal basis functions $\psi_i \hat{\boldsymbol{\rho}}$ and $\psi_i \hat{\boldsymbol{z}}$, we arrive at the finite element matrix form of the problem, expressed as

$$\boldsymbol{K}\boldsymbol{d} = \boldsymbol{F}, \tag{5.9}$$

with

$$\boldsymbol{K} = \boldsymbol{K}^a + \boldsymbol{K}^b, \qquad \boldsymbol{K}^a = \begin{bmatrix} \boldsymbol{K}^a_{\rho\rho} & \boldsymbol{K}^a_{\rho z} \\ \boldsymbol{K}^a_{z\rho} & \boldsymbol{K}^a_{zz} \end{bmatrix}, \qquad \boldsymbol{K}^b = \begin{bmatrix} \boldsymbol{K}^b_{\rho\rho} & \boldsymbol{K}^b_{\rho z} \\ \boldsymbol{K}^b_{z\rho} & \boldsymbol{K}^b_{zz} \end{bmatrix},$$

and

$$\boldsymbol{d} = \begin{bmatrix} \boldsymbol{d}_\rho \\ \boldsymbol{d}_z \end{bmatrix}, \qquad \boldsymbol{F} = \begin{bmatrix} \boldsymbol{F}_\rho \\ \boldsymbol{F}_z \end{bmatrix},$$

where

$$\begin{aligned} [\boldsymbol{K}^a_{\rho\rho}]_{ij} &= a(\psi_i \hat{\boldsymbol{\rho}}, \psi_j \hat{\boldsymbol{\rho}}), & [\boldsymbol{K}^a_{\rho z}]_{ij} &= a(\psi_i \hat{\boldsymbol{\rho}}, \psi_j \hat{\boldsymbol{z}}), \\ [\boldsymbol{K}^a_{z\rho}]_{ij} &= a(\psi_i \hat{\boldsymbol{z}}, \psi_j \hat{\boldsymbol{\rho}}), & [\boldsymbol{K}^a_{zz}]_{ij} &= a(\psi_i \hat{\boldsymbol{z}}, \psi_j \hat{\boldsymbol{z}}), \end{aligned} \tag{5.10}$$

$$[\boldsymbol{K}^b_{\rho\rho}]_{ij} = b(\psi_i\hat{\boldsymbol{\rho}}, \psi_j\hat{\boldsymbol{\rho}}), \qquad [\boldsymbol{K}^b_{\rho z}]_{ij} = b(\psi_i\hat{\boldsymbol{\rho}}, \psi_j\hat{\boldsymbol{z}}),$$
$$[\boldsymbol{K}^b_{z\rho}]_{ij} = b(\psi_i\hat{\boldsymbol{z}}, \psi_j\hat{\boldsymbol{\rho}}), \qquad [\boldsymbol{K}^b_{zz}]_{ij} = b(\psi_i\hat{\boldsymbol{z}}, \psi_j\hat{\boldsymbol{z}}), \tag{5.11}$$

$$[\boldsymbol{d}_\rho]_j = d_{\rho j}, \qquad [\boldsymbol{d}_z]_j = d_{zj}, \tag{5.12}$$

$$[\boldsymbol{F}_\rho]_i = (\boldsymbol{f}, \psi_i\hat{\boldsymbol{\rho}})_{\Gamma_\mathrm{p}}, \qquad [\boldsymbol{F}_z]_i = (\boldsymbol{f}, \psi_i\hat{\boldsymbol{z}})_{\Gamma_\mathrm{p}}. \tag{5.13}$$

The entries of matrix $\boldsymbol{K}^a$ and vector $\boldsymbol{F}$ are computed by standard numerical integration techniques. However, this is not possible in the case of matrix $\boldsymbol{K}^b$. Substituting (5.5) in (5.11), we reexpress the entries of $\boldsymbol{K}^b$ as

$$[\boldsymbol{K}^b_{\rho\rho}]_{ij} = \int_{\Gamma_R} \psi_i\hat{\boldsymbol{\rho}} \cdot \boldsymbol{\mathcal{M}}\psi_j\hat{\boldsymbol{\rho}}\,\mathrm{d}\Gamma_R, \qquad [\boldsymbol{K}^b_{\rho z}]_{ij} = \int_{\Gamma_R} \psi_i\hat{\boldsymbol{\rho}} \cdot \boldsymbol{\mathcal{M}}\psi_j\hat{\boldsymbol{z}}\,\mathrm{d}\Gamma_R, \tag{5.14a}$$

$$[\boldsymbol{K}^b_{z\rho}]_{ij} = \int_{\Gamma_R} \psi_i\hat{\boldsymbol{z}} \cdot \boldsymbol{\mathcal{M}}\psi_j\hat{\boldsymbol{\rho}}\,\mathrm{d}\Gamma_R, \qquad [\boldsymbol{K}^b_{zz}]_{ij} = \int_{\Gamma_R} \psi_i\hat{\boldsymbol{z}} \cdot \boldsymbol{\mathcal{M}}\psi_j\hat{\boldsymbol{z}}\,\mathrm{d}\Gamma_R. \tag{5.14b}$$

Computing these terms is far from being straightforward, since they involve the DtN map $\boldsymbol{\mathcal{M}}$, which has to be calculated in an accurate way. Notice that these terms are different from zero only if $i, j \in \mathcal{I}_R$, where $\mathcal{I}_R \subset \mathcal{I}$ denotes the set of mesh nodes lying on Γ_R. A correct calculation of the nonzero entries of matrix $\boldsymbol{K}^b$ is critical for obtaining an accurate solution of (5.2), since $\boldsymbol{K}^b$ accounts for the contribution from the exact ABCs in the standard finite element scheme used for numerical discretisation. This crucial issue is thoroughly treated in the next section.

5.3. Approximation of the exact artificial boundary conditions

5.3.1. Definition of the DtN map

Next, we provide the mathematical definition of the DtN map $\boldsymbol{\mathcal{M}}$ introduced in the previous section. Let us consider the residual semi-infinite domain lying outside the artificial boundary Γ_R, denoted by Ω^e. The resulting unbounded parts of boundaries Γ_∞ and Γ_s are respectively denoted by Γ^e_∞ and $\Gamma^\mathrm{e}_\mathrm{s}$ (cf. Figure 5.3). Let $H^s(\Gamma_R)$ be the standard Sobolev space on Γ_R of real order s. Given any $\boldsymbol{v} \in [H^{1/2}(\Gamma_R)]^2$, we obtain $\boldsymbol{\mathcal{M}v} \in [H^{-1/2}(\Gamma_R)]^2$ as

$$\boldsymbol{\mathcal{M}v} = -\boldsymbol{\sigma}(\boldsymbol{u})\hat{\boldsymbol{r}}\big|_{\Gamma_R}, \tag{5.15}$$

where $\boldsymbol{u}$ is the solution of the following BVP in Ω^{e}: Find $\boldsymbol{u} : \Omega^{\mathrm{e}} \to \mathbb{R}^2$ such that

$$\nabla \cdot \boldsymbol{\sigma}(\boldsymbol{u}) = \boldsymbol{0} \qquad \text{in } \Omega^{\mathrm{e}}, \tag{5.16a}$$

$$\boldsymbol{\sigma}(\boldsymbol{u})\hat{\boldsymbol{z}} = \boldsymbol{0} \qquad \text{on } \Gamma^{\mathrm{e}}_{\infty}, \tag{5.16b}$$

$$\boldsymbol{u} = \boldsymbol{v} \qquad \text{on } \Gamma_R, \tag{5.16c}$$

$$\boldsymbol{\sigma}(\boldsymbol{u})\hat{\boldsymbol{\rho}} \cdot \hat{\boldsymbol{z}} = \boldsymbol{u} \cdot \hat{\boldsymbol{\rho}} = 0 \qquad \text{on } \Gamma^{\mathrm{e}}_{\mathrm{s}}, \tag{5.16d}$$

$$|\boldsymbol{u}| = O\big(r^{-1}\big) \qquad \text{as } r \to \infty. \tag{5.16e}$$

As already mentioned, unlike most exterior BVPs, in this case the method of separation of variables fails in obtaining a full analytical closed-form expression for the solution $\boldsymbol{u}$ of (5.16) in function of a generic Dirichlet datum $\boldsymbol{v}$ on Γ_R. This drawback is overcome by solving (5.16) approximately, just for those $\boldsymbol{v}$ required to compute the nonzero entries of matrix $\boldsymbol{K}^b$. By virtue of (5.14), the required right-hand sides in (5.16c) are $\boldsymbol{v} = \psi_j \hat{\boldsymbol{\rho}}$ and $\boldsymbol{v} = \psi_j \hat{\boldsymbol{z}}$, for every $j \in \mathcal{I}_R$.

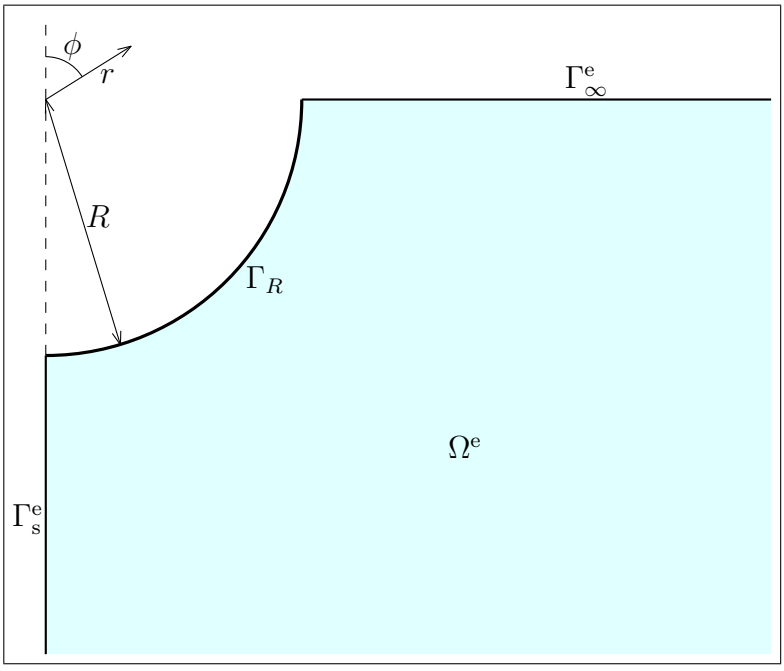

Figure 5.3. Axisymmetric semi-infinite residual domain.

5.3.2. Numerical enforcement of exact boundary conditions on the artificial boundary

In order to solve (5.16), we apply the semi-analytical method presented in Chapter 4 with some suitable modifications. Proceeding analogously as in Section 4.1, we obtain an analytical solution in series form satisfying (5.16a), (5.16b), (5.16b) and (5.16e). This solution reads exactly as (4.20a)-(4.20b), but with h substituted by R. In the same way as we did in Section 4.2, this solution is numerically forced to satisfy (5.16c), leading to determine the coefficients A_n and B_n associated with a particular right-hand side $\boldsymbol{v}$. In the next subsection, this procedure will be applied to the particular right-hand sides $\boldsymbol{v} = \psi_j \hat{\boldsymbol{\rho}}$ and $\boldsymbol{v} = \psi_j \hat{\boldsymbol{z}}$. First, we truncate the series in the aforementioned analytical solution at a finite order N. The resulting expressions for the displacement vector $\boldsymbol{u}_N$ and the stress tensor $\boldsymbol{\sigma}_N$ are

$$\boldsymbol{u}_N(r,\phi) = \sum_{n=0}^{N} A_n \Big(\frac{R}{r}\Big)^{2n+2} \boldsymbol{w}_n^{(A)}(\phi) + \sum_{n=-1}^{N} B_n \Big(\frac{R}{r}\Big)^{2n+3} \boldsymbol{w}_n^{(B)}(\phi), \tag{5.17a}$$

$$\boldsymbol{\sigma}_N(r,\phi) = \frac{1}{R}\Bigg[\sum_{n=0}^{N} A_n \Big(\frac{R}{r}\Big)^{2n+3} \boldsymbol{\tau}_n^{(A)}(\phi) + \sum_{n=-1}^{N} B_n \Big(\frac{R}{r}\Big)^{2n+4} \boldsymbol{\tau}_n^{(B)}(\phi)\Bigg], \tag{5.17b}$$

and this time we consider the quadratic energy functional $\mathcal{J}$ defined as

$$\mathcal{J}(\boldsymbol{u}_N) = \frac{1}{2R}\int_{\Gamma_R} \boldsymbol{\sigma}_N \hat{\boldsymbol{n}} \cdot \boldsymbol{u}_N \,\mathrm{d}\Gamma_R - \frac{1}{R}\int_{\Gamma_R} \boldsymbol{\sigma}_N \hat{\boldsymbol{n}} \cdot \boldsymbol{v} \,\mathrm{d}\Gamma_R, \tag{5.18}$$

where $\hat{\boldsymbol{n}} = -\hat{\boldsymbol{r}}$ is the unit normal vector on Γ_R, pointing outwards Ω^{e}. The first term in (5.18) is quadratic in $\boldsymbol{u}_N$ and represents the surface elastic potential energy on Γ_R, whereas the second term is linear in $\boldsymbol{u}_N$ and is related to the Dirichlet boundary condition assumed on Γ_R. The functional $\mathcal{J}$ has been defined in such a way that its minimisation provides numerical values for coefficients $A_0, A_1, A_2, \ldots, A_N$ and $B_{-1}, B_0, B_1, \ldots, B_N$ so that (5.16c) holds approximately. By expanding terms in (5.18), replacing $\hat{\boldsymbol{n}} = -\hat{\boldsymbol{r}}$ and making explicit

the integrals (notice that $\mathrm{d}\Gamma_R = R^2 \sin\phi \, \mathrm{d}\phi$), we arrive at

$$\mathcal{J}(\boldsymbol{u}_N) = -\frac{R}{2}\int_{\pi/2}^{\pi} \Big([\sigma_N]_r(R,\phi)\,[u_N]_r(R,\phi) + [\sigma_N]_{r\phi}(R,\phi)\,[u_N]_\phi(R,\phi) \Big) \sin\phi \, \mathrm{d}\phi \\ + R\int_{\pi/2}^{\pi} \Big([\sigma_N]_r(R,\phi)\, v_r(R,\phi) + [\sigma_N]_{r\phi}(R,\phi)\, v_\phi(R,\phi) \Big) \sin\phi \, \mathrm{d}\phi. \tag{5.19}$$

As we did in Subsection 4.2.2, we define the column vectors $\boldsymbol{A} \in \mathbb{R}^{N+1}$ and $\boldsymbol{B} \in \mathbb{R}^{N+2}$ as those whose entries are the coefficients $A_0, A_1, A_2, \ldots, A_N$ and $B_{-1}, B_0, B_1, \ldots, B_N$, respectively. By evaluating the corresponding components of $\boldsymbol{u}_N$ and $\boldsymbol{\sigma}_N$ at $r = R$ in (5.17a) and (5.17b), substituting in (5.19) and expanding terms appropriately, $\mathcal{J}$ is reexpressed as an explicit function of $\boldsymbol{A}$ and $\boldsymbol{B}$ as

$$\mathcal{J}(\boldsymbol{A},\boldsymbol{B}) = \frac{1}{2}\sum_{n=0}^{N}\sum_{k=0}^{N} Q_{nk}^{(AA)} A_n A_k + \frac{1}{2}\sum_{n=0}^{N}\sum_{k=-1}^{N} Q_{nk}^{(AB)} A_n B_k + \frac{1}{2}\sum_{n=-1}^{N}\sum_{k=0}^{N} Q_{nk}^{(BA)} B_n A_k \\ + \frac{1}{2}\sum_{n=-1}^{N}\sum_{k=-1}^{N} Q_{nk}^{(BB)} B_n B_k - \sum_{n=0}^{N} y_n^{(A)} A_n - \sum_{n=-1}^{N} y_n^{(B)} B_n, \tag{5.20}$$

where the coefficients $Q_{nk}^{\alpha\beta}$ are given by (4.31a)-(4.33d) and

$$y_n^{(\alpha)} = -\int_{\pi/2}^{\pi} \Big([\tau_n^{(\alpha)}]_r(\phi) v_r(R,\phi) + [\tau_n^{(\alpha)}]_{r\phi}(\phi) v_\phi(R,\phi) \Big) \sin\phi \, \mathrm{d}\phi. \tag{5.21}$$

where $\alpha = A, B$. Coefficients $y_n^{(\alpha)}$ depend on the particular right-hand side $\boldsymbol{v}$ assumed in (5.16c), so their calculation is discussed in the next subsection. Defining matrix $\boldsymbol{Q} \in M_{2N+3}(\mathbb{R})$ and vectors $\boldsymbol{x}, \boldsymbol{y} \in \mathbb{R}^{2N+3}$ exactly as in Subsection 4.2.2, it is possible to reexpress $\mathcal{J}$ in (5.20) as a quadratic form in $\boldsymbol{x}$

$$\mathcal{J}(\boldsymbol{x}) = \frac{1}{2}\boldsymbol{x}^T \boldsymbol{Q} \boldsymbol{x} - \boldsymbol{x}^T \boldsymbol{y}. \tag{5.22}$$

whose minimization yields again a linear sistem of equations for the coefficients $A_0, A_1, \ldots, A_N$ and $B_{-1}, B_0, B_1, \ldots, B_N$ stored in the vector $\boldsymbol{x}$. The procedure and associated algorithm to solve the system are completely analogous to those presented in Section 4.2.3. This

algorithm has to be applied repeatedly for each pair of vectors $\boldsymbol{y}^{(A)}$ and $\boldsymbol{y}^{(B)}$ necessary in the computations. Nevertheless, as matrices $\boldsymbol{Q}^{(\alpha\beta)}$ remain unchanged, each one of them, together with the coefficients for inversion of $\boldsymbol{Q}^{(AA)}$ and $\widetilde{\boldsymbol{Q}}^{(BB)}$, are computed and stored only once.

5.3.3. Numerical approximation of integral terms involving the DtN map in the FEM formulation

In what follows, the numerical procedure described in the previous subsection is applied to approximate the terms in (5.14). First, coefficients $y_n^{(\alpha)}$ in (5.21) are to be calculated for $\boldsymbol{v} = \psi_j \hat{\boldsymbol{\rho}}$ and $\boldsymbol{v} = \psi_j \hat{\boldsymbol{z}}$ for every $j \in \mathcal{I}_R$. Combining with (2.1a), we obtain that these two cases are respectively equivalent to consider

$$\boldsymbol{y}^{(A)} = \boldsymbol{C}_\rho^j, \quad \boldsymbol{y}^{(B)} = \boldsymbol{D}_\rho^j,$$

and

$$\boldsymbol{y}^{(A)} = \boldsymbol{C}_z^j, \quad \boldsymbol{y}^{(B)} = \boldsymbol{D}_z^j,$$

where $\boldsymbol{C}_\rho^j, \boldsymbol{C}_z^j \in \mathbb{R}^{N+1}$ and $\boldsymbol{D}_\rho^j, \boldsymbol{D}_z^j \in \mathbb{R}^{N+2}$ are the vectors of components

$$C_{\rho,n}^j = -\int_{\pi/2}^{\pi} \big([\tau_n^{(A)}]_r(\phi)\sin\phi + [\tau_n^{(A)}]_{r\phi}(\phi)\cos\phi\big)\psi_j(R,\phi)\sin\phi\,\mathrm{d}\phi \qquad n = 0,\dots,N, \tag{5.23a}$$

$$C_{z,n}^j = -\int_{\pi/2}^{\pi} \big([\tau_n^{(A)}]_r(\phi)\cos\phi - [\tau_n^{(A)}]_{r\phi}(\phi)\sin\phi\big)\psi_j(R,\phi)\sin\phi\,\mathrm{d}\phi \qquad n = 0,\dots,N, \tag{5.23b}$$

$$D_{\rho,n}^j = -\int_{\pi/2}^{\pi} \big([\tau_n^{(B)}]_r(\phi)\sin\phi + [\tau_n^{(B)}]_{r\phi}(\phi)\cos\phi\big)\psi_j(R,\phi)\sin\phi\,\mathrm{d}\phi \qquad n = 0,\dots,N, \tag{5.23c}$$

$$D_{z,n}^j = -\int_{\pi/2}^{\pi} \big([\tau_n^{(B)}]_r(\phi)\cos\phi - [\tau_n^{(B)}]_{r\phi}(\phi)\sin\phi\big)\psi_j(R,\phi)\sin\phi\,\mathrm{d}\phi \qquad n = 0,\dots,N, \tag{5.23d}$$

respectively. By substituting (4.21c), (4.21f), (4.22c), (4.22f), (4.23c) and (4.23f) in (5.23) and expanding, components of vectors $\boldsymbol{C}_\rho^j, \boldsymbol{C}_z^j, \boldsymbol{D}_\rho^j, \boldsymbol{D}_z^j$ are rewritten as

$$\begin{aligned} C_{s,n}^j = &-(2n+1)(2n+2)\big(\alpha_{2n}\, l_{s,2n}^j + \beta_{2n}\, l_{s,2n+2}^j\big) \\ &- (2n+2)\alpha_{2n}\, m_{s,2n}^j - (2n+1)\alpha_{2n+1}\, m_{s,2n+2}^j \qquad n = 0, \ldots, N, \end{aligned} \tag{5.24a}$$

$$D_{s,-1}^j = -3\, l_{s,1}^j - (1-2\nu) q_s^j, \tag{5.24b}$$

$$\begin{aligned} D_{s,n}^j = &-(2n+2)(2n+3)\big(\alpha_{2n+2}\, l_{s,2n+1}^j + \beta_{2n+1}\, l_{s,2n+3}^j\big) \\ &- \alpha_{2n+2}\big((2n+3) m_{s,2n+1}^j + (2n+2) m_{s,2n+3}^j\big) \qquad n = 0, \ldots, N, \end{aligned} \tag{5.24c}$$

where $s = \rho, z$ and

$$l_{\rho,n}^j = \int_{\pi/2}^{\pi} \sin^2\phi P_n(\cos\phi)\psi_j(R,\phi)\mathrm{d}\phi, \tag{5.25a}$$

$$l_{z,n}^j = \int_{\pi/2}^{\pi} \sin\phi\cos\phi P_n(\cos\phi)\psi_j(R,\phi)\mathrm{d}\phi, \tag{5.25b}$$

$$m_{\rho,n}^j = \int_{\pi/2}^{\pi} \sin^2\phi\cos\phi P_n'(\cos\phi)\psi_j(R,\phi)\mathrm{d}\phi, \tag{5.25c}$$

$$m_{z,n}^j = -\int_{\pi/2}^{\pi} \sin^3\phi P_n'(\cos\phi)\psi_j(R,\phi)\mathrm{d}\phi, \tag{5.25d}$$

$$q_\rho^j = \int_{\pi/2}^{\pi} (1+\cos\phi)\psi_j(R,\phi)\mathrm{d}\phi, \tag{5.25e}$$

$$q_z^j = 0. \tag{5.25f}$$

To compute these integrals, we observe that the mesh $\mathcal{T}_h$ restricted to Γ_R gives rise to a partition of the quarter circle into segments (usually equispaced). Let J be the number of these segments. Then the set $\mathcal{I}_R$ necessarily consists of $J+1$ mesh nodes, which we assume for simplicity to be correlatively numbered, that is, $\mathcal{I}_R = \{1, 2, \ldots, J, J+1\}$. We associate with each node $j \in \mathcal{I}_R$ an angle ϕ_j, in such a way that $\pi/2 = \phi_1 < \phi_2 < \ldots < \phi_J < \phi_{J+1} = \pi$. The $P1$-nodal shape functions ψ_j, restricted to Γ_R, do not depend on the

radius R, and have the following explicit expressions

$$\psi_1(\phi) = \mathbb{1}_{[\phi_1,\phi_2]}(\phi)\left(\frac{\phi_2-\phi}{\phi_2-\phi_1}\right), \tag{5.26a}$$

$$\psi_j(\phi) = \mathbb{1}_{[\phi_{j-1},\phi_j]}(\phi)\left(\frac{\phi-\phi_{j-1}}{\phi_j-\phi_{j-1}}\right) + \mathbb{1}_{[\phi_j,\phi_{j+1}]}(\phi)\left(\frac{\phi_{j+1}-\phi}{\phi_{j+1}-\phi_j}\right) \quad j=2,\ldots,J, \tag{5.26b}$$

$$\psi_{J+1}(\phi) = \mathbb{1}_{[\phi_J,\phi_{J+1}]}(\phi)\left(\frac{\phi-\phi_J}{\phi_{J+1}-\phi_J}\right), \tag{5.26c}$$

where $\mathbb{1}_{[a,b]}(\cdot)$ stands for the indicator function of the interval $[a,b]$. Substituting (5.26) in (5.25), coefficients $l^s_{n,j}$, $m^s_{n,j}$ and q^ρ_j are decomposed as

$$\begin{aligned}
&l^1_{s,n} = l^{1,+}_{s,n}, && m^1_{s,n} = m^{1,+}_{s,n}, && q^1_{\rho,n} = q^{1,+}_{\rho,n},\\
&l^j_{s,n} = l^{j,-}_{s,n} + l^{j,+}_{s,n}, && m^j_{s,n} = m^{j,-}_{s,n} + m^{j,+}_{s,n}, && q^j_{\rho,n} = q^{j,-}_{\rho,n} + q^{j,+}_{\rho,n}, \quad j=2,\ldots,J,\\
&l^{J+1}_{s,n} = l^{J+1,-}_{s,n}, && m^{J+1}_{s,n} = m^{J+1,-}_{s,n}, && q^{J+1}_{\rho,n} = q^{J+1,-}_{\rho,n},
\end{aligned}$$

where for $j=2,\ldots,J+1$,

$$l^{j,-}_{\rho,n} = \int_{\phi_{j-1}}^{\phi_j} \sin^2\phi P_n(\cos\phi)\left(\frac{\phi-\phi_{j-1}}{\phi_j-\phi_{j-1}}\right)\mathrm{d}\phi, \tag{5.27a}$$

$$m^{j,-}_{\rho,n} = \int_{\phi_{j-1}}^{\phi_j} \sin^2\phi\cos\phi P_n'(\cos\phi)\left(\frac{\phi-\phi_{j-1}}{\phi_j-\phi_{j-1}}\right)\mathrm{d}\phi, \tag{5.27b}$$

$$q^{j,-}_{\rho} = \int_{\phi_{j-1}}^{\phi_j} (1+\cos\phi)\left(\frac{\phi-\phi_{j-1}}{\phi_j-\phi_{j-1}}\right)\mathrm{d}\phi, \tag{5.27c}$$

$$l^{j,-}_{z,n} = \int_{\phi_{j-1}}^{\phi_j} \sin\phi\cos\phi P_n(\cos\phi)\left(\frac{\phi-\phi_{j-1}}{\phi_j-\phi_{j-1}}\right)\mathrm{d}\phi, \tag{5.27d}$$

$$m^{j,-}_{z,n} = -\int_{\phi_{j-1}}^{\phi_j} \sin^3\phi P_n'(\cos\phi)\left(\frac{\phi-\phi_{j-1}}{\phi_j-\phi_{j-1}}\right)\mathrm{d}\phi, \tag{5.27e}$$

and for $j=1,\ldots,J$,

$$l^{j,+}_{\rho,n} = \int_{\phi_j}^{\phi_{j+1}} \sin^2\phi P_n(\cos\phi)\left(\frac{\phi_{j+1}-\phi}{\phi_{j+1}-\phi_j}\right)\mathrm{d}\phi, \tag{5.28a}$$

$$m^{j,+}_{\rho,n} = \int_{\phi_j}^{\phi_{j+1}} \sin^2\phi\cos\phi P_n'(\cos\phi)\left(\frac{\phi_{j+1}-\phi}{\phi_{j+1}-\phi_j}\right)\mathrm{d}\phi, \tag{5.28b}$$

$$q_{\rho}^{j,+} = \int_{\phi_j}^{\phi_{j+1}} (1+\cos\phi)\left(\frac{\phi_{j+1}-\phi}{\phi_{j+1}-\phi_j}\right)\mathrm{d}\phi, \tag{5.28c}$$

$$l_{z,n}^{j,+} = \int_{\phi_j}^{\phi_{j+1}} \sin\phi\cos\phi P_n(\cos\phi)\left(\frac{\phi_{j+1}-\phi}{\phi_{j+1}-\phi_j}\right)\mathrm{d}\phi, \tag{5.28d}$$

$$m_{z,n}^{j,+} = -\int_{\phi_j}^{\phi_{j+1}} \sin^3\phi P_n'(\cos\phi)\left(\frac{\phi_{j+1}-\phi}{\phi_{j+1}-\phi_j}\right)\mathrm{d}\phi. \tag{5.28e}$$

Explicit expressions for a few coefficients $l_{s,n}^{j,\pm}$, $m_{s,n}^{j,\pm}$ and $q_s^{j,\pm}$ are given next

$$l_{\rho,0}^{j,-} = \frac{\phi_j-\phi_{j-1}}{4} - \frac{1}{2}\cos\phi_j\sin\phi_j - \frac{\cos^2\phi_j-\cos^2\phi_{j-1}}{4(\phi_j-\phi_{j-1})},$$

$$l_{\rho,0}^{j,+} = \frac{\phi_{j+1}-\phi_j}{4} + \frac{1}{2}\cos\phi_j\sin\phi_j + \frac{\cos^2\phi_{j+1}-\cos^2\phi_j}{4(\phi_{j+1}-\phi_j)},$$

$$l_{\rho,1}^{j,-} = m_{\rho,1}^{j,-} = \frac{1}{3}\sin^3\phi_j + \frac{(2+\sin^2\phi_j)\cos\phi_j - (2+\sin^2\phi_{j-1})\cos\phi_{j-1}}{9(\phi_j-\phi_{j-1})},$$

$$l_{\rho,1}^{j,+} = m_{\rho,1}^{j,+} = -\frac{1}{3}\sin^3\phi_j - \frac{(2+\sin^2\phi_{j+1})\cos\phi_{j+1} - (2+\sin^2\phi_j)\cos\phi_j}{9(\phi_{j+1}-\phi_j)},$$

$$\begin{aligned} l_{\rho,2}^{j,-} = &-\frac{\phi_j-\phi_{j-1}}{32} - \frac{\cos\phi_j\sin\phi_j(6\cos^2\phi_j-7)}{16} \\ &- \frac{(\cos^2\phi_j-\cos^2\phi_{j-1})\big(3(\cos^2\phi_j+\cos^2\phi_{j-1})-7\big)}{32(\phi_j-\phi_{j-1})} \end{aligned}$$

$$\begin{aligned} l_{\rho,2}^{j,+} = &-\frac{\phi_{j+1}-\phi_j}{32} + \frac{\cos\phi_j\sin\phi_j(6\cos^2\phi_j-7)}{16} \\ &+ \frac{(\cos^2\phi_{j+1}-\cos^2\phi_j)\big(3(\cos^2\phi_j+\cos^2\phi_{j+1})-7\big)}{32(\phi_{j+1}-\phi_j)} \end{aligned}$$

$$q_{\rho}^{j,-} = \frac{\phi_j-\phi_{j-1}}{2} + \sin\phi_j + \frac{\cos\phi_j-\cos\phi_{j-1}}{\phi_j-\phi_{j-1}},$$

$$q_{\rho}^{j,+} = \frac{\phi_{j+1}-\phi_j}{2} - \sin\phi_j - \frac{\cos\phi_{j+1}-\cos\phi_j}{\phi_{j+1}-\phi_j},$$

$$l_{z,0}^{j,-} = -\frac{\cos^2\phi_j-\sin^2\phi_j}{4} + \frac{\sin\phi_j\cos\phi_j-\sin\phi_{j-1}\cos\phi_{j-1}}{4(\phi_j-\phi_{j-1})},$$

$$l_{z,0}^{j,+} = \frac{\cos^2\phi_j-\sin^2\phi_j}{4} - \frac{\sin\phi_{j+1}\cos\phi_{j+1}-\sin\phi_j\cos\phi_j}{4(\phi_{j+1}-\phi_j)},$$

$$l_{z,1}^{j,-} = -\frac{1}{3}\cos^3\phi_j + \frac{(2+\cos^2\phi_j)\sin\phi_j - (2+\cos^2\phi_{j-1})\sin\phi_{j-1}}{9(\phi_j-\phi_{j-1})},$$

$$
\begin{aligned}
l_{z,1}^{j,+} &= \frac{1}{3}\cos^3\phi_j - \frac{(2+\cos^2\phi_{j+1})\sin\phi_{j+1} - (2+\cos^2\phi_j)\sin\phi_j}{9(\phi_{j+1}-\phi_j)},\\
m_{z,1}^{j,-} &= \frac{(2+\sin^2\phi_j)\cos\phi_j}{3} - \frac{(6+\sin^2\phi_j)\sin\phi_j - (6+\sin^2\phi_{j-1})\sin\phi_{j-1}}{9(\phi_j-\phi_{j-1})},\\
m_{z,1}^{j,+} &= -\frac{(2+\sin^2\phi_j)\cos\phi_j}{3} + \frac{(6+\sin^2\phi_{j+1})\sin\phi_{j+1} - (6+\sin^2\phi_j)\sin\phi_j}{9(\phi_{j+1}-\phi_j)},\\
l_{z,2}^{j,-} &= -\frac{8(\cos^2\phi_j-1)(3\cos^2\phi_j+1)+7}{64}\\
&\quad + \frac{\cos\phi_j\sin\phi_j(6\cos^2\phi_j+1) - \cos\phi_{j-1}\sin\phi_{j-1}(6\cos^2\phi_{j-1}+1)}{64(\phi_j-\phi_{j-1})}\\
l_{z,2}^{j,+} &= \frac{8(\cos^2\phi_j-1)(3\cos^2\phi_j+1)+7}{64}\\
&\quad - \frac{\cos\phi_{j+1}\sin\phi_{j+1}(6\cos^2\phi_{j+1}+1) - \cos\phi_j\sin\phi_j(6\cos^2\phi_j+1)}{64(\phi_{j+1}-\phi_j)}
\end{aligned}
$$

Integrals in (5.27) and (5.28) are computed analytically with the aid of symbolic computation techniques. The resulting expressions become more and more unwieldy as n increases, so only a few of them are provided by the way of example. We denote by $A_{s,n}^j$ and $B_{s,n}^j$ the coefficients A_n and B_n obtained by applying the algorithm of the previous subsection with $\boldsymbol{y}^{(A)} = \boldsymbol{C}_s^j$ and $\boldsymbol{y}^{(B)} = \boldsymbol{D}_s^j$, respectively. Notice that as for each $j = 1, 2, \ldots, J, J+1$ two cases need to be considered ($s = \rho$ and $s = z$), the algorithm is to be applied $2(J+1)$ times in total. Additionally, let us define the vectors $\boldsymbol{A}_s^j \in \mathbb{R}^{N+1}$ and $\boldsymbol{B}_s^j \in \mathbb{R}^{N+2}$ as those whose components are the coefficients $A_{s,n}^j$ and $B_{s,n}^j$, respectively, which by virtue of (4.40a) and (4.40b) are given by

$$
\begin{aligned}
\boldsymbol{A}_s^j &= \big([\boldsymbol{Q}^{(AA)}]^{-1} + [\boldsymbol{Q}^{(AA)}]^{-1}\boldsymbol{Q}^{(AB)}[\widetilde{\boldsymbol{Q}}^{(BB)}]^{-1}[\boldsymbol{Q}^{(AB)}]^T[\boldsymbol{Q}^{(AA)}]^{-1}\big)\boldsymbol{C}_s^j\\
&\quad - [\boldsymbol{Q}^{(AA)}]^{-1}\boldsymbol{Q}^{(AB)}[\widetilde{\boldsymbol{Q}}^{(BB)}]^{-1}\boldsymbol{D}_s^j,
\end{aligned}
\tag{5.29a}
$$

$$
\boldsymbol{B}_s^j = -[\widetilde{\boldsymbol{Q}}^{(BB)}]^{-1}[\boldsymbol{Q}^{(AB)}]^T[\boldsymbol{Q}^{(AA)}]^{-1}\boldsymbol{C}_s^j + [\widetilde{\boldsymbol{Q}}^{(BB)}]^{-1}\boldsymbol{D}_s^j. \tag{5.29b}
$$

Thus, using the definition of the DtN map (5.15) and combining with (4.26a) and (5.17b) yields the approximations

$$\begin{aligned}
\boldsymbol{\mathcal{M}}\psi_j\hat{\boldsymbol{\rho}}(\phi) \approx -\frac{1}{R}\Bigg[&\sum_{n=0}^{N} A^j_{\rho,n}\Big([\tau_n^{(A)}]_r(\phi)\hat{\boldsymbol{r}} + [\tau_n^{(A)}]_{r\phi}(\phi)\hat{\boldsymbol{\phi}}\Big) \\
&+ \sum_{n=-1}^{N} B^j_{\rho,n}\Big([\tau_n^{(B)}]_r(\phi)\hat{\boldsymbol{r}} + [\tau_n^{(B)}]_{r\phi}(\phi)\hat{\boldsymbol{\phi}}\Big)\Bigg], \\
\boldsymbol{\mathcal{M}}\psi_j\hat{\boldsymbol{z}}(\phi) \approx -\frac{1}{R}\Bigg[&\sum_{n=0}^{N} A^j_{z,n}\Big([\tau_n^{(A)}]_r(\phi)\hat{\boldsymbol{r}} + [\tau_n^{(A)}]_{r\phi}(\phi)\hat{\boldsymbol{\phi}}\Big) \\
&+ \sum_{n=-1}^{N} B^j_{z,n}\Big([\tau_n^{(B)}]_r(\phi)\hat{\boldsymbol{r}} + [\tau_n^{(B)}]_{r\phi}(\phi)\hat{\boldsymbol{\phi}}\Big)\Bigg].
\end{aligned}$$

By replacing these expressions in (5.14), combining with (2.1a) and expanding, we arrive at

$$\begin{aligned}
[\boldsymbol{K}^b_{\rho\rho}]_{ij} \approx &- R\sum_{n=0}^{N} A^j_{\rho,n}\int_{\pi/2}^{\pi}\Big([\tau_n^{(A)}]_r(\phi)\sin\phi + [\tau_n^{(A)}]_{r\phi}(\phi)\cos\phi\Big)\psi_i(R,\phi)\sin\phi\,\mathrm{d}\phi \\
&- R\sum_{n=-1}^{N} B^j_{\rho,n}\int_{\pi/2}^{\pi}\Big([\tau_n^{(B)}]_r(\phi)\sin\phi + [\tau_n^{(B)}]_{r\phi}(\phi)\cos\phi\Big)\psi_i(R,\phi)\sin\phi\,\mathrm{d}\phi, \\
[\boldsymbol{K}^b_{\rho z}]_{ij} \approx &- R\sum_{n=0}^{N} A^j_{z,n}\int_{\pi/2}^{\pi}\Big([\tau_n^{(A)}]_r(\phi)\sin\phi + [\tau_n^{(A)}]_{r\phi}(\phi)\cos\phi\Big)\psi_i(R,\phi)\sin\phi\,\mathrm{d}\phi \\
&- R\sum_{n=-1}^{N} B^j_{z,n}\int_{\pi/2}^{\pi}\Big([\tau_n^{(B)}]_r(\phi)\sin\phi + [\tau_n^{(B)}]_{r\phi}(\phi)\cos\phi\Big)\psi_i(R,\phi)\sin\phi\,\mathrm{d}\phi, \\
[\boldsymbol{K}^b_{z\rho}]_{ij} \approx &- R\sum_{n=0}^{N} A^j_{\rho,n}\int_{\pi/2}^{\pi}\Big([\tau_n^{(A)}]_r(\phi)\cos\phi - [\tau_n^{(A)}]_{r\phi}(\phi)\sin\phi\Big)\psi_i(R,\phi)\sin\phi\,\mathrm{d}\phi \\
&- R\sum_{n=-1}^{N} B^j_{\rho,n}\int_{\pi/2}^{\pi}\Big([\tau_n^{(B)}]_r(\phi)\cos\phi - [\tau_n^{(B)}]_{r\phi}(\phi)\sin\phi\Big)\psi_i(R,\phi)\sin\phi\,\mathrm{d}\phi,
\end{aligned}$$

$$[\boldsymbol{K}^b_{zz}]_{ij} \approx -\,R\sum_{n=0}^{N} A^j_{z,n}\int_{\pi/2}^{\pi}\Big([\tau_n^{(A)}]_r(\phi)\cos\phi - [\tau_n^{(A)}]_{r\phi}(\phi)\sin\phi\Big)\psi_i(R,\phi)\sin\phi\,\mathrm{d}\phi$$
$$-\,R\sum_{n=-1}^{N} B^j_{z,n}\int_{\pi/2}^{\pi}\Big([\tau_n^{(B)}]_r(\phi)\cos\phi - [\tau_n^{(B)}]_{r\phi}(\phi)\sin\phi\Big)\psi_i(R,\phi)\sin\phi\,\mathrm{d}\phi,$$

and combining with (5.23), these terms are conveniently reexpressed as

$$[\boldsymbol{K}^b_{\rho\rho}]_{ij} \approx R\Big[\sum_{n=0}^{N} C^i_{\rho,n}A^j_{\rho,n} + \sum_{n=-1}^{N} D^i_{\rho,n}B^j_{\rho,n}\Big] = R\big(\boldsymbol{C}^i_\rho\cdot\boldsymbol{A}^j_\rho + \boldsymbol{D}^i_\rho\cdot\boldsymbol{B}^j_\rho\big), \tag{5.30a}$$

$$[\boldsymbol{K}^b_{\rho z}]_{ij} \approx R\Big[\sum_{n=0}^{N} C^i_{\rho,n}A^j_{z,n} + \sum_{n=-1}^{N} D^i_{\rho,n}B^j_{z,n}\Big] = R\big(\boldsymbol{C}^i_\rho\cdot\boldsymbol{A}^j_z + \boldsymbol{D}^i_\rho\cdot\boldsymbol{B}^j_z\big), \tag{5.30b}$$

$$[\boldsymbol{K}^b_{z\rho}]_{ij} \approx R\Big[\sum_{n=0}^{N} C^i_{z,n}A^j_{\rho,n} + \sum_{n=-1}^{N} D^i_{z,n}B^j_{\rho,n}\Big] = R\big(\boldsymbol{C}^i_z\cdot\boldsymbol{A}^j_\rho + \boldsymbol{D}^i_z\cdot\boldsymbol{B}^j_\rho\big), \tag{5.30c}$$

$$[\boldsymbol{K}^b_{zz}]_{ij} \approx R\Big[\sum_{n=0}^{N} C^i_{z,n}A^j_{z,n} + \sum_{n=-1}^{N} D^i_{z,n}B^j_{z,n}\Big] = R\big(\boldsymbol{C}^i_z\cdot\boldsymbol{A}^j_z + \boldsymbol{D}^i_z\cdot\boldsymbol{B}^j_z\big). \tag{5.30d}$$

It should be observed that vectors $\boldsymbol{C}^i_\rho, \boldsymbol{C}^i_z, \boldsymbol{D}^i_\rho, \boldsymbol{D}^i_z$ actually do not depend on the radius R, and so do vectors $\boldsymbol{A}^i_\rho, \boldsymbol{A}^i_z, \boldsymbol{B}^i_\rho, \boldsymbol{B}^i_z$. Hence, by virtue of (5.30), the entries of matrix $\boldsymbol{K}^b$ are linear in R.

5.4. Numerical experiments

5.4.1. Model problem

Throughout this section we consider a model problem whose exact solution is available. Let us assume the perturbed boundary Γ_{p} to be a quarter circle of radius $a > 0$. In this case, it holds in axisymmetric spherical coordinates that

$$\Omega = \{(r,\phi):\ a < r < \infty,\ \pi/2 < \phi < \pi\},$$
$$\Gamma_{\mathrm{p}} = \{(r,\phi):\ r = a,\ \pi/2 < \phi < \pi\}.$$

We define the function $\boldsymbol{f} = f_r\,\hat{\boldsymbol{r}} + f_\phi\,\hat{\boldsymbol{\phi}} : \Gamma_p \to \mathbb{R}^2$ as

$$f_r(\phi) = 2\mu c\big(1 - 2\nu + 2(2-\nu)\cos\phi\big), \tag{5.31a}$$

$$f_\phi(\phi) = 2\mu c\,(1-2\nu)\left(\frac{\cos\phi\sin\phi}{1-\cos\phi}\right), \tag{5.31b}$$

where c is a scale factor. Then the displacement $\boldsymbol{u} = u_r\,\hat{\boldsymbol{r}} + u_\phi\,\hat{\boldsymbol{\phi}} : \Omega \to \mathbb{R}^2$, defined as

$$u_r(r,\phi) = -\frac{c\,a^2}{r}\left(1 - 2\nu + 4(1-\nu)\cos\phi\right), \tag{5.32a}$$

$$u_\phi(r,\phi) = \frac{c\,a^2}{r}\left(3 - 4\nu - \frac{1-2\nu}{1-\cos\phi}\right)\sin\phi, \tag{5.32b}$$

is an exact solution of (5.1) with $\boldsymbol{f}$ given by (5.31). This solution is obtained from (4.20a) with R replaced by a and setting $A_n = B_n = 0$ for all $n = 0, 1, 2, \ldots$ and $B_{-1} = 2\mu c\,a$. The stress components associated with (5.32) are obtained by setting these same values of coefficients A_n and B_n in (4.20b) with R replaced by a, or simply by substituting (5.32) in (2.8), yielding

$$\sigma_r(r,\phi) = \frac{2\mu c\,a^2}{r^2}\big(1 - 2\nu + 2(2-\nu)\cos\phi\big), \tag{5.33a}$$

$$\sigma_\phi(r,\phi) = \frac{2\mu c\,a^2(1-2\nu)}{r^2}\left(\frac{\cos^2\phi}{1-\cos\phi}\right), \tag{5.33b}$$

$$\sigma_\theta(r,\phi) = -\frac{2\mu c\,a^2(1-2\nu)}{r^2}\left(\frac{1+\cos\phi-\cos^2\phi}{1-\cos\phi}\right), \tag{5.33c}$$

$$\sigma_{r\phi}(r,\phi) = \frac{2\mu c\,a^2(1-2\nu)}{r^2}\left(\frac{\cos\phi\sin\phi}{1-\cos\phi}\right). \tag{5.33d}$$

In axisymmetric cylindrical coordinates, (5.32) reads $\boldsymbol{u} = u_\rho\,\hat{\boldsymbol{\rho}} + u_z\,\hat{\boldsymbol{z}}$, with

$$u_\rho(\rho,z) = -\frac{c\,a^2\rho}{(\rho^2+z^2)^{1/2}}\left(\frac{1-2\nu}{(\rho^2+z^2)^{1/2}-z} + \frac{z}{\rho^2+z^2}\right), \tag{5.34a}$$

$$u_z(\rho,z) = -\frac{c\,a^2}{(\rho^2+z^2)^{1/2}}\left(2(1-\nu) + \frac{z^2}{\rho^2+z^2}\right), \tag{5.34b}$$

and associated stress components given by

$$\sigma_\rho(\rho,z) = \frac{2\mu c\,a^2}{(\rho^2+z^2)^{1/2}}\left(\frac{1-2\nu}{(\rho^2+z^2)^{1/2}-z} + \frac{3\rho^2 z}{(\rho^2+z^2)^2}\right), \tag{5.35a}$$

$$\sigma_\theta(\rho,z) = -\frac{2\mu c\, a^2(1-2\nu)}{(\rho^2+z^2)^{1/2}}\left(\frac{1}{(\rho^2+z^2)^{1/2}-z}+\frac{z}{\rho^2+z^2}\right), \tag{5.35b}$$

$$\sigma_z(\rho,z) = \frac{6\mu c\, a^2 z^3}{(\rho^2+z^2)^{5/2}}, \tag{5.35c}$$

$$\sigma_{\rho z}(\rho,z) = \frac{6\mu c\, a^2 \rho z^2}{(\rho^2+z^2)^{5/2}}, \tag{5.35d}$$

which follow from substituting (5.34) in (2.7). This exact solution will be used as a benchmark to test the performance of the DtN FEM approach.

5.4.2. Implementation aspects

To apply the DtN FEM to solve the model problem, the radius of the artificial boundary R must be, of course, greater than a. The resulting computational domain Ω^{i} is described in axisymmetric spherical coordinates (r,ϕ) as

$$\Omega^{\mathrm{i}} = \{(r,\phi):\ a<r<R,\ \pi/2<\phi<\pi\}.$$

In general, in any DtN FEM approach, the radius R is to be chosen large enough so that any possible irregularity (anisotropy, inhomogeneity) is enclosed by Γ_R, but at the same time small enough to minimise the size of Ω^{i} and thus the number of finite elements considered (cf. (Givoli & Vigdergauz, 1993)). In our case, for the purpose of solving the model problem in order to test the accuracy of the DtN FEM, it is reasonable to assume, for instance, $R=(3/2)a$. In addition, as we have deduced a linear dependence of the matrix $\boldsymbol{K}^b$ on R, the accuracy of the method should not be strongly affected by the location of Γ_R. Thus, from now on, R is assumed to be fixed at the same value.

In order to maintain a constant mesh quality, we consider structured triangular meshes of Ω^{i} generated as follows: We assume equispaced partitions of intervals $[a,R]$ and $[\pi/2,\pi]$ consisting respectively of I and J segments, delimited by nodes satisfying $a=r_1<r_2<\ldots<r_I<r_{I+1}=R$ and $\pi/2=\phi_1<\phi_2<\ldots<\phi_J<\phi_{J+1}=\pi$ (the latter partition already introduced in Section 5.3), in such a way that $r_i = a+(i-1)(R-a)/I$ and $\phi_j=(\pi/2)(1+(j-1)/J)$. The cartesian product of both partitions gives rise to a structured quadrilateral mesh of Ω^{i}, which consists of $(I+1)(J+1)$ nodes and IJ elements. If each

quadrilateral element is split by its diagonal, two triangles are created. Then the resulting triangular mesh consists of $(I+1)(J+1)$ nodes and $2IJ$ elements in total. Given that we have assumed $R = (3/2)a$, and in order to ensure relatively good quality triangles, it is reasonable to set $J = 4I$. The mesh size h is calculated using relatively simple geometrical considerations, arriving at the formula

$$h = \frac{R}{3I}\left(1 + 6I(3I-1)\left(1 - \cos\left(\frac{\pi}{8I}\right)\right)\right)^{1/2}. \tag{5.36}$$

To choose an optimal value of the truncation order N for fixed R and h, we use the simple crude formula first proposed in (Keller & Givoli, 1989) for the Laplace equation, and subsequently modified and used in (Givoli & Keller, 1989) and (Givoli & Vigdergauz, 1993) for the 2D elasticity equation. According to this formula, the optimal N is estimated as

$$N_{\text{opt}} = \left\lceil -(p+1)\frac{\ln(h/a)}{\ln(R/a)} \right\rceil, \tag{5.37}$$

where $\lceil \cdot \rceil$ stands for the ceiling function and p is the highest degree of complete polynomial in $\mathcal{V}^h$ (in this case $p = 1$ since we are considering $P1$ finite elements). Substituting $R = (3/2)a$ and approximating $\ln(3/2) \approx 2/5$, (5.37) becomes

$$N_{\text{opt}} = \left\lceil -\left(2 + 5\ln\left(\frac{h}{R}\right)\right) \right\rceil. \tag{5.38}$$

This formula provides a good estimation of N, as we shall see below.

5.4.3. Results and accuracy

Next, we present numerical results obtained by solving the model problem using our DtN FEM procedure. We assume $a = 600$ m and $R = (3/2)a = 900$ m. Six meshes of Ω^{i} for different values of I are considered, whose parameters are summarised in Table 5.1. The optimal series truncation order N_{opt} is computed from (5.38) and is shown in the last column of the table. The meshes corresponding to $I = 5$ and $I = 10$ are depicted in Figure 5.4 by the way of example.

We assume an elastic solid with Young's modulus $E = 70$ GPa and Poisson's ratio $\nu = 0.3$. The Lamé constants are immediate from E and ν through the standard formulae

Table 5.1. Parameters of the structured triangular meshes considered.

I	J	No. nodes	No. elements	h m	N_{opt}
3	12	52	72	149.39679	7
5	20	126	200	90.89000	10
10	40	451	800	45.90566	13
18	72	1387	2592	25.61552	16
32	128	4257	8192	14.44309	19
60	240	14701	28800	7.71394	22

$\lambda = E\nu/(1+\nu)/(1-2\nu)$ and $\mu = E/2/(1+\nu)$. In order to get displacements and stresses of physically realistic magnitudes, we set $c = 10^{-4}$. Then the model problem is solved by the DtN FEM in the six triangular meshes described in Table 5.1. For each mesh, the optimal series truncation order N_{opt} indicated in the same table is assumed in all the development of Section 5.3. The results calculated in the finest mesh ($I = 60$) are presented next. Figures 5.5 shows the components of the computed displacement vector $\boldsymbol{u}^h$. The

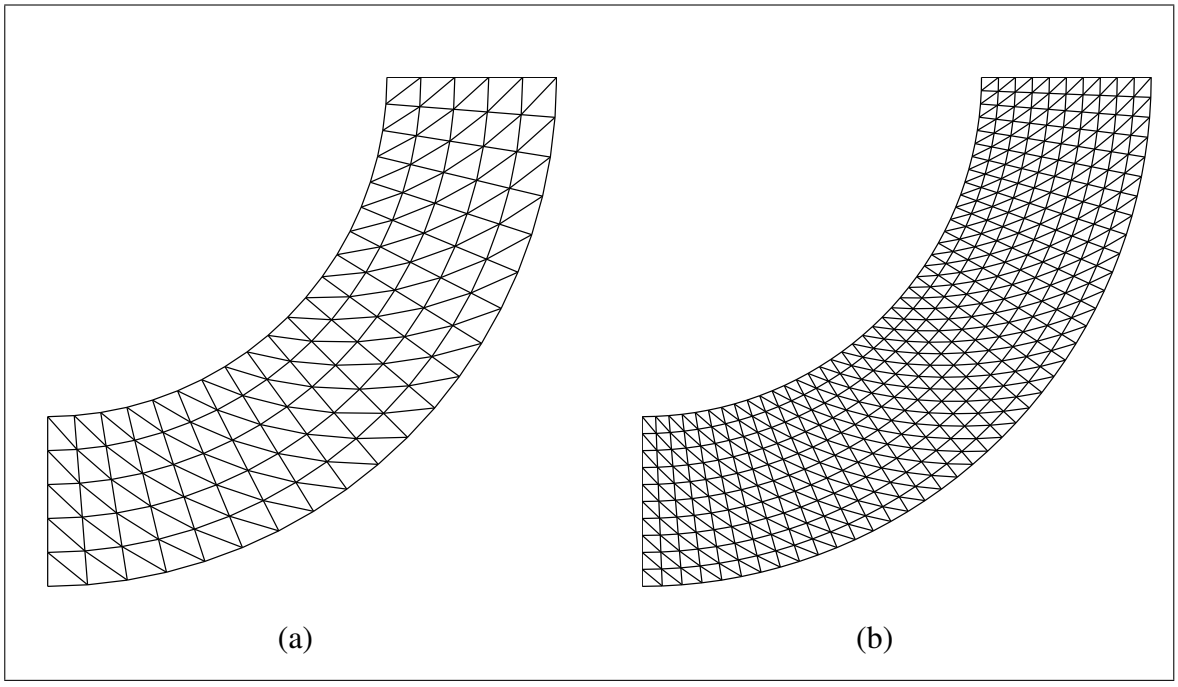

Figure 5.4. Two of the considered structured triangular meshes. (a) $I = 5$. (b) $I = 10$.

associated stress tensor $\boldsymbol{\sigma}^h$ is numerically computed from $\boldsymbol{u}^h$ by substituting the displacement components in (2.7), with the derivatives calculated numerically in the mesh. The components of $\boldsymbol{\sigma}^h$ are presented in Figure 5.6.

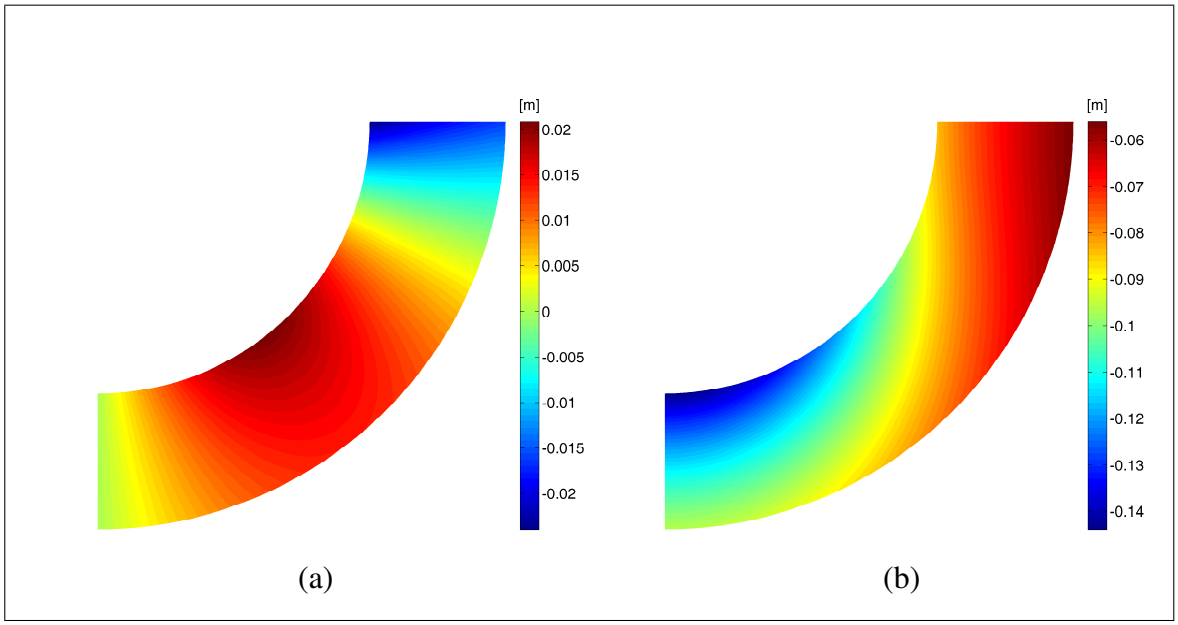

Figure 5.5. Computed displacement components. (a) $u_\rho^h(\rho, z)$. (b) $u_z^h(\rho, z)$.

In order to test preliminarily the effectiveness of our DtN FEM, the numerical solutions calculated in each mesh are compared against the exact solution given by (5.34) and (5.35) at some specific points of the domain. Table 5.2 presents numerical values of some displacement and stress components evaluated at the extreme points of Γ_R. From this table we see that, as the mesh size decreases, the values of the numerical solution get closer to the values of the exact one at the considered points. Moreover, in the case of the displacement, this approximation is faster.

To study more rigorously the accuracy and convergence of the DtN FEM procedure, we employ the relative error between the numerical and the exact solution, defined as

$$E_{\boldsymbol{u}}(h) = \frac{\|\boldsymbol{u}^h - \boldsymbol{\Pi}^h \boldsymbol{u}\|_{0,\Omega^{\mathrm{i}}}}{\|\boldsymbol{\Pi}^h \boldsymbol{u}\|_{0,\Omega^{\mathrm{i}}}},$$

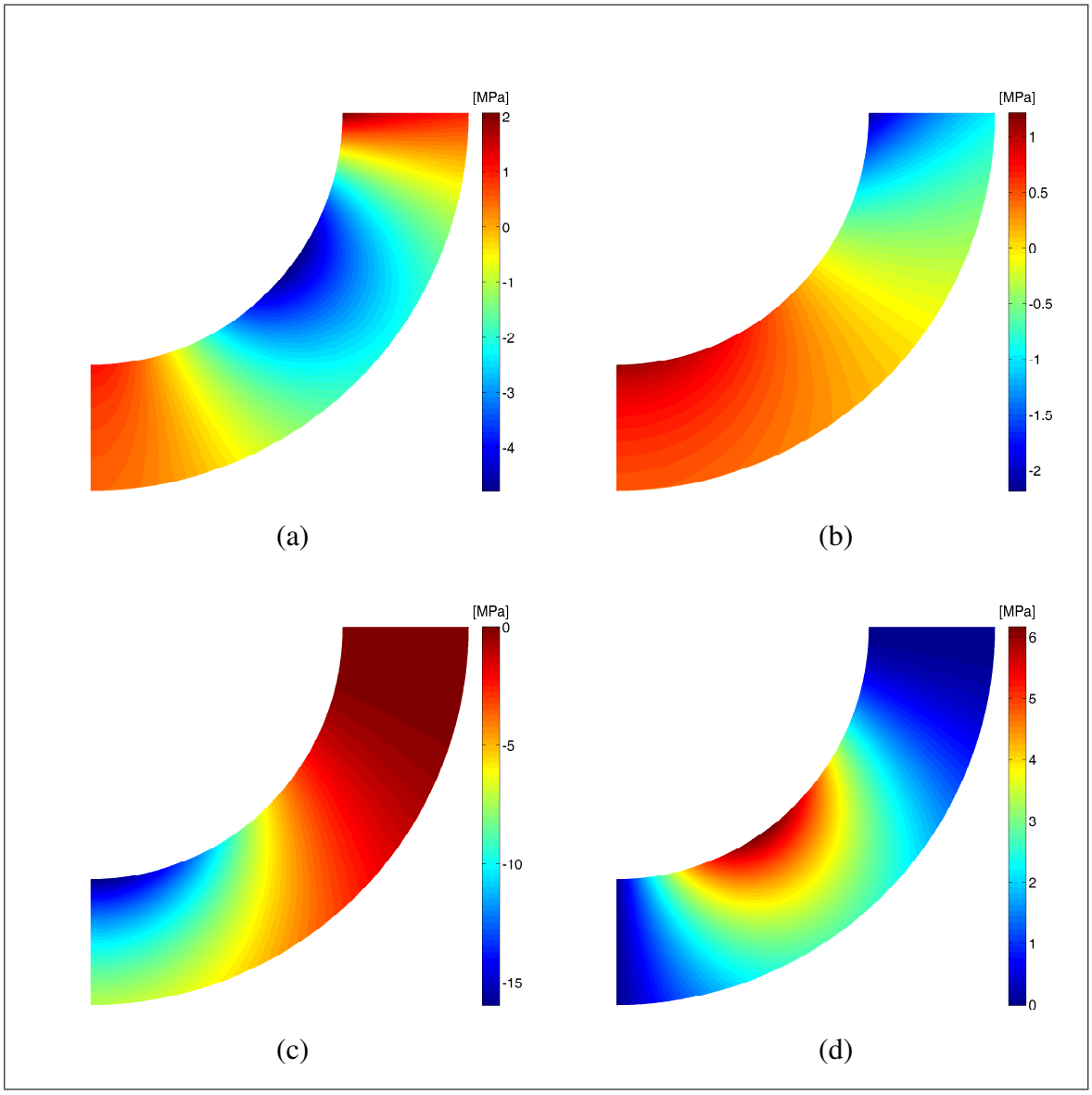

Figure 5.6. Computed stress components. (a) $\sigma_\rho^h(\rho, z)$. (b) $\sigma_\theta^h(\rho, z)$. (c) $\sigma_z^h(\rho, z)$. (d) $\sigma_{\rho z}^h(\rho, z)$.

where $\|\cdot\|_{0,\Omega^{\mathrm{i}}}$ is the usual L^2-norm in Ω^{i} and $\mathbf{\Pi}^h \boldsymbol{u}$ denotes the Lagrange interpolation of the exact solution $\boldsymbol{u}$ over the mesh of size h. Figure 5.7 presents a log-log plot of $E_{\boldsymbol{u}}$ in function of h, where we observe that the relative error decays as mesh size diminishes. Therefore, the whole numerical solution computed by the DtN FEM converges to the exact solution as the mesh is refined, which confirms the effectiveness of the method. In fact, the

Table 5.2. Some components of the solution evaluated at points $(0, R)$ and $(-R, 0)$.

Solution	$u_\rho(0,R)$ m	$u_z(-R,0)$ m	$\sigma_\rho(0,R)$ MPa	$\sigma_\rho(-R,0)$ MPa	$\sigma_z(-R,0)$ MPa
$I = 3$	-0.01709	-0.09664	0.29365	0.08399	-7.58848
$I = 5$	-0.01648	-0.09633	0.59049	0.20644	-7.49848
$I = 10$	-0.01615	-0.09613	0.78277	0.37847	-7.33654
$I = 18$	-0.01606	-0.09605	0.85841	0.42163	-7.27821
$I = 32$	-0.01602	-0.09602	0.89876	0.44859	-7.23198
$I = 60$	-0.01601	-0.09601	0.92393	0.46549	-7.20743
Exact	-0.01600	-0.09600	0.95726	0.47863	-7.17949

relative error in the finest mesh is approximately 0.003%. This good agreement between the numerical and the exact solution is achieved with a relatively low number of terms in the series of the DtN map ($N = 22$). In addition, the graph of $E_{\boldsymbol{u}}$ in the log-log plot is nearly a straight line, which suggests that the DtN FEM has a constant rate of convergence. To estimate it, we compute the slope of this line, using for this the relative errors associated with the two finest meshes, since in these cases the method yields the best approximations. The computed slope is 2.00257. A slope nearly 2 in the relative error of the solution predicts that the rate of convergence of the method is 2. Hence, the numerical evidence indicates that the DtN FEM presented throughout this work has second-order accuracy.

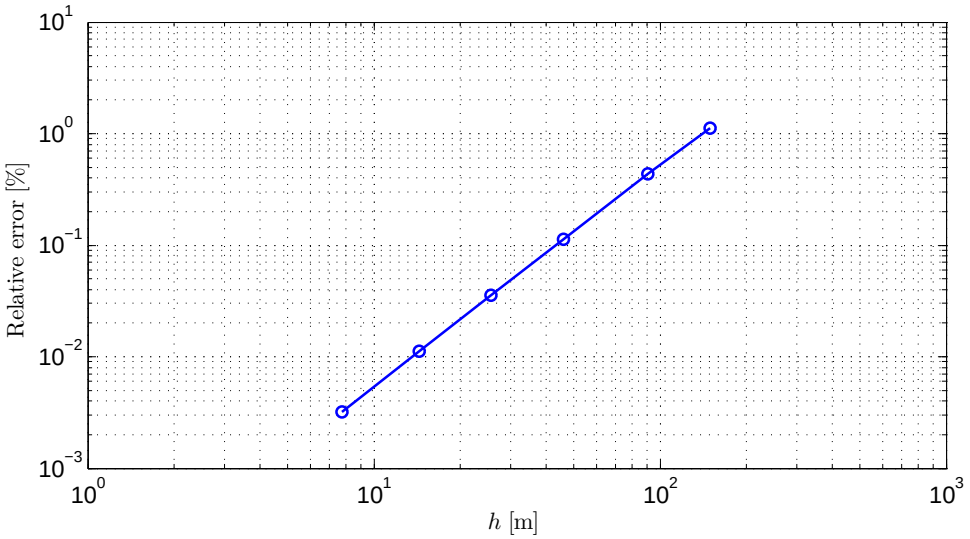

Figure 5.7. Log-log plot of $E_{\boldsymbol{u}}$ in function of h.

References

Abramowitz, M., & Stegun, I. (1965). *Handbook of mathematical functions with formulas, graphs, and mathematical tables.* New York: Dover Publications.

Aladl, U. E., Deakin, A. S., & Rasmussen, H. (2002). Nonreflecting boundary condition for the wave equation. *J. Comput. Appl. Math.*, *138*, 309–323.

Amenzade, Y. A. (1979). *Theory of elasticity*. Moscow: Mir Publishers.

Andrews, L. C. (1985). *Special functions for engineers and applied mathematicians*. New York: Macmillan Publishing Co.

Arfken, G. B., & Weber, H. J. (2001). *Mathematical methods for physicists*. London: Harcourt/Academic Press.

Bell, W. W. (1968). *Special functions for scientists and engineers*. London: Van Nostrand.

Björck, A. (1996). *Numerical methods for least square problems*. Philadelphia: SIAM.

Brown, J. W., & Churchill, R. (2006). *Fourier series and boundary value problems*. New York: McGraw-Hill.

Cerit, M., Genel, K., & Eksi, S. (2009, October). Numerical investigation on stress concentration of corrosion pit. *Engineering Failure Analysis*, *16*(7), 2467–2472. doi: 10.1016/j.engfailanal.2009.04.004

Deakin, A. S., & Rasmussen, H. (2001). Nonreflecting boundary condition for the Helmholtz equation. *Comput. Math. Appl.*, *41*, 307–318.

Eubanks, R. (1953). Stress concentration due to a hemispherical pit at a free surface. *Journal of Applied Mechanics*, *21*, 57.

Eubanks, R., & Sternberg, E. (1956). On the completeness of the boussinesq-papkovich stress functions. *Jour. Rational Mech. Anal.*, *5*, 735 - 746.

Eubanks, R. A. (1954). Stress concentration due to a hemispherical pit at a free surface. *J. Appl. Mech.*, *21*, 57–62.

Fujita, T., Sadayasu, T., Tsuchida, E., & Nakahara, I. (1978). Stress concentration due to a hemispherical pit at a free surface of a thick plate under all-around tension. *Bulletin of JSME*, *21*(154), 561-565.

Fujita, T., Tsuchida, E., & Nakahara, I. (1982, April). Asymmetric problem of a semi-infinite body having a hemispherical pit under uniaxial tension. *Journal of Elasticity*, *12*(2), 177–192. doi: 10.1007/BF00042214

Gächter, G., & Grote, M. J. (2003). Dirichlet-to-Neumann map for three-dimensional elastic waves. *Wave Motion*, *37*, 293–311.

Givoli, D. (1992). *Numerical methods for problems in infinite domains*. Amsterdam: Elsevier.

Givoli, D. (1999a). Exact representations on artificial interfaces and applications in mechanics. *Appl. Mech. Rev.*, *52*(11), 333–349.

Givoli, D. (1999b). Recent advances in the DtN FE method. *Arch. Comput. Method E.*, *6*(2), 71–116.

Givoli, D., & Keller, J. B. (1989). A finite element method for large domains. *Comput. Methods Appl. Mech. Engrg.*, *76*, 41-66.

Givoli, D., & Keller, J. B. (1990). Non-reflecting boundary conditions for elastic waves. *Wave Motion*, *12*, 261–279.

Givoli, D., & Vigdergauz, S. (1993). Artificial boundary conditions for 2D problems in geophysics. *Comput. Methods Appl. Mech. Engrg.*, *110*, 87-101.

Golub, G. H., & Loan, C. F. V. (1996). *Matrix computations*. Baltimore: Johns Hopkins University Press.

Gradshteyn, I. S., & Ryzhik, I. M. (2007). *Table of integrals, series and products*. Amsterdam: Elsevier/Academic Press.

Griffiths, D., & Lane, P. (1999). Slope stability analysis by finite elements. *Geotechnique*, *49*(3), 387–403.

Grote, M. J. (2000). Nonreflecting boundary conditions for elastodynamic scattering. *J. Comput. Phys.*, *161*, 331–353.

Grote, M. J., & Keller, J. B. (1995a). Exact nonreflecting boundary condition for the time dependent wave equation. *SIAM J. Appl. Math.*, *55*, 280–297.

Grote, M. J., & Keller, J. B. (1995b). On nonreflecting boundary conditions. *J. Comput. Phys.*, *122*, 231–243.

Grote, M. J., & Keller, J. B. (1996). Nonreflecting boundary conditions for time-dependent scattering. *J. Comput. Phys.*, *127*, 52–65.

Grote, M. J., & Keller, J. B. (2000). Exact nonreflecting boundary condition for elastic waves. *SIAM J. Appl. Math.*, *60*, 803–819.

Han, H., Bao, W., & Wang, T. (1997). Numerical simulation for the problem of infinite elastic foundation. *Comput. Methods Appl. Mech. Engrg.*, *147*, 369–385.

Han, H. D., & Wu, X. N. (1985). Approximations of infinite boundary conditions and its application to finite elements methods. *J. Comput. Math.*, *3*, 179–192.

Han, H. D., & Wu, X. N. (1992). The approximation of the exact boundary conditions at an artificial boundary for linear elastic equations and its application. *Math. Comput.*, *59*(199), 21–37.

Han, H. D., & Wu, X. N. (2013a). *Artificial boundary method*. Beijing-Berlin-Heidelberg: Tsinghua University Press and Springer-Verlag.

Han, H. D., & Wu, X. N. (2013b). A survey on artificial boundary method. *Sci. China Math.*, *56*, 2439–2488.

Han, H. D., & Zheng, C. X. (2005). Artificial boundary method for the three-dimensional exterior problem of elasticity. *J. Comput. Math.*, *23*, 603-–618.

Harari, I., & Shohet, Z. (1998). On non-reflecting boundary conditions in unbounded elastic solids. *Comput. Methods Appl. Mech. Engrg.*, *163*, 123—139.

Huttelmaier, H. P., & Glockner, P. G. (1985). Stresses and displacements due to underground mining using a finite element procedure. *Geotechnical and Geological Engineering*, *3*(1), 49 - 63. doi: DOI:10.1007/BF00881341

Keller, J. B., & Givoli, D. (1989). Exact non-reflecting boundary conditions. *J. Comput. Phys.*, *82*, 172–192.

Kulhawy, F. H. (1974). Finite element modeling criteria for underground openings in rock. *International Journal of Rock Mechanics and Mining Sciences and Geomechanics Abstracts*, *11*(12), 465 - 472. doi: DOI:10.1016/0148-9062(74)91996-2

Multiphysics, C. (1994). Comsol. *Inc., Burlington, MA, www. comsol. com*.

Ou, C.-Y., Chiou, D.-C., & Wu, T.-S. (1996). *Three-Dimensional Finite Element Analysis of Deep Excavations* (Vol. 122) (No. 5). doi: 10.1061/(ASCE)0733-9410(1996)122:5(337)

Ovsyannikov, A. S., & Starikov, V. A. (1987, September). Numerical solution of an axisymmetric problem of the theory of elasticity for a half-space with a notch. *Soviet Applied Mechanics*, *23*(9), 849–852. doi: 10.1007/BF00887788

Sadd, M. H. (2005). *Elasticity: Theory, applications, and numerics*. Boston: Elsevier Butterworth-Heinemann.

Szabo, B., & Babuška, I. (1991). *Finite element analysis*. New York: John Wiley & Sons.

Turnbull, A., Horner, D., & Connolly, B. (2009, March). Challenges in modelling the evolution of stress corrosion cracks from pits. *Engineering Fracture Mechanics*, *76*(5), 633–640. doi: 10.1016/j.engfracmech.2008.09.004

6. APPENDIX

6.1. Some properties of Legendre polynomials

The Legendre polynomial $P_n(\cos\phi)$ as a function of ϕ is a solution of the Legendre's differential equation, given by

$$\frac{1}{\sin\phi}\frac{\mathrm{d}}{\mathrm{d}\phi}\left(\sin\phi\frac{\mathrm{d}}{\mathrm{d}\phi}P_n(\cos\phi)\right)+n(n+1)P_n(\cos\phi)=0. \tag{6.1}$$

Some useful recurrence relations fulfilled by the Legendre polynomials and their derivatives are (cf. (Andrews, 1985; Bell, 1968)):

$$(n+1)P_{n+1}(\cos\phi)-(2n+1)\cos\phi\,P_n(\cos\phi)+nP_{n-1}(\cos\phi)=0, \tag{6.2a}$$

$$P'_{n+1}(\cos\phi)-P'_{n-1}(\cos\phi)=(2n+1)P_n(\cos\phi), \tag{6.2b}$$

$$\sin^2\phi\,P'_n(\cos\phi)=(n+1)\big(\cos\phi\,P_n(\cos\phi)-P_{n+1}(\cos\phi)\big), \tag{6.2c}$$

$$\sin^2\phi\,P'_n(\cos\phi)=n\big(P_{n-1}(\cos\phi)-\cos\phi\,P_n(\cos\phi)\big), \tag{6.2d}$$

where $n\geq 1$. The Legendre polynomials also satisfy the following properties for $n\geq 0$:

$$P_{2n}(0)=\frac{(-1)^n(2n)!}{2^{2n}(n!)^2}, \tag{6.3a}$$

$$P_{2n+1}(0)=0, \tag{6.3b}$$

$$P_{2n+2}(0)=-\frac{2n+1}{2n+2}\,P_{2n}(0), \tag{6.3c}$$

$$P'_{2n}(0)=0, \tag{6.3d}$$

$$P'_{2n+1}(0)=(2n+1)\,P_{2n}(0). \tag{6.3e}$$

Properties (6.3a) and (6.3b) are standard and can be found, for instance, in (Andrews, 1985) or (Bell, 1968). Property (6.3c) is a consequence of formula (6.2a). Property (6.3d) follows from (6.2c) and (6.3b). Property (6.3e) is obtained from (6.2d). Moreover, the Legendre polynomials fulfil the following integral formulae for $n\geq 0$ and $k\geq 0$:

$$\int_{\pi/2}^{\pi}P_{2n}(\cos\phi)\,P_{2k}(\cos\phi)\sin\phi\,\mathrm{d}\phi=\frac{\delta_{n,k}}{4n+1}, \tag{6.4a}$$

$$\int_{\pi/2}^{\pi} P_{2n+1}(\cos\phi)\, P_{2k+1}(\cos\phi)\sin\phi\,\mathrm{d}\phi = \frac{\delta_{n,k}}{4n+3}, \tag{6.4b}$$

$$\int_{\pi/2}^{\pi} P_{2n}(\cos\phi)\, P_{2k+1}(\cos\phi)\sin\phi\,\mathrm{d}\phi = -\frac{(2k+1)P_{2n}(0)P_{2k}(0)}{(2k+1-2n)(2k+2+2n)}, \tag{6.4c}$$

$$\int_{\pi/2}^{\pi} P'_{2n}(\cos\phi)\, P'_{2k}(\cos\phi)\sin^3\phi\,\mathrm{d}\phi = \frac{2n(2n+1)\delta_{n,k}}{4n+1}, \tag{6.4d}$$

$$\int_{\pi/2}^{\pi} P'_{2n+1}(\cos\phi)\, P'_{2k+1}(\cos\phi)\sin^3\phi\,\mathrm{d}\phi = \frac{(2n+1)(2n+2)\delta_{n,k}}{4n+3}, \tag{6.4e}$$

$$\int_{\pi/2}^{\pi} P'_{2n}(\cos\phi)\, P'_{2k+1}(\cos\phi)\sin^3\phi\,\mathrm{d}\phi = -\frac{2n(2n+1)(2k+1)P_{2n}(0)P_{2k}(0)}{(2k+1-2n)(2k+2+2n)}. \tag{6.4f}$$

Formulae (6.4a), (6.4b), and (6.4c) can be deduced from (Gradshteyn & Ryzhik, 2007), Subsection 7.221. To obtain (6.4c) it is, in addition, necessary to combine with (6.3a). Formulae (6.4d), (6.4e), and (6.4f) follow from formulae (6.4a), (6.4b), and (6.4c), respectively, together with the Legendre's differential equation (6.1). The following two additional integral formulae are also valid

$$\int_{\pi/2}^{\pi} P'_{2n}(\cos\phi)(1+\cos\phi)\sin\phi\,\mathrm{d}\phi = P_{2n}(0), \tag{6.5a}$$

$$\int_{\pi/2}^{\pi} P'_{2n+1}(\cos\phi)(1+\cos\phi)\sin\phi\,\mathrm{d}\phi = \frac{P_{2n}(0)}{2n+2}, \tag{6.5b}$$

which are obtained by integrating by parts and combining with (6.4a) and (6.4c), respectively.

6.1.1. Expansion of the odd terms in pair terms from the Legendre polynomials

We need to show that $\forall k = 0, 1, \ldots$ and $-1 \le x \le 0$

$$P_{2k+1}(x) = -(2k+1)P_{2k}(0)\sum_{n=0}^{\infty}\omega_k^{(n)}P_{2n}(x), \tag{6.6}$$

where

$$\omega_k^{(n)} = \frac{(4n+1)P_{2n}(0)}{(2k+1-2n)(2k+2+2n)}. \tag{6.7}$$

The set $\{P_{2n}(x)\}_{n=0}^{\infty}$ is an orthogonal basis (Brown & Churchill, 2006) in $[-1, 0]$ (and in $[0, 1]$) such that

$$\int_{-1}^{0} P_{2n}(x)P_{2m}(x)\mathrm{d}x = \frac{\delta_{nm}}{4n+1}, \tag{6.8}$$

then we can expand $P_{2k+1}(x)$ in a Legendre series

$$P_{2k+1}(x) = \sum_{n=0}^{\infty}(4n+1)\int_{-1}^{0} P_{2k+1}(t)P_{2k}(t)\mathrm{d}tP_{2n}(x). \tag{6.9}$$

Then, our problem becomes

$$\int_{-1}^{0} P_{2k+1}(x)P_{2n}(x)\mathrm{d}x = -\frac{(2k+1)P_{2k}(0)P_{2n}(0)}{(2k+1-2n)(2k+2+2n)}\forall n, k = 0, 1\ldots \tag{6.10}$$

which can also be written as

$$\int_{0}^{1} P_{2n}(x)P_{2k+1}(x)\mathrm{d}x = \frac{(2k+1)P_{2k}(0)P_{2n}(0)}{(2k+1-2n)(2k+2+2n)}\forall n, k = 0, 1\ldots \tag{6.11}$$

We define

$$A_{n,k} = \int_{0}^{1} P_{2n}(x)P_{2k+1}(x)\mathrm{d}x. \tag{6.12}$$

This will be proved by induction. We have the following hypothesis

(i) The statement (6.12) is valid for $n = k = 0$.

(ii) If the statement holds for some $N > 0$ for any n, k with $n + k = N$, then the statement also holds for any n, k when $n + k = N + 1$.

Basis: Show that the statement holds for $n = k = 0$.

$$A_{0,0} = \int_{0}^{1} P_0(x)P_1(x)\mathrm{d}x = \int_{0}^{1} x\mathrm{d}x = \frac{x^2}{2}\bigg|_{0}^{1} = \frac{1}{2}.$$

On the other hand if $n = k = 0$

$$\frac{(2k+1)P_{2k}(0)P_{2n}(0)}{(2k+1-2n)(2k+2+2n)} = \frac{1\cdot 1\cdot 1}{1\cdot 2} = \frac{1}{2}. \tag{6.13}$$

The two sides are equal, so the statement is true for $n = k = 0$. Thus it has been shown that $A_{0,0}$ holds.

Inductive step: Show that if $A_{n,k}$ with $n+k=N$ holds, then also $A_{n,k}$ with $n+k=N+1$ holds, where

$$A_{n,k} = \frac{(2k+1)P_{2k}(0)P_{2n}(0)}{(2k+1-2n)(2k+2+2n)}. \tag{6.14}$$

This only can occur in two cases, $(n+1,k)$ and $(n,k+1)$. Then we need to prove two statements

$$A_{n+1,k} = \int_0^1 P_{2n+2}(x)P_{2k+1}(x)\mathrm{d}x = \frac{(2k+1)P_{2k}(0)P_{2n+2}(0)}{(2k-1-2n)(2k+4+2n)}, \tag{6.15}$$

and

$$A_{n,k+1} = \int_0^1 P_{2n}(x)P_{2k+3}(x)\mathrm{d}x = \frac{(2k+3)P_{2k+2}(0)P_{2n}(0)}{(2k+3-2n)(2k+4+2n)}. \tag{6.16}$$

The Legendre polynomials satisfy the recurrence relations

$$\begin{aligned}
&(n+1)P_{n+1}(x) - (2n-1)xP_n(x) + nP_{n-1}(x) = 0,\\
&(1-x^2)P_n'(x) = -nxP_n(x) + nP_{n-1}(x) = (n+1)\big(xP_n(x) - P_{n+1}\big).
\end{aligned} \tag{6.17}$$

Combining this we obtain

$$P_{2n+2}(x) = P_{2n}(x) - \frac{(4n+3)}{(2n+1)(2n+2)}(1-x^2)P_{2n+1}'(x), \tag{6.18}$$

multiplying by $P_{2k+1}(x)$ and integrating between 0 and 1 we have

$$A_{n+1,k} = A_{n,k} - \frac{(4n+3)}{(2n+1)(2n+2)}\int_0^1 (1-x^2)P_{2n+1}'(x)P_{2k+1}(x)\mathrm{d}x. \tag{6.19}$$

Using integration by parts we obtain

$$\int_0^1 (1-x^2)P_{2n+1}'(x)P_{2k+1}(x)\mathrm{d}x = -\int_0^1 P_{2n+1}(x)\big((1-x^2)P_{2k+1}'(x) - 2xP_{2k+1}(x)\big)\mathrm{d}x. \tag{6.20}$$

Using this we obtain

$$A_{n+1,k} = A_{n,k} + \frac{(4n+3)}{(2n+1)(2n+2)}\int_0^1 \big((1-x^2)P_{2n+1}'(x) - 2P_{2n+1}(x)\big)\,P_{2k+1}(x)\mathrm{d}x. \tag{6.21}$$

With (6.17), this becomes

$$A_{n+1,k} = A_{n,k} + \frac{(4n+3)}{(2n+1)(2n+2)} \left((2k+1) \int_0^1 P_{2n+1}(x) P_{2k}(x) \mathrm{d}x \right.$$
$$\left. -(2k+3) \int_0^1 x P_{2n+1}(x) P_{2k+1}(x) \mathrm{d}x \right) \tag{6.22}$$

Again using the recurrence relations (6.17) multiplying by $P_{2k+1}(x)$ and integration between 0 and 1, and using the definition of $A_{k,n}$ we obtain

$$\int_0^1 x P_{2n+1}(x) P_{2k+1}(x) \mathrm{d}x = \frac{(2n+1)}{(4n+3)} A_{n,k} + \frac{(2n+2)}{(4n+3)} A_{n+1,k}. \tag{6.23}$$

This yields

$$A_{n+1,k} = A_{n,k} + \frac{(4n+3)}{(2n+1)(2n+2)} \left((2k+1) A_{k,n} - \frac{(2k+3)(2n+1)}{(4n+3)} A_{n,k} \right.$$
$$\left. -\frac{(2k+3)(2n+2)}{(4n+3)} A_{n+1,k} \right). \tag{6.24}$$

Rearranging in a suitable way gives us

$$A_{n+1,k} = -\frac{(2n+1)(2k+1-2n)}{(2n+2)(2k+4+2n)} A_{n,k} + \frac{(4n+3)(2k+1)}{(2n+2)(2k+4+2n)} A_{k,n}. \tag{6.25}$$

Applying (6.14) in this expression and using that $(2n+2)P_{2n+2}(0) = -(2n+1)P_{2n}(0)$ yields

$$A_{n+1,k} = \frac{(2k+1)}{(2k-1-2n)(2k+4+2n)} P_{2k}(0) - \frac{(2n+1)}{(2n+2)} P_{2n}(0)$$
$$= \frac{(2k+1) P_{2k}(0) P_{2n+2}(0)}{(2k-1-2n)(2k+4+2n)}, \tag{6.26}$$

thereby showing that indeed $A_{n+1,k}$ holds. Next we need to show te same for $A_{n,k+1}$, in order to do that we use (6.17)

$$P_{2k+3}(x) = P_{2k+1} - \frac{(4k+5)}{(2k+2)(2k+3)} (1-x^2) P'_{2k+2}(x). \tag{6.27}$$

Multiplying by $P_{2n}(x)$ and integration between 0 and 1 gives us

$$A_{n,k+1} = A_{n,k} - \frac{(4n+5)}{(2k+2)(2k+3)} \int_0^1 (1-x^2) P'_{2k+2}(x) P_{2n}(x) \mathrm{d}x. \tag{6.28}$$

Since

$$\int_0^1 (1-x^2) P'_{2k+2}(x) P_{2n}(x) \mathrm{d}x = -P_{2n}(0) P_{2k+2}(x) - \int_0^1 \big((1-x^2) P'_{2n}(x) - 2x P_{2n}(x)\big) P_{2k+2}(x) \mathrm{d}x. \tag{6.29}$$

Hence

$$A_{n,k+1} = A_{n,k} + \frac{(4k+5)}{(2k+2)(2k+3)} \bigg(P_{2n}(0) P_{2k+2}(0) + \int_0^1 (1-x^2) P'_{2n}(x) P_{2k+2}(x) \mathrm{d}x - 2 \int_0^1 x P_{2n}(x) P_{2k+2}(x) \mathrm{d}x \bigg). \tag{6.30}$$

Using (6.17) yields

$$A_{n,k+1} = A_{n,k} + \frac{(4k+5)}{(2k+2)(2k+3)} \bigg(P_{2n}(0) P_{2k+2}(0) + (2n-1) \int_0^1 x P_{2n}(x) P_{2k+2}(x) \mathrm{d}x - (2n+1) \int_0^1 P_{2n+1}(x) P_{2k+2}(x) \mathrm{d}x \bigg). \tag{6.31}$$

Again using the recurrence relations (6.17) multiplying by $P_{2n}(x)$ and integration between 0 and 1, and using the definition of $A_{k+1,n}$ we obtain

$$\int_0^1 x P_{2n}(x) P_{2k+2}(x) \mathrm{d}x = \frac{(2k+3)}{(4k+5)} A_{n,k+1} + \frac{(2k+2)}{(4k+5)} A_{n,k}, \tag{6.32}$$

hence

$$A_{n,k+1} = A_{n,k} + \frac{(4k+5)}{(2k+2)(2k+3)} \bigg(P_{2n}(0) P_{2k+2}(0) + \frac{(2n-1)(2k+3)}{(4k+5)} A_{n,k+1} + \frac{(2n-1)(2k+2)}{(4k+5)} A_{n,k} - (2n+1) A_{k+1,n} \bigg). \tag{6.33}$$

Rearranging in a suitable way gives us

$$A_{n,k+1} = \frac{(2k+2)(2k+2+2n)}{(2k+3)(2k+3-2n)} A_{n,k} - \frac{(4k+5)(2n+1)}{(2k+3)(2k+3-2n)} A_{k+1,n} + \frac{(4k+5)}{(2k+3)(2k+3-2n)} P_{2n}(0) P_{2k+2}(0). \tag{6.34}$$

If we interchange k by n in (6.25) we obtain

$$\begin{aligned} &(2k+2)(2k+3)(2k+3-2n)(2k+4+2n) A_{n,k+1} \\ &+ (2k+1)(4k+5)(2k-1-2n)(2n+1) A_{k,n} \\ &+ \big((4k+3)(4k+5)(2n+1)^2 - (2k+2)^2(2k+2+2n)(2k+4+2n)\big) A_{n,k} \\ &= -(2k+1)(4k+5)(2k+4+2n) P_{2n}(0) P_{2k}(0). \end{aligned} \tag{6.35}$$

Using (6.14) yields

$$A_{n,k+1} = \frac{(2k+3) P_{2k+2}(0) P_{2n}(0)}{(2k+3-2n)(2k+4+2n)}. \tag{6.36}$$

End of proof.